

UC Davis

UC Davis Electronic Theses and Dissertations

Title

Optimization and evaluation of NK cells for immunotherapy in canine clinical trials

Permalink

<https://escholarship.org/uc/item/8m7042d4>

Author

Razmara, Aryana

Publication Date

2024

Peer reviewed|Thesis/dissertation

Optimization and Evaluation of NK Cells for Immunotherapy in Canine Clinical Trials
By

ARYANA RAZMARA
DISSERTATION

Submitted in partial satisfaction of the requirements for the degree of

DOCTOR OF PHILOSOPHY

in

IMMUNOLOGY

in the

OFFICE OF GRADUATE STUDIES

of the

UNIVERSITY OF CALIFORNIA

DAVIS

Approved:

Robert Canter, Chair

Michael Kent

Titus Brown

Committee in Charge

2024

Natural killer (NK) cells are key effectors in anti-tumor responses with great potential to extend the promise of cancer immunotherapy. Dogs develop spontaneous cancers with striking similarities to humans and can serve as a crucial link to inform NK biology, optimize NK immunotherapy for both dog and human patients, and identify potential biomarkers of response. Previously, CD5 depletion of peripheral blood mononuclear cells (PBMCs) was used in dogs to isolate a CD5dim-expressing NK subset prior to co-culture with an irradiated feeder line, but this can limit the yield of the final NK product. We assessed NK activation, expansion, and preliminary clinical activity in first-in-dog clinical trials using a novel system with unmanipulated PBMCs to generate our NK cell product. Calculated cell counts, viability, killing, and cytokine secretion were equivalent or higher in expanded NK cells from canine PBMCs versus CD5-depleted cells, and immune phenotyping confirmed a CD3-NKp46+ product from PBMC-expanded cells at day 14. Transcriptomic analysis of expanded cell populations confirmed upregulation of NK activation genes and related pathways, and human NK cells using well-characterized NK markers closely mirrored canine gene expression patterns. Autologous and allogeneic PBMC-derived NK cells were successfully expanded for use in first-in-dog clinical trials, resulting in no serious adverse events and preliminary efficacy data. RNA sequencing of PBMCs from dogs receiving allogeneic NK transfer showed patient-unique gene signatures with NK gene expression trends in response to treatment. Overall, the use of unmanipulated PBMCs appears safe and potentially effective for canine NK immunotherapy with equivalent to superior results to CD5 depletion in NK expansion, activation, and cytotoxicity. Our preclinical and clinical data support further evaluation of this technique as a novel platform for optimizing NK immunotherapy in dogs. To characterize the heterogeneity of canine NK cells regarding NK ontogeny, subset, and patterns of activation and inhibition we assessed canine NK cell populations by single cell RNA sequencing (scRNAseq) across blood and tissues, including canine soft tissue sarcoma, and canine and human lung, liver, spleen, and placenta. We observed tissue-specific NK cell signatures consistent with immature, stem-like NK cells in the

placenta, mature and activated NK cells in the lung, and NK cells with a mixed activated and inhibited signature in the liver with significant cross-species homology. NK cells from both canine and human undifferentiated sarcoma exhibited an exhausted signature that most closely correlated with NK cells in the liver. We also analyzed NK cells in the peripheral blood of dogs on first-in-dog clinical trials undergoing three distinct NK-targeting regimens, observing that dogs with favorable response (good responders) demonstrated increased NK proportions post treatment. Genes upregulated in NK cells in the peripheral blood of good responders included genes associated with activated NK cells in the lung and revealed post-treatment gene expression changes in the blood as a better predictor of response than baseline NK gene expression. Together, our results point to heterogeneous canine NK populations highly comparable to human NK cells with effector functions adapted to their tissue of residence and dysregulated sarcoma infiltrating NK cells with features of both activation and inhibition. We provide a comprehensive atlas of canine NK cells across organs and sarcomas which will inform future cross-species NK studies and further substantiate the spontaneous canine model in immuno-oncology to optimize NK immunotherapy across species.

TABLE OF CONTENTS

Table of Contents.....	iv
CHAPTER	
1. Research Background and Review.....	1
1.1 Natural Killer and T Cell Infiltration in Canine Osteosarcoma.....	1
1.1.1 Abstract.....	1
1.1.2 Introduction.....	1
1.1.3 Blood vs Tumor.....	3
1.1.4 T cells.....	5
1.1.5 Checkpoint Inhibitors.....	7
1.1.6 NK cells.....	8
1.1.7 Conclusion.....	10
1.1.8 Figures.....	11
1.1.9 References.....	12
1.2 Improved characterization of NK cells for canine immunotherapy.....	18
1.2.1 Abstract.....	18
1.2.2 Introduction.....	18
1.2.3 Identification and characterization of canine NK cells.....	19
1.2.4 NK cells in canine immunotherapy.....	22
1.2.5 Discussion.....	27
1.2.6 Figures.....	29
1.2.7 References.....	30
2. Pre-clinical evaluation and first-in-dog trials of PBMC-expanded adoptive NK cells.....	36
2.1 Background.....	36
2.2 Materials and methods.....	37
2.2.1 PBMC isolation and CD5 depletion of canine cells.....	38
2.2.2 PBMC isolation and NK purification of human cells.....	38
2.2.3 NK expansion of canine and human cells.....	38
2.2.4 Flow cytometry, killing assays, and cytokines.....	38
2.2.5 RNA sequencing.....	40

2.2.6 Autologous and allogeneic NK immunotherapy in dogs.....	40
2.2.7 Statistics.....	42
2.3 Results.....	42
2.3.1 Canine NK Expansions in Vitro.....	42
2.3.2 Genomic analysis of PMBC-expanded canine NK cells.....	43
2.3.3 Functional assessment of expanded NK cells.....	45
2.3.4 Genomic analysis of PBMC-expanded human NK cells.....	46
2.3.5 First-in-dog clinical trial of autologous canine NK cells.....	47
2.3.6 First-in-dog clinical trial of allogeneic canine NK cells.....	48
2.3.6 Figures.....	51
2.4 Discussion.....	65
2.5 References.....	70
3. Single Cell Atlas of Canine NK Cells	79
3.1 Introduction.....	79
3.2 Materials and methods.....	82
3.2.1 Sample acquisition and processing.....	82
3.2.2 Fluorescence-activated Cell Sorting.....	83
3.2.3 Single-Cell RNA Sequencing and Analysis.....	83
3.2.4 Publicly available data	84
3.3 Results.....	85
3.3.1 Canine NK cells vary in abundance and interactions across tissues.....	85
3.3.2 Canine NK cells demonstrate tissue-specific gene signatures.....	86
3.3.3 Canine NK cells can be categorized into distinct subsets.....	88
3.3.4 Canine tumor NK cells have unique activation and exhaustion features....	89
3.3.5 Human Tissues have unique NK proportions and interactions.....	90
3.3.6 Canine and human NK cells show homology across compartments.....	92

3.3.7 NK proportions increase in response to treatment in good responders.....	94
3.3.8 Good responders upregulate NK activation in response to treatment.....	95
3.3.9 Figures.....	97
3.4 Discussion.....	114
3.5 References.....	117

1 Research Background and Review

1.1 Natural Killer and T Cell Infiltration in Canine Osteosarcoma

1.1.1 Abstract

Metastatic osteosarcoma has a bleak prognosis in both humans and dogs, and there have been minimal therapeutic advances in recent decades to improve outcomes. Naturally occurring osteosarcoma in dogs is shown to be a highly suitable model for human osteosarcoma, and limited data suggest the similarities between species extend into immune responses to cancer. Studies show that immune infiltrates in canine osteosarcoma resemble those of human osteosarcoma, and the analysis of tumor immune constituents as predictors of therapeutic response is a promising direction for future research. Additionally, clinical studies in dogs have piloted the use of NK transfer to treat osteosarcoma and can serve as valuable precursors to clinical trials in humans. Cytotoxic lymphocytes in dogs and humans with osteosarcoma have increased activation and exhaustion markers within tumors compared with blood. Accordingly, NK and T cells have complex interactions among cancer cells and other immune cells, which can lead to changes in pathways that work both for and against the tumor. Studies focused on NK and T cell interactions within the tumor microenvironment can open the door to targeted therapies, such as checkpoint inhibitors. Specifically, PD-1/PD-L1 checkpoint expression is conserved across tumors in both species, but further characterization of PD-L1 in canine osteosarcoma is needed to assess its prognostic significance compared with humans. Ultimately, a comparative understanding of T and NK cells in the osteosarcoma tumor microenvironment in both dogs and humans can be a platform for translational studies that improve outcomes in both dogs and humans with this frequently aggressive disease.

1.1.2 Introduction

Osteosarcoma (OSA) is an aggressive cancer of the skeleton in both dogs and humans with high rates of metastasis. Untreated, 90% of dogs with OSA develop metastasis within 1 year, and 85–90% of humans do so within 2 years (1). When gross metastatic disease develops, survival is dismal, and fewer than 20% of human patients survive 5 years and fewer than 5% of dogs survive 2 years with disseminated disease (2, 3). In the past few decades, there has been limited advancement of OSA therapies, and outcomes for patients with metastatic disease have remained stagnant (4, 5). Canine OSA (cOSA) occurs spontaneously and shares notable genomic profiles, clinical presentations, and progression patterns with human OSA (hOSA) (1, 6–8). The intact immune system of dogs with naturally occurring cancer along with the relatively high incidence of cOSA and extensive similarities between cOSA and hOSA make companion dogs an ideal platform for translational oncology, especially in the investigation of novel immunotherapies (9, 10). NK cells are innate immune cells with cytokine-producing and cytotoxic effector capabilities that have been identified in the OSA tumor microenvironment (TME) along with cytotoxic and helper T cells (11, 12). Both NK and CD8⁺ T cells have the capability to kill cancer cells using their cytotoxic functions, but their potential cooperation is complex. The downregulation of MHC-I by certain cancer cells effectively circumvents recognition by CD8⁺ T cells but simultaneously increases activation of NK cells by removing a major inhibitory signal (13). Additionally, IFN- γ secreted by NK cells stimulates CD4⁺ T cell activation and is required for proliferation of CD8⁺ T cell precursors (13). In many cancers, such as melanoma, gastric cancer, and myeloma, among others, secretion of IFN- γ is also shown to induce PD-L1 expression in tumor cells (14). IFN- γ -induced upregulation of PD-L1 expression on immune and tumor target cells is recognized as a conserved mechanism of adaptive immune resistance and tolerance as a response to chronic antigen stimulation, which is observed in both cancers and chronic pathogen exposure (15–17). These cooperative antitumor properties of NK and both CD4⁺ and CD8⁺ T cells are contrasted by studies showing that NK cells kill activated T cells to protect against virus-induced immunopathology (18, 19). Even among tumor-

infiltrating T cells, tumor and immune cells expressing PD-L1 can inhibit neighboring PD-1+ T cells through the PD-1/PD-L1 axis, an immune checkpoint that cancer cells can exploit to inhibit antitumor immune responses (20). In humans, NK and T cells also show increased exhaustion markers in the solid TME, making reversal of the resulting immunosuppression a key aim of emerging immunotherapies (21). Veterinary studies also identify features of immune exhaustion in dogs with cancer (22, 23), but focused studies are needed to answer lingering questions of the consistency of these markers and how to target them. Analyses establishing the extent to which cOSA infiltrating NK and T cells are comparable to hOSA support a deeper understanding of the OSA TME and advance bench-to-bedside studies to speed the translation of novel immunotherapies. This review focuses on the recent literature characterizing NK and T cell infiltrates in OSA tumors and their prognostic significance in humans and dogs.

1.1.3 Blood vs Tumor

The TME is made up of tumor cells, healthy stromal and nonimmune cells, and immune cells, all of which are communicating in dynamic interactions that work both for and against the tumor (24). These interactions occur in the context of a systemic immune response, including immune cell activity within the peripheral circulation, which, interestingly, does not inherently parallel activity in the TME (25–29). In healthy dogs, CD4+ and CD8+ T cells comprise approximately 49 and 22% of lymphocytes, respectively, in peripheral blood, and T regulatory cells (Tregs) account for 4.5% of CD4+ T cells (25). Walter et al. (12) looked at peripheral immune responses in dogs prior to and following chemotherapy and found that dogs with osteosarcoma have fewer pretreatment CD4+ and CD8+ T cells in the blood than healthy dogs. Canine Tregs have also been identified and found to be higher in blood from dogs with OSA compared with healthy dogs (25, 30, 31). Later, the same working group established the clinical relevance of circulating lymphocytes in cOSA. For example, Sottnik et al. (32) observed that dogs with lower monocyte counts and lymphopenia prior to treatment with amputation and adjuvant chemotherapy had an

increased disease-free interval (DFI). The authors call attention to the fact that this contrasts with human studies in which lymphopenia is associated with worse outcomes in sarcomas and other cancers (33). However, recent hOSA studies largely focus on lymphocytes in the context of other blood parameters, such as high neutrophil-to-lymphocyte ratios (NLRs) or low lymphocyte-to-monocyte ratios (LMRs), which are both associated with poor prognosis (34, 35). The necessity of lymphocyte ratios could be explained by the importance of other immune cell populations and the conflicting functions of different lymphocyte subsets, such as Tregs. For example, Biller et al. (25) analyzed CD4+ T, CD8+ T, and Treg (defined as CD4+FOXP3+) cells by flow cytometry in cOSA and found that low circulating CD8/Treg ratios were associated with shorter survival time. Investigation of NLR and LMR within cOSA are needed for an accurate comparison of the prognostic significance of circulating lymphocytes in dogs. Although circulating CD8/Treg ratios were associated with a significantly worse prognosis, this was not seen in cOSA tumorinfiltrating lymphocytes (TIL), an indication of the differing immune populations between blood and tumors (25). This discordance is further substantiated with evidence from the same study that Tregs are highest in cOSA tumors, making up 21% of lymphocytes in the TME, compared with Tregs in the lymph nodes and circulation (25). The pattern stays consistent in mouse and human OSA, where, compared with blood, tumors have a higher concentration of Tregs as well as more activated Tregs based on cellular proliferation and increased expression of activation markers (26). The similarities extend to other immune cell subsets. A recent comparative study by Judge et al. (27) observed that proportions of T and NK cells (using CD3, CD8, and NKG2D by PCR as readouts) were significantly higher in peripheral blood compared with the TME in both cOSA and human sarcomas. The authors also found that, though tumors have low infiltration of lymphocytes, activation and exhaustion markers of infiltrating CD8+ T and NK cells are higher than those found in circulation (28). In another study, CD3+ T cells in hOSA similarly had significantly higher expression of exhaustion markers than those in peripheral blood (29). Based on the current literature, both human and dog OSA tumors

contain CD3⁺ T, CD8⁺ T, and NK cells, and the activation and exhaustion of these immune cell subsets varies significantly between the tumor and circulation. The immune landscape of both the TME and peripheral circulation is important in identifying novel immunotherapies and patients most likely to respond to them (36). However, immunotherapies targeting immune cells in the TME, such as PD-1/PD-L1 inhibitors, have the added benefit of eliciting targeted antitumor responses, sometimes with minimal side effects (37). As a critical window into the mechanism of immune cell and solid tumor interaction, summarized in Figure 1, the remainder of this review focuses on the OSA TME specifically and characteristics of infiltrating T and NK cells.

1.1.4 T cells

Recent evaluation of cOSA tumors from our group using immunohistochemistry (IHC) confirmed minimal CD3 infiltration compared with normal lymph nodes (27). There was varied cOSA intratumoral CD3 and CD8 gene expression after radiotherapy (RT) plus NK transfer, which did not correlate significantly with survival, acknowledging that sample size was a limiting factor (27). However, these results suggest that an immune “cold” cOSA tumor could be transformed into a “hot” tumor with immunotherapy (27). This hypothesis stems from increasing studies of lymphocyte infiltration, or immune score, in human cancers with higher levels indicating hot tumors and those with low infiltration being cold tumors, which may be more accurate in predicting survival than the tumor-node-metastasis staging system (38). The ability to increase immune scores therapeutically is demonstrated by Modiano et al. (39), who found that the percentage of CD3⁺ T cells in cOSA jumps from 8 to 17% after fas-ligand gene therapy. The increase in TILs also correlates with survival because dogs with greater lymphocyte infiltration after treatment had longer survival times than dogs with lower infiltration (39). Similarly, in hOSA, CD8⁺ cells were observed in the majority of tumors but only made up 1% of intra-tumor cells (40). Even with low CD8⁺ staining within hOSA tumors, CD8⁺ cells were still significantly

associated with improved prognosis and also favorably predicted survival posttreatment with zoledronic acid (40). These results together provide evidence of OSA being an immunologically cold tumor that can be treated to increase immune cell activity and improve survival. On the other hand, some studies show cOSA to have varying patterns of TILs. Biller et al. (25) were among the first to evaluate tumor infiltrates of cOSA, finding that tumors were relatively highly infiltrated, made up of 19.2% CD4+ and 8.6% CD8+ T cells, but TILs were not associated with survival. The discrepancy may be due to varying techniques as this study determined percentage of cells by flow cytometric analysis of strained tumor samples rather than IHC evaluation. But Withers et al. (41) later also showed evidence of varying degrees of infiltration using IHC with CD3+ cells ranging from 4.6 to 607.6 cells/mm² in cOSA tumors. Although CD3+ infiltrates alone were not prognostic, increased infiltration of CD204+ macrophages was associated with increased DFI, leading the authors to suggest that cOSA is an immunogenic tumor (41). In a second study, Withers et al. (42) further examined heterogeneity of infiltrates by comparing infiltrates within matched primary and metastatic cOSA tumors. They reported that overall immune infiltrates of the primary tumor correlated with a patient's metastatic lesions, but importantly, they also found that CD3+ and CD204+ macrophages were significantly higher in metastatic lung lesions compared with their primary tumor (42). The range of TILs in cOSA and inconsistent associations with survival, rather than conflicting each other, may point to intra-tumoral heterogeneity within cOSA and complicate the idea of cOSA being uniformly cold. Cascio et al. (43) found cOSA to have virtually no infiltration of CD3+ and CD8+ T cells within the tumors but found both subsets in much higher concentrations in the peritumor areas. This aligns well with the definition of "altered" or "excluded" tumors, an intermediate between hot and cold, that have T cells present in tumor margins that are excluded from entering the tumor (38). The presence of distinct immune subtypes with low, intermediate, and high immune infiltrate has already been described in hOSA and is shown to affect response to immunotherapy treatments (44). Each tumor type— cold, altered, or hot—has distinct features that make them more or less

likely to respond to a specific treatment, such as checkpoint inhibitors or adoptive cell therapy (38, 44, 45). Based on the available literature, cOSA recapitulates the heterogeneity of immune infiltrates and distinct immune score subtypes seen in hOSA. Still, choosing therapeutics based on levels of immune infiltrates has not yet been explored expressly in cOSA, and further studies are needed to corroborate the use of immune score to predict response to treatment and survival as seen in humans.

1.1.5 Checkpoint Inhibitors

Although beyond the scope of this review and reviewed in detail elsewhere (46, 47), an understanding of the PD-1/PDL1 pathway is critical to understanding the interactions of T cells with tumor cells as well as other immune cells. PD-L1 is frequently upregulated on tumor cells, and its interaction with PD-1 on immune cells induces tumor tolerance and allows for immune evasion (46). PD-L1 is also found to be expressed on T cells in mouse models with PD-1+ T cells exhibiting multiform interactions that lead to protumor effects (20). Both anticancer PD-1 and PD-L1 therapeutic antibodies have been developed and proven to possess antitumor activity in dogs with cancer (48, 49). The first study to look at PD-L1 in cOSA did not find expression in samples using IHC, although the study only had three cOSA samples (50). Subsequent studies have found that the majority or all cOSA samples evaluated by IHC express PDL1 (51, 52). PD-L1 expression in cOSA tumors was likewise consistently found by Cascio et al. (43), whose results show that expression of PD-L1 is associated with resistance to T cell infiltration from the peri-tumor environment to within the tumor, but the study did not evaluate prognostic significance. Although the expression of PD-L1 varies in hOSA, it is consistently associated with TILs. Studies found that PD-L1 is expressed in up to 25% of hOSA tumors and correlates with increased infiltration of PD-1+, CD3+, and CD56+ cells; however, there is no significant correlation to survival (53). A later study found that more than 43% of hOSA harbor PDL1+ tumor cells with positive correlations to TILs (54). Similar to overall levels of immune

infiltration in OSA, the impact of PD-L1 expression in hOSA is conflicting because PD-L1 expression is associated with a negative prognosis secondary to immune dysfunction and also better event-free survival and overall survival because of greater density of TILs and other immune cells (54). Additionally, an increase in PD-L1-expressing tumor-infiltrating immune cells is significantly associated with response to humanized anti-PD-L1 antibody (55), though the specific indications of these biomarkers for response to treatment varies within different cancer types (56). Consequently, further characterization of PD-L1 expressing cells in cOSA is needed for accurate comparison to human studies and investigation of cOSA's sensitivity to PD-1/PD-L1 blockade.

1.1.6 NK cells

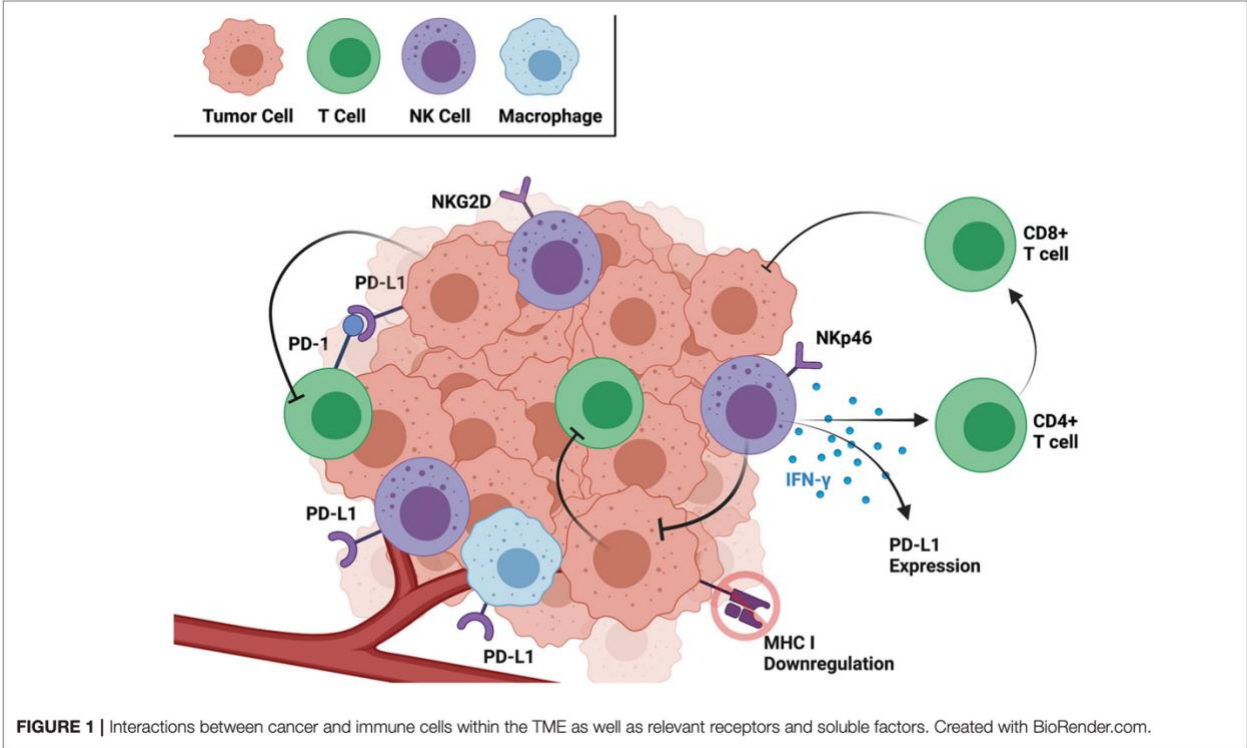
Even in scenarios in which T cells are present in the TME, cancer cells can suppress MHC-I expression, which is necessary for CD8+ T cells to recognize a target and enact their cytotoxic functions. NK cells, on the other hand, recognize “missingself ” or the lack of MHC-I molecules and can exert their cytotoxic functions in situations in which CD8+ T cells cannot, forming a basis of reasoning for their use in immunotherapies (13). This is seen specifically in hOSA, in which the majority of tumors showed diminished expression of MHC-I, and its downregulation is associated with a worse prognosis (57). NK cells are proven to be capable of lysing hOSA cells (58), and adoptive transfer of NK cells serves as a mechanism to increase the numbers of cytotoxic cells capable of targeting OSA cells in vivo. Canine and human NKp46+ NK cells show impressive similarities in expression of natural cytotoxicity receptors and secretion of factors, such as IFN- γ and TNF- α (59). In addition, NKp46+ is not expressed uniformly across NK cells, and its absence correlates with decreased cytotoxicity across species (59). The similarities in both NK cells and OSA in general make dogs an ideal candidate for comparative studies of NK cell infiltrates in OSA. Mouse models of osteomyelitis with concurrent OSA were early implications of the role of innate immune cells, including NK cells, in the OSA antitumor

response (60). Through NK cell depletion, NK cells were found to be critical in OSA tumor growth inhibition (60). One mechanism by which tumors continue to grow in the presence of NK cells may be through overexpression of TGF- β , a potent inhibitor of NK cells. Canine OSA tumors consistently stain positive for TGF β RI and TGF β RII (61), providing a rationale for the expansion and transfer of expanded and TGF- β -imprinted NK cells in cOSA therapy (62, 63). Imprinting of NK cells involves prolonged coculture with IL-2 and TGF- β to produce NK cells that are desensitized to the inhibitory effects of TGF- β and thereby capable of prolonged hyperfunctionality with increased cytotoxicity, cytokine production, and longevity. This approach has the potential for novel use in NK immunotherapies (63). In their phase I trial using hypofractionated RT and autologous intratumoral NK cell transfer in dogs with naturally occurring OSA, Canter et al. (64) demonstrate increased progression-free survival in dogs with OSA compared with historical controls. The same group collected tumor specimens from patients in this first-in-dog clinical trial and found that pre- to post-treatment immune-related gene transcript changes varied considerably between dogs (27). NK gene transcripts have significantly less expression of both CD3+ and CD8+ cells in untreated cOSA tumor samples, but there were no patterns of expression that significantly correlated with survival at six months posttreatment in paired samples (27). Intra-tumoral changes in expression of IL-6, a gene linked to cytotoxic lymphocytes, was higher in dogs with prolonged survival though statistical significance may have been limited by the sample size (27). Future clinical trials with increased sample sizes are needed to better evaluate the prognostic value of cOSA tumor-infiltrating NK cells and the therapeutic benefit of NK cell immunotherapy. It should be noted that the full characterization of canine NK cells and their surface markers is still in progress compared with human NK cells and could provide critical information in their use for NK immunotherapies (65). The use of NK cell transfer has not been explored extensively in hOSA, likely due to limiting factors in the sourcing and expansion of NK cells (66, 67), but early successes seen in cOSA can potentially drive translation of NK immunotherapy to clinical trials in humans.

1.1.7 Conclusion

Osteosarcoma is an aggressive disease for which novel therapeutics are needed, and dogs with spontaneously occurring cancer are a useful model for hOSA studies. Both cOSA and hOSA share extensive similarities, including the frequency and phenotype of immune cells within the TME and peripheral circulation. The OSA TME constitutes a complex web of interactions, especially among NK and T cells, that can be targeted with immunotherapies. OSA tumors in both humans and dogs fall on a spectrum of immune infiltrate levels that correlate with prognosis, express PD-L1 with association to increased TILs, and show sensitivity to NK cell cytotoxicity. The parallels between cOSA and hOSA can be best put to use after filling the gaps in current knowledge regarding the characterization of the cOSA TME and immunotherapies to target it. Future studies in cOSA are needed to characterize NK cells and the expression of PD-1/PD-L1 in TILs as well as to validate the use of immune infiltrates to predict immune response to therapeutics. Increased understanding of intra-tumoral NK and T cells will influence clinical applications of TIL-targeting treatments in both dogs and humans, ultimately leading to better outcomes for patients with OSA.

1.1.8 Figures



1.1.9 References

1. Fenger JM, London CA, Kisseberth WC. Canine osteosarcoma: a naturally occurring disease to inform pediatric oncology. *ILAR J.* (2014) 55:69– 85. doi: 10.1093/ilar/ilu009
2. Durfee RA, Mohammed M, Luu HH. Review of osteosarcoma and current management. *Rheumatol Ther.* (2016) 3:221– 43. doi: 10.1007/s40744-016-0046-y
3. Boston SE, Ehrhart NP, Dernell WS, Lafferty M, Withrow SJ. Evaluation of survival time in dogs with stage III osteosarcoma that undergo treatment: 90 cases (1985-2004). *J Am Vet Med Assoc.* (2006) 228:1905– 8. doi: 10.2460/javma.228.12.1905
4. Mirabello L, Troisi RJ, Savage SA. Osteosarcoma incidence and survival rates from 1973 to 2004: data from the Surveillance, Epidemiology, and End Results Program. *Cancer.* (2009) 115:1531–43. doi: 10.1002/cncr.24121
5. Harrison DJ, Geller DS, Gill JD, Lewis VO, Gorlick R. Current and future therapeutic approaches for osteosarcoma. *Expert Rev Anticancer Ther.* (2018) 18:39–50. doi: 10.1080/14737140.2018.1413939
6. Simpson S, Dunning MD, de Brot S, Grau-Roma L, Mongan NP, Rutland CS. Comparative review of human and canine osteosarcoma: morphology, epidemiology, prognosis, treatment and genetics. *Acta Vet Scand.* (2017) 59:71. doi: 10.1186/s13028-017-0341-9
7. Gardner HL, Sivaprakasam K, Briones N, Zismann V, Perdigonos N, Drenner K, et al. Canine osteosarcoma genome sequencing identifies recurrent mutations in DMD and the histone methyltransferase gene SETD2. *Commun Biol.* (2019) 2:266. doi: 10.1038/s42003-019-0487-2
8. Scott MC, Temiz NA, Sarver AE, LaRue RS, Rathe SK, Varshney J, et al. Comparative transcriptome analysis quantifies immune cell transcript levels, metastatic progression, and survival in osteosarcoma. *Cancer Res.* (2018) 78:326–37. doi: 10.1158/0008-5472.CAN-17-0576
9. Castillo-Tandazo W, Mutsaers AJ, Walkley CR. Osteosarcoma in the post genome era: preclinical models and approaches to identify tractable therapeutic targets. *Curr Osteoporos Rep.* (2019) 17:343–52. doi: 10.1007/s11914-019-00534-w

10. Tarone L, Barutello G, Iussich S, Giacobino D, Quaglino E, Buracco P, et al. Naturally occurring cancers in pet dogs as pre-clinical models for cancer immunotherapy. *Cancer Immunol Immunother.* (2019) 68:1839– 53. doi: 10.1007/s00262-019-02360-6
11. Mason NJ. Comparative immunology and immunotherapy of canine osteosarcoma. *Adv Exp Med Biol.* (2020) 1258:199– 221. doi: 10.1007/978-3-030-43085-6_14
12. Walter CU, Biller BJ, Lana SE, Bachand AM, Dow SW. Effects of chemotherapy on immune responses in dogs with cancer. *J Vet Intern Med.* (2006) 20:342–7. doi: 10.1111/j.1939-1676.2006.tb02866.x
13. Myers JA, Miller JS. Exploring the NK cell platform for cancer immunotherapy. *Nat Rev Clin Oncol.* (2020) 18:85– 100. doi: 10.1038/s41571-020-0426-7
14. Shi Y. Regulatory mechanisms of PD-L1 expression in cancer cells. *Cancer Immunol Immunother.* (2018) 67:1481–9. doi: 10.1007/s00262-018-2226-9
15. Loke P, Allison JP. PD-L1 and PD-L2 are differentially regulated by Th1 and Th2 cells. *Proc Natl Acad Sci U S A.* (2003) 100:5336– 41. doi: 10.1073/pnas.0931259100
16. Garcia-Diaz A, Shin DS, Moreno BH, Saco J, Escuin-Ordinas H, Rodriguez GA, et al. Interferon receptor signaling pathways regulating PD-L1 and PD-L2 expression. *Cell Rep.* (2017) 19:1189–201. doi: 10.1016/j.celrep.2017.04.031
17. Lee SJ, Jang BC, Lee SW, Yang YI, Suh SI, Park YM, et al. Interferon regulatory factor-1 is prerequisite to the constitutive expression and IFN γ -induced upregulation of B7-H1 (CD274). *FEBS Lett.* (2006) 580:755– 62. doi: 10.1016/j.febslet.2005.12.093
18. Lee SH, Kim KS, Fodil-Cornu N, Vidal SM, Biron CA. Activating receptors promote NK cell expansion for maintenance, IL-10 production, and CD8 T cell regulation during viral infection. *J Exp Med.* (2009) 206:2235– 51. doi: 10.1084/jem.20082387
19. Waggoner SN, Cornberg M, Selin LK, Welsh RM. Natural killer cells act as rheostats modulating antiviral T cells. *Nature.* (2011) 481:394– 8. doi: 10.1038/nature10624

20. Diskin B, Adam S, Cassini MF, Sanchez G, Liria M, Aykut B, et al. PD-L1 engagement on T cells promotes self-tolerance and suppression of neighboring macrophages and effector T cells in cancer. *Nat Immunol.* (2020) 21:442–54. doi: 10.1038/s41590-020-0620-x
21. Balta E, Wabnitz GH, Samstag Y. Hijacked immune cells in the tumor microenvironment: molecular mechanisms of immunosuppression and cues to improve T cell-based immunotherapy of solid tumors. *Int J Mol Sci.* (2021) 22:5736. doi: 10.3390/ijms22115736
22. Lee SH, Shin DJ, Kim Y, Kim CJ, Lee JJ, Yoon MS, et al. Comparison of phenotypic and functional characteristics between canine non-B, non-T natural killer lymphocytes and CD3. *Front Immunol.* (2018) 9:841. doi: 10.3389/fimmu.2018.00841
23. Bujak JK, Pingwara R, Nelson MH, Majchrzak K. Adoptive cell transfer: new perspective treatment in veterinary oncology. *Acta Vet Scand.* (2018) 60:60. doi: 10.1186/s13028-018-0414-4
24. Giraldo NA, Sanchez-Salas R, Peske JD, Vano Y, Becht E, Petitprez F, et al. The clinical role of the TME in solid cancer. *Br J Cancer.* (2019) 120:45– 53. doi: 10.1038/s41416-018-0327-z
25. Biller BJ, Guth A, Burton JH, Dow SW. Decreased ratio of CD8+ T cells to regulatory T cells associated with decreased survival in dogs with osteosarcoma. *J Vet Intern Med.* (2010) 24:1118–23. doi: 10.1111/j.1939-1676.2010.0557.x
26. Qin FX. Dynamic behavior and function of Foxp3+ regulatory T cells in tumor bearing host. *Cell Mol Immunol.* (2009) 6:3–13. doi: 10.1038/cmi.2009.2
27. Judge SJ, Yanagisawa M, Sturgill IR, Bateni SB, Gingrich AA, Foltz JA, et al. Blood and tissue biomarker analysis in dogs with osteosarcoma treated with palliative radiation and intratumoral autologous natural killer cell transfer. *PLoS One.* (2020) 15:e0224775. doi: 10.1371/journal.pone.0224775
28. Judge SJ, Darrow MA, Thorpe SW, Gingrich AA, O'Donnell EF, Bellini AR, et al. Analysis of tumor-infiltrating NK and T cells highlights IL15 stimulation and TIGIT blockade as a

- combination immunotherapy strategy for soft tissue sarcomas. *J Immunother Cancer*. (2020) 8:e001355. doi: 10.1136/jitc-2020-001355
29. Han Q, Shi H, Liu F. CD163(+) M2-type tumor-associated macrophage support the suppression of tumor-infiltrating T cells in osteosarcoma. *Int Immunopharmacol*. (2016) 34:101–6. doi: 10.1016/j.intimp.2016.01.023
30. Biller BJ, Elmslie RE, Burnett RC, Avery AC, Dow SW. Use of FoxP3 expression to identify regulatory T cells in healthy dogs and dogs with cancer. *Vet Immunol Immunopathol*. (2007) 116:69–78. doi: 10.1016/j.vetimm.2006.12.002
31. O’Neill K, Guth A, Biller B, Elmslie R, Dow S. Changes in regulatory T cells in dogs with cancer and associations with tumor type. *J Vet Intern Med*. (2009) 23:875–81. doi: 10.1111/j.1939-1676.2009.03333.x
32. Sottnik JL, Rao S, Lafferty MH, Thamm DH, Morley PS, Withrow SJ, et al. Association of blood monocyte and lymphocyte count and disease-free interval in dogs with osteosarcoma. *J Vet Intern Med*. (2010) 24:1439–44. doi: 10.1111/j.1939-1676.2010.0591.x
33. Ray-Coquard I, Cropet C, Van Glabbeke M, Sebban C, Le Cesne A, Judson I, et al. Lymphopenia as a prognostic factor for overall survival in advanced carcinomas, sarcomas, and lymphomas. *Cancer Res*. (2009) 69:5383–91. doi: 10.1158/0008-5472.CAN-08-3845
34. Liu B, Huang Y, Sun Y, Zhang J, Yao Y, Shen Z, et al. Prognostic value of inflammation-based scores in patients with osteosarcoma. *Sci Rep*. (2016) 6:39862. doi: 10.1038/srep39862
35. Liu T, Fang XC, Ding Z, Sun ZG, Sun LM, Wang YL. Pre-operative lymphocyte-to-monocyte ratio as a predictor of overall survival in patients suffering from osteosarcoma. *FEBS Open Bio*. (2015) 5:682–7. doi: 10.1016/j.fob.2015.08.002
36. Gnjatic S, Bronte V, Brunet LR, Butler MO, Disis ML, Galon J, et al. Identifying baseline immune-related biomarkers to predict clinical outcome of immunotherapy. *J Immunother Cancer*. (2017) 5:44. doi: 10.1186/s40425-017-0243-4

37. Lei X, Lei Y, Li JK, Du WX, Li RG, Yang J, et al. Immune cells within the tumor microenvironment: biological functions and roles in cancer immunotherapy. *Cancer Lett.* (2020) 470:126–33. doi: 10.1016/j.canlet.2019.11.009
38. Galon J, Bruni D. Approaches to treat immune hot, altered and cold tumours with combination immunotherapies. *Nat Rev Drug Discov.* (2019) 18:197– 218. doi: 10.1038/s41573-018-0007-y
39. Modiano JF, Bellgrau D, Cutter GR, Lana SE, Ehrhart NP, Ehrhart E, et al. Inflammation, apoptosis, and necrosis induced by neoadjuvant fas ligand gene therapy improves survival of dogs with spontaneous bone cancer. *Mol Ther.* (2012) 20:2234–43. doi: 10.1038/mt.2012.149
40. Gomez-Brouchet A, Illac C, Gilhodes J, Bouvier C, Aubert S, Guinebretiere JM, et al. CD163-positive tumor-associated macrophages and CD8-positive cytotoxic lymphocytes are powerful diagnostic markers for the therapeutic stratification of osteosarcoma patients: an immunohistochemical analysis of the biopsies from the French OS2006 phase 3 trial. *Oncoimmunology.* (2017) 6:e1331193. doi: 10.1080/2162402X.2017.1331193
41. Withers SS, Skorupski KA, York D, Choi JW, Woolard KD, Laufer Amorim R, et al. Association of macrophage and lymphocyte infiltration with outcome in canine osteosarcoma. *Vet Comp Oncol.* (2019) 17:49– 60. doi: 10.1111/vco.12444
42. Withers SS, York D, Choi JW, Woolard KD, Laufer-Amorim R, Sparger EE, et al. Metastatic immune infiltrates correlate with those of the primary tumour in canine osteosarcoma. *Vet Comp Oncol.* (2019) 17:242– 52. doi: 10.1111/vco.12459
43. Cascio MJ, Whitley EM, Sahay B, Cortes-Hinojosa G, Chang LJ, Cowart J, et al. Canine osteosarcoma checkpoint expression correlates with metastasis and T-cell infiltrate. *Vet Immunol Immunopathol.* (2021) 232:110169. doi: 10.1016/j.vetimm.2020.110169
44. Wu CC, Beird HC, Andrew Livingston J, Advani S, Mitra A, Cao S, et al. Immuno-genomic landscape of osteosarcoma. *Nat Commun.* (2020) 11:1008. doi: 10.1038/s41467-020-14646-w

45. Song YJ, Xu Y, Deng C, Zhu X, Fu J, Chen H, et al. Gene expression classifier reveals prognostic osteosarcoma microenvironment molecular subtypes. *Front Immunol.* (2021) 12:623762. doi: 10.3389/fimmu.2021.623762
46. Han Y, Liu D, Li L. PD-1/PD-L1 pathway: current researches in cancer. *Am J Cancer Res.* (2020) 10:727–42.
47. Thanindrarn P, Dean DC, Nelson SD, Hornicek FJ, Duan Z. Advances in immune checkpoint inhibitors for bone sarcoma therapy. *J Bone Oncol.* (2019) 15:100221. doi: 10.1016/j.jbo.2019.100221
48. Maekawa N, Konnai S, Takagi S, Kagawa Y, Okagawa T, Nishimori A, et al. A canine chimeric monoclonal antibody targeting PD-L1 and its clinical efficacy in canine oral malignant melanoma or undifferentiated sarcoma. *Sci Rep.* (2017) 7:8951. doi: 10.1038/s41598-017-09444-2
49. Igase M, Nemoto Y, Itamoto K, Tani K, Nakaichi M, Sakurai M, et al. A pilot clinical study of the therapeutic antibody against canine PD-1 for advanced spontaneous cancers in dogs. *Sci Rep.* (2020) 10:18311. doi: 10.1038/s41598-020-75533-4
50. Shosu K, Sakurai M, Inoue K, Nakagawa T, Sakai H, Morimoto M, et al. Programmed cell death ligand 1 expression in canine cancer. *In Vivo.* (2016) 30:195–204. Available online at: <https://iv.iiarjournals.org/content/invivo/30/3/195.full.pdf>
51. Takeuchi H, Konnai S, Maekawa N, Minato E, Ichikawa Y, Kobayashi A, et al. Expression analysis of canine CMTM6 and CMTM4 as potential regulators of the PD-L1 protein in canine cancers. *Front Vet Sci.* (2020) 7:330. doi: 10.3389/fvets.2020.00330

1.2 Improved characterization of NK cells for canine immunotherapy

1.2.1 Abstract

The field of cancer immunology has seen a meteoric rise in interest and application due to the discovery of immunotherapies that target immune cells, often leading to dramatic anti-tumor effects. However, successful cellular immunotherapy for solid tumors remains a challenge, and the application of immunotherapy to dogs with naturally occurring cancers has emerged as a high yield large animal model to bridge the bench-to-bedside challenges of immunotherapies, including those based on natural killer (NK) cells. Here, we review recent developments in the characterization and understanding of canine NK cells, a critical springboard for future translational NK immunotherapy research. The characterization of canine NK cells is exceptionally pertinent given the ongoing challenges in defining them and contextualizing their similarities and differences compared to human and murine NK cells compounded by the limited availability of validated canine specific reagents. Additionally, we summarize the current landscape of the clinical and translational literature employing strategies to capitalize on endogenous and exogenous NK cell immunotherapy in canine cancer patients. The insights regarding efficacy and immune correlates from these trials provide a solid foundation to design and test novel combinational therapies to enhance NK cell activity with the added benefit of motivating comparative work to translate these findings to human cancers with extensive similarities to their canine counterparts. The compilation of knowledge from basic canine NK phenotype and function to applications in first-in-dog clinical trials will support the canine cancer model and enhance translational work to improve cancer outcomes for both dogs and humans.

1.2.2 Introduction

The advent of immunotherapy has propelled the field of oncology beyond the standard therapies of surgery, radiation, and chemotherapy. While the vast majority of successful immunotherapy

methods to date have been T-cell based, such as PD-1/PD-L1 inhibition and CAR-T cells, such strategies are not universally successful in all patients. Thus, researchers have broadened their focus to harness and manipulate other immune cell types. Of these, natural killer (NK) cells have emerged as an attractive candidate given their innate cytotoxicity against a diverse array of targets and their potent cytokine production. NK cells are considered sentinels of the innate immune system, capable of identifying and killing virusinfected and cancer-transformed cells via mechanisms that do not require antigen-specific recognition. NK cells have been a focus of potential therapy for decades, since initial trials by Rosenberg et al. in the 1980s, among others (1–3). However, severe toxicity was seen in early attempts, largely due to amplified cytotoxic lymphocyte responses and the concomitant use of high-dose IL-2 to support adoptive transfer of these cells into patients. These findings emphasized the need to minimize such responses while still harnessing NK cells' anti-tumor effects. Companion canines have emerged as a useful model for studying novel cancer therapies given that dogs are a large, outbred species which develop spontaneous cancers in the setting of an intact immune system. To study NK cells in particular, the canine model is invaluable since the complex interplay between neoplasia development and a functional immune system can be evaluated. Here, we review recent canine immunotherapy trials which directly or indirectly act via NK cells while also summarizing the progress made and hurdles which still exist to advance canine NK immunotherapies.

1.2.3 Identification and characterization of canine NK cells

Populations of innate lymphoid cells (ILCs) have been extensively studied in humans and mice for decades. By comparison, canine ILCs are less defined, although recent studies have sought to advance our understanding (4). The identification and clarification of the canine NK cell populations based on surface markers has been a longstanding effort (5–8). Early work established that they are CD4-/CD20-, as these are the canine T and B cell markers, respectively (9). A detailed review regarding the evolution of the collective understanding of

canine NK cell identification was published by Gingrich et al. (10). To summarize, many early efforts focused on phenotypic identification of canine NK cells using surface markers, as such markers differ from those in humans and mice (10). Huang et al. were the first to describe canine NK cells using the surface density of the CD5 marker, a member of the scavenger receptor cysteine-rich superfamily and typically classified as a T cell marker (11). This study noted important differences in lymphoid phenotype based on CD5 density, as cells with CD5dim expression were larger, contained more cytoplasmic granules, and demonstrated antigen-independent cytotoxicity, especially in the setting of IL-2 enrichment (11). Further studies by Shin et al. continued to focus on the density of the CD5 receptor as an NK marker, particularly contrasting CD3+CD5dimCD21- with CD3+CD5-CD21- cells (12). Following expansion and co-culture with K562 feeder cells and cytokines for 21 days, CD5dim expressing cells did not express TCR $\alpha\beta$ nor TCR $\gamma\delta$ (12). Additionally, CD3+CD5dimCD21- cells exhibited significantly higher IFN- γ cytokine production compared to CD3+CD5-CD21- (12). Based on these findings, the authors proposed that each population represents canine NK cells at different levels of maturation (12), although the stages of canine NK cell maturation and development remain a poorly understood topic in contrast to key discoveries in mouse and human studies (13–15). The “pan-mammalian” NK cell receptor, NCR1/NKp46, has also been identified as a marker of canine NK cells (10). Studies by Grondahl-Rosado et al. noted that CD3-NCR1+ cells comprised 2.5% of canine PBMCs, a proportion much lower than NK cells seen in other mammals (6, 7). Foltz et al. developed a novel antibody to canine NKp46 for use in flow cytometry (5). Their work also identified a CD3-NKp46+ NK subset, representing approximately 2–3% of PBMCs (5). These cells were found to be highly cytotoxic against multiple canine cancer lines. Using a novel expansion technique, the authors also identified a population of CD3+TCR+NKp46+ cells (5). The CD3 positivity in canine NK cells was postulated to represent a different stage of maturation, although a conclusive trajectory has not been described to date (5, 10). More recently, Grudzien et al. established a canine NK cell line (CNK-89) derived from a

dog with NK cell neoplasia (16). This cell line is CD5+CD8+CD45+CD56+CD79a+NKp46+.

Although CD79a is classically a B cell marker, the presence of the NKp46 protein and mRNA expression of NKG2D, NKp30, NKp44, NKp46 and perforin suggested NK cell properties for this cell line. Following treatment with IL-12, IL-15, IL-18 and IL-21, increased expression of granzyme B, perforin and CD16 was observed (16). Secretion of TNF α and IFN γ was also noted. These findings were not observed following treatment with IL-2, suggesting these neoplastic-derived cells are an IL-2 independent cell line and potentially useful for studying alternate pathways of canine NK cell activation (16). Gingrich et al. detailed differential gene expression analyses of the two most widely accepted canine NK cell populations: CD3-CD5dim and CD3-NKp46+ cells (17). Marked differences were seen in steady-state cells, including non-detectable mRNA expression of granzyme B, perforin, IFN γ and KLRD1/CD94 in CD3-CD5dim cells, but detectable expression in CD3+NKp46+ cells (17). Remarkably, following co-culture with irradiated human feeder cells [K562cl9, (18)], the two cell populations converged on a nearly identical mRNA expression phenotype (17). The findings suggested each population likely contains NK cells that are selected for rapid and dominant growth under stimulatory co-culture conditions. The authors then conducted single-cell RNA sequencing of FACSsorted CD3-CD5dim and CD3-NKp46+ cells to explore overlap between the two populations. In these studies, at steady-state the CD3-CD5dim population was found to be more heterogeneous than the CD3-NKp46+ one. Gene expression driving the variance for CD5dim cells was predominantly non-NKC gene expression, reinforcing that CD5dim appears to be a less specific marker. Further single-cell studies following the activation of the two cell populations in co-culture demonstrated a conserved trajectory to activation based on uniform, discrete changes in gene expression in canonical NK transcription factors as well as marked changes in expression of granzyme A, IL2RB, and KLRB1. These data described the transition in both CD3-CD5dim and CD3-NKp46- canine NK cells from a resting state to an activated state which may lend insight to the stages of NK cell maturation in dogs, a physiologic process which has yet to

be clearly elucidated. Overall, the precise identification of canine NK cell populations remains elusive, likely in part due to a lack of understanding of the maturation process as well as variable gene expression and protein surface markers associated with different stages of development. However, based on the studies above, populations of innate, canine lymphocytes capable of cytokine-dependent, antigen-independent cytotoxicity have been demonstrated to exist, paving the way for clinical applications of NK-based immunotherapies in dogs.

1.2.4 NK cells in canine immunotherapy

Ultimately, immunotherapy needs to be tested in immunocompetent hosts. This underscores a strength of the dog model, especially when novel immunotherapies are combined with serial immune correlates (19). The investigation of immune populations before, during, and following immunotherapy can not only provide insight to the presence or absence of clinical benefit in the relevant study but can also be hypothesis generating in the pursuit of improving efficacy.

Additionally, immune correlates can bring to light potential biomarkers of response, leading to improved selection of dogs that are likely to respond to treatment and the identification of canine patient subsets that require innovative interventions. A concerted effort to combine the lessons learned from canine clinical trials performed or in progress is essential to the future of the field. To date, several canine immunotherapy trials have been completed with either direct or indirect effects on putative NK cell populations. Trials have used adoptive cell therapy, cytokine therapy, virus-based therapy, radio- and chemo-immunotherapy, and checkpoint blockade to treat dogs with spontaneous cancers with various methods of NK cell identification and analysis (Figure 1 and Table 1). Our group has completed several first-in-dog trials using adoptive NK cell transfer to treat dogs with spontaneous cancers. In 2017, we treated dogs with unresectable limb osteosarcoma (OSA) using palliative radiotherapy (RT) and two intratumor injections of autologous NK cells (20). NK cells were expanded from CD5-depleted PBMCs over a 14day co-culture with irradiated K562-C9-mIL21 feeder cells and 100IU/mL recombinant human IL-2 (21).

We observed a significant increase in CD45+GZMB+ cells in PBMCs post-treatment by flow cytometry suggesting systemic immune effects of the treatment, although there did not appear to be an association between survival and frequency of GZMB+ or IFN γ + cells in peripheral blood (30). Given the intra-tumor route of administration, we also analyzed tumor biopsies by flow cytometry and observed that approximately 50% of intratumor CD45+ cells stained positive for an intracellular dye label consistent with persistence of the adoptively transferred NK cells for one-week post-transfer in the tumor microenvironment (TME) (20). We analyzed tumor tissue by qPCR and showed gene expression varied greatly by patient, with no difference in fold change gene expression between dogs that were alive or dead at 6months (30). Though, it is interesting to note that the longest surviving dog, 18months, showed the greatest fold-change in the expression of CD3, CD8, and IDO1 genes following RT and intratumor NK transfer (30). Immunotherapies can also stimulate endogenous NK cells through cytokines that are responsible for the activation, migration, and expansion of NK cells in vivo. Our group also completed a first-in-dog dose escalation trial in dogs with pulmonary metastatic melanoma and osteosarcoma using inhaled recombinant human IL-15 to stimulate NK cells in the lung at metastasis sites (31). Seven of the initial enrollees were also analyzed in a preliminary assessment of peripheral NK cells using flow cytometry and RNA sequencing (17, 22). The proportion of total NK cells and NK cells expressing Ki67 increased during inhaled IL-15 treatment and had a significant increase in Granzyme B fold change (22). Conversely, there was evidence of upregulation of TIGIT gene expression, an inhibitory marker, at both day 7 and 14 post enrollment (22). The increase in both Granzyme B and TIGIT suggests concurrent stimulation of activating and inhibitory pathways, the balance of which potentially determines response to treatment. RNA sequencing of patient PBMCs offers preliminary evidence that the activating/inhibitory balance may be patient specific, since principal component analysis (PCA) variance was driven largely by two dogs that responded to treatment (17). At the completion of trial, among 21 dogs total, we observed a 39% clinical benefit rate (31). Cytotoxicity of patient

PBMCs against osteosarcoma (OSA) and melanoma (M5) targets significantly increased from pre- to post-therapy and maximal cytotoxicity was significantly correlated with patient survival (31). The finding of increased peripheral blood cytotoxicity across the entire cohort post-treatment suggests that tumor cell death is occurring, but only leading to improved survival in certain patients. There are many immunotherapies that are not traditionally NK-targeting or are non-specific in nature, which still result in NK activation, making them attractive candidates for multimodal treatments (23, 32). For instance, oncolytic viruses are a unique type of immunotherapy in that their primary function is to invade and replicate within cancer cells, leading to lysis, but it was soon recognized that this process also increases the immunogenicity of cancer cells, leading to the recruitment of and elimination by immune cells. This is a similar mechanism through which viruses, like cowpea mosaic virus, are used as therapy to bind non-specific receptors and stimulate the induction of an immune response in the TME. Martín-Carrasco et al. tested an intratumor oncolytic virus based on canine wild-type adenovirus which was engineered to selectively replicate in mutated cells to treat canine patients with cancer (24). The strength of the study was the availability of serial sample collections from patients before and up to one year after treatment. At least four of the eight patients had an increase in peripheral NK cells within the first month after treatment as assessed by flow cytometry (24). However, CD56 was used as the identifying marker, which is not known to be expressed on canine NK cells, highlighting the importance of validating both the reagents used as well as the underlying biology given the extensive cross-species differences in NK cells. In another trial, the authors treated canine oligodendroglioma and astrocytoma using intratumor injections of M032, a genetically modified herpes simplex virus. The authors observed enrichment of tumor mRNA gene signatures associated with NK cells in four of six patients with available specimens (25). In this study, NK cell gene signatures were labeled as belonging to “NK CD56dim cells” and assessed by the NanoString Technologies gene expression panel (25). The classification of NK cells as CD56dim by this method is described as based on expression of IL21R in an evaluation

of nearly 10,000 samples from The Cancer Genome Atlas (TCGA) (26). So, while CD56 or CD56dim are not validated as canine NK markers, IL21R is thought to be expressed on canine NK cells and capable of being activated by its respective IL-21 ligand. The same immune profiling method was used to investigate the abundance of NK cells in the TME of dogs with canine inflammatory mammary cancer treated with intratumor delivery of immunotherapy using empty cowpea mosaic virus-like particles (eCPMV) (27), which are recognized by toll-like receptors (TLRs). They found no significant change in cells labeled as “NK CD56dim cells,” or cells enriched for IL21R, and the fold change of other genes associated with NK cells including KLRA1, KLRD1, and GZMB were increased in treated tumor tissue, but not significantly (27). Conversely, there was significant upregulation in treated versus untreated tumor tissue of IL18R1 and significant downregulation of IL12RB2, which are both implicated in NK cell functions (27), supporting the pattern across canine immunotherapies in which both activation and inhibition are observed simultaneously. Another study treated patients with canine mammary cancer using eCPMV (33). This trial gave two injections into the largest tumor followed by tumor resection. In line with findings from dogs treated with eCPMV alone, NK-related genes were not differentially expressed using RNA-seq to analyze the tumors treated with neoadjuvant immunotherapy. Additionally, flow cytometry was used to define CD45+CD21-CD3-GZMB+ PBMCs as NK cells. This analysis showed insignificant changes in peripheral NK cells in response to eCPMV and surgery (33). To bypass hurdles associated with non-surgical tumors and improve systemic effects, autologous canine mesenchymal stem cells can be infected with a canine oncolytic adenovirus and administered to patients. This was performed on 27 dogs with extracranial cancer and assessed by the same group in 10 subsequent dogs with highgrade gliomas (34, 35). In the initial trial, peripheral immune cells including NK cells increased after each dose, although the changes were not statistically significant (34). In the subsequent trial, dogs with gliomas received eight weekly treatments of cellular virotherapy (35). Using CIBERSORT analysis of bulk-RNAseq on tumor tissue, they

found that NK cell fractions were not changed between responders and non-responders post-treatment (35). Together, these virus-based therapies have shown preliminary efficacy in dogs but inconsistent association with NK cell numbers and related gene signatures as biomarkers of clinical effects. Changes in NK cells are more likely to be seen in the TME rather than in peripheral blood, especially with intra-tumor immunotherapies (28). These studies also expose the real and ongoing difficulties in identifying canine NK cells, with virtually every trial using different markers. The future of canine NK immunotherapy is likely a combinatorial approach that enhances multiple anti-tumor methods. Several groups have spearheaded combination radioimmunotherapy and chemoimmunotherapy trials in dogs with spontaneous cancer with varying involvement of NK cells or related cytokines and genes (29, 36). Four dogs with advanced stage melanoma were treated with trimodal immuno-radiotherapy which included sub-ablative external beam radiation therapy (EBRT), targeted radionuclide therapy (TRT), and intratumor immunocytokine (IT-IC) (37). Numbers of NK cells in circulating blood identified by flow cytometry using CD3-CD5dim did not change significantly with treatment (37). However, RNA-seq analysis of tumor tissue from dogs before and following treatment indicated significant upregulation of KLRA1, KLRB1, NCR3 IL18R1, and TNF α at selected timepoints (37). The small sample size precludes conclusions regarding survival outcomes but may aid in contextualizing the contribution of NK cells in response to therapy. The importance of placing immune changes in the framework of progression or survival is well-illustrated in an unrelated trial which enrolled 18 dogs with B cell lymphoma that were treated with doxorubicin chemotherapy, anti-CD20 monoclonal antibody, and a small molecule inhibitor (38). Lymph node aspirates analyzed by RNA-seq demonstrated genes associated with NK function as the most significantly upregulated gene set in dogs with poor survival, but samples were obtained from only one time point limiting conclusions regarding immune changes in response to therapy (38). Serial sampling of patient lymph nodes and tracking of changes in response to treatment would help clarify the conclusions of the study and identify predictive in addition to prognostic biomarkers. Prognostic

biomarkers of response were similarly investigated in a trial treating dogs with oral malignant melanoma using checkpoint blockade (39). The Ohashi Laboratory pioneered PD-L1 antibody therapy in dogs and have completed two clinical trials to date (40–42). The mechanism of anti-PD-L1 therapy is based on the understanding that PD-L1 on tumor cells binds to PD-1 on T cells, providing an inhibitory signal that interferes with anti-tumor T cell functions. In the context of NK cells, binding of anti-PD-L1 antibody to PD-L1 expressed on NK cells can increase activation and effector function (43). Thus, the treatment has the potential to both remove T cell inhibition and enhance NK cell function. While the initial canine anti-PD-L1 trial publications did not include immune correlates of response, a follow-up investigation of serum biomarkers by the same group found that overall survival following treatment was positively correlated with low PGE2, higher IL-2, and higher IL-12 in pre-treatment sera, helping to identify COX-2 as a potential target for future trials (39). NK cells were not the primary focus of the trial, but the authors noted that PGE2 is capable of suppressing the function of NK cells and IL-12 is well-established as necessary for the release of IFN γ by NK cells, the most prominent producers of the inflammatory cytokine (39). These studies illustrate the potential for clinical trials to inform future studies, identifying dogs exhibiting high baseline PGE2 serum levels as candidates for the addition of a COX-2 inhibitor. Given the successful development of anti-canine PD-1/L1 antibodies, determining whether these and other immune checkpoints are found on canine NK cells would have a profound impact on prospective targets and combinatorial approaches. Taken together, these data provide preliminary support for future investigations into combination NK immunotherapies to holistically impart anti-tumor effects.

1.2.5 Discussion

NK immunotherapy in dogs is progressing at an escalating rate with larger sample sizes and collaboration between university hospitals and specialty centers. At the time of this publication, the American Veterinary Medical Association (AVMA) Animal Health Studies Database lists five

trials currently recruiting, and 35 trials with completed recruitment based on a search for “immunotherapy” in dogs with cancer. Studies from the University of Minnesota have demonstrated increased Antibody-Dependent Cellular Cytotoxicity (ADCC) efficacy in engineered human NK cells expressing recombinant CD64, opening the doors for the development of engineered canine NK cells that have similar effector capabilities (44). Investigators at The Ohio State University have simultaneously made progress in attempting to improve adoptive NK cell products for canine immunotherapy by imprinting NK cells with TGF- β during expansion to override potential inhibition in the TME (45). This group is using this method of TGF β -imprinted NK cell therapy combined with carboplatin chemotherapy to treat dogs with OSA in an ongoing phase I clinical trial. Our own group has sought to improve the canine NK product using the expansion of unmanipulated PBMCs from healthy donors for allogeneic adoptive NK cell transfer. These works provide the infrastructure from which canine NK cells can be manipulated to enhance persistence and efficacy in future immunotherapy trials and this multiinstitutional, rapid innovation in canine NK immunotherapy is indicative of the growing interest and recognized potential in the field. By reviewing recent trials with available NK cell correlates, we begin to elucidate an intricate framework of NK responses to treatment. Overall, there is evidence of both NK activation and inhibition in canine immunotherapy with moderate and irregular impacts on NK cell proportions which vary based on intratumor versus peripheral sampling. Timing of sampling is also highly relevant, given that NK correlation to improved response can be negative or positive based on the treatment stage, a concept that can be expected in the context of limited NK cell half-life. Resolution of the role of NK cells in canine immunotherapy requires additional trials with intra-tumor and peripheral immune serial sampling and adequate enrollment for response assessments. The current literature clearly points to the potential promise of NK cell targeting, especially in combination therapies, to benefit both dogs and people for whom novel immunotherapies are needed.

1.2.6 Figures

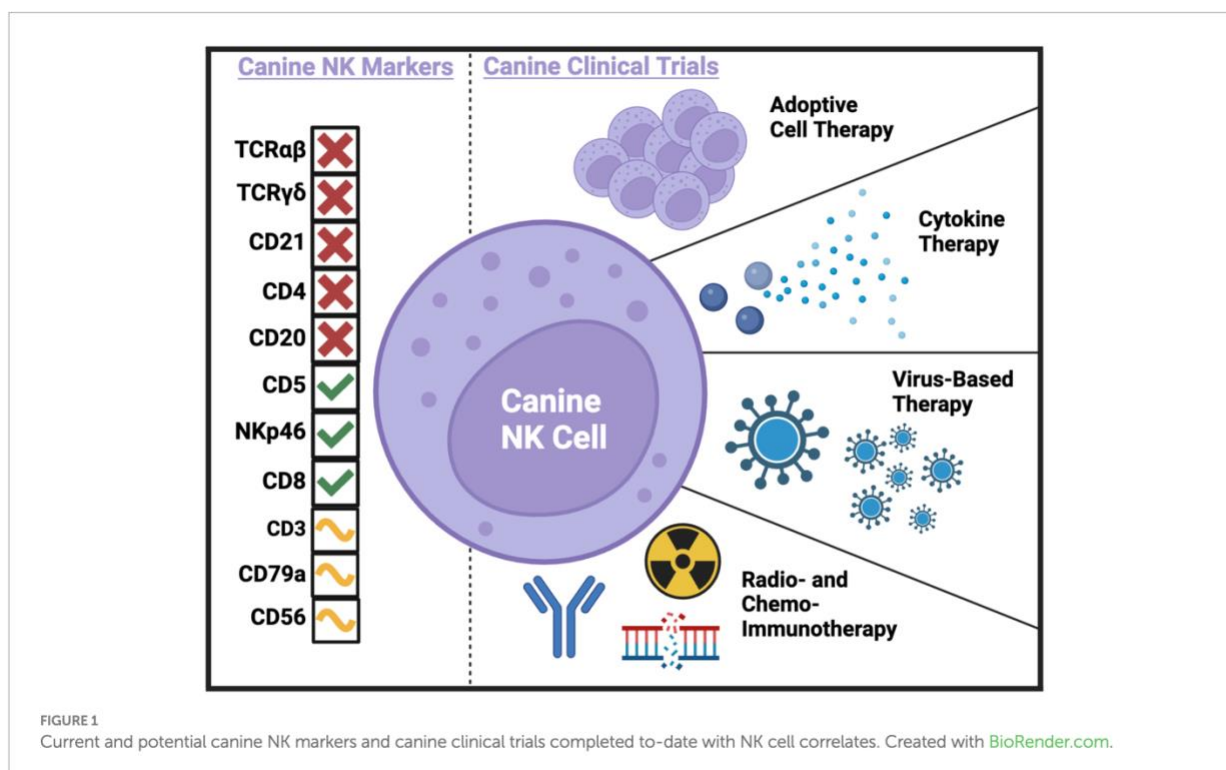


TABLE 1 Canine clinical trials with NK immune correlates.

General therapy	Specific therapy	Cancer diagnosis	NK correlates	Method of analysis	References
Adoptive cell therapy	Autologous NK cell transfer	Osteosarcoma	Number of NK cells	Flow cytometry	(20, 30)
			Serum cytokines	ELISA	
			Activation markers	Flow cytometry	
			Gene expression	qPCR	
Cytokine therapy	Inhaled IL-15	Osteosarcoma, melanoma	Number of NK cells	Flow cytometry	(31, 17, 22)
			Serum cytokines	ELISA	
			Activation markers	Flow cytometry	
			Gene expression	RNA sequencing	
			Cytotoxicity	Killing assay/flow cytometry	
Virus-based therapy	Oncolytic virus	Carcinoma, Adenocarcinoma	Number of NK cells	Flow cytometry	(24)
	Genetically modified HSV	Glioma	Gene expression	RNA seqencing/nanostring	(25)
	eCPMV	Inflammatory mammary cancer	Gene expression	RNA seqencing/nanostring	(27)
	eCPMV	Mammary cancer	Gene expression	RNA sequencing	(33)
			Number of NK cells	Flow cytometry	
	Cellular virotherapy	Various	Number of NK cells	Flow cytometry	(34, 35)
		Gene expression	RNA seqencing/CIBERSORT		
Radio- and chemo-immunotherapy	RT, TRT, IT-IC	Melanoma	Number of NK cells	Flow cytometry	(37)
			Gene expression	RNA sequencing	
	Chemotherapy, anti-CD20, SMI	B cell lymphoma	Gene expression	RNA sequencing	(38)

HSV, Herpes Simplex Virus; eCPMV, Empty Cowpea Mosaic Virus; RT, Radiotherapy; TRT, Targeted Radionuclide Therapy; IT-IC, intratumoral immunocytokine; SMI, Small Molecule Inhibitor.

1.2.7 References

1. Rosenberg SA, Lotze MT, Muul LM, Chang AE, Avis FP, Leitman S, et al. A progress report on the treatment of 157 patients with advanced cancer using lymphokine-activated killer cells and interleukin-2 or high-dose interleukin-2 alone. *N Engl J Med.* (1987) 316:889–97. doi: 10.1056/NEJM198704093161501
2. Rosenberg SA, Lotze MT, Muul LM, Leitman S, Chang AE, Ettinghausen SE, et al. Observations on the systemic administration of autologous lymphokine-activated killer cells and recombinant interleukin-2 to patients with metastatic cancer. *N Engl J Med.* (1985) 313:1485–92. doi: 10.1056/NEJM198512053132327
3. Myers JA, Miller JS. Exploring the NK cell platform for cancer immunotherapy. *Nat Rev Clin Oncol.* (2020) 18:85–100. doi: 10.1038/s41571-020-0426-7
4. McDonough SP, Moore PF. Clinical, hematologic, and immunophenotypic characterization of canine large granular lymphocytosis. *Vet Pathol.* (2000) 37:637–46. doi: 10.1354/vp.37-6-637
5. Foltz JA, Somanchi SS, Yang Y, Aquino-Lopez A, Bishop EE, Lee DA. NCR1 expression identifies canine natural killer cell subsets with phenotypic similarity to human natural killer cells. *Front Immunol.* (2016) 7:521. doi: 10.3389/fimmu.2016.00521
6. Grøndahl-Rosado C, Bønsdorff TB, Brun-Hansen HC, Storset AK. NCR1+ cells in dogs show phenotypic characteristics of natural killer cells. *Vet Res Commun.* (2015) 39:19–30. doi: 10.1007/s11259-014-9624-z
7. Grøndahl-Rosado C, Boysen P, Johansen GM, Brun-Hansen H, Storset AK. NCR1 is an activating receptor expressed on a subset of canine NK cells. *Vet Immunol Immunopathol.* (2016) 177:7–15. doi: 10.1016/j.vetimm.2016.05.001
8. Graves SS, Gyurkocza B, Stone DM, Parker MH, Abrams K, Jochum C, et al. Development and characterization of a canine-specific anti-CD94 (KLRD-1) monoclonal antibody. *Vet Immunol Immunopathol.* (2019) 211:10–8. doi: 10.1016/j.vetimm.2019.03.005

9. Lin YC, Huang YC, Wang YS, Juang RH, Liao KW, Chu RM. Canine CD8 T cells showing NK cytotoxic activity express mRNAs for NK cell-associated surface molecules. *Vet Immunol Immunopathol.* (2010) 133:144–53. doi: 10.1016/j.vetimm.2009.07.013
10. Gingrich AA, Modiano JF, Canter RJ. Characterization and potential applications of dog natural killer cells in Cancer immunotherapy. *J Clin Med.* (2019) 8:1802. doi: 10.3390/jcm8111802
11. Huang YC, Hung SW, Jan TR, Liao KW, Cheng CH, Wang YS, et al. CD5-low expression lymphocytes in canine peripheral blood show characteristics of natural killer cells. *J Leukoc Biol.* (2008) 84:1501–10. doi: 10.1189/jlb.0408255
12. Shin DJ, Park JY, Jang YY, Lee JJ, Lee YK, Shin MG, et al. Ex vivo expansion of canine cytotoxic large granular lymphocytes exhibiting characteristics of natural killer cells. *Vet Immunol Immunopathol.* (2013) 153:249–59. doi: 10.1016/j.vetimm.2013.03.006
13. Freud AG, Caligiuri MA. Human natural killer cell development. *Immunol Rev.* (2006) 214:56–72. doi: 10.1111/j.1600-065X.2006.00451.x
14. Freud AG, Yu J, Caligiuri MA. Human natural killer cell development in secondary lymphoid tissues. *Semin Immunol.* (2014) 26:132–7. doi: 10.1016/j.smim.2014.02.008
15. Kim S, Iizuka K, Kang HS, Dokun A, French AR, Greco S, et al. In vivo developmental stages in murine natural killer cell maturation. *Nat Immunol.* (2002) 3:523–8. doi: 10.1038/ni796
16. Grudzien M, Pawlak A, Kutkowska J, Ziolo E, Wysokińska E, Hildebrand W, et al. A newly established canine NK-type cell line and its cytotoxic properties. *Vet Comp Oncol.* (2021) 19:567–77. Epub 20210426. doi: 10.1111/vco.12695
17. Gingrich AA, Reiter TE, Judge SJ, York D, Yanagisawa M, Razmara A, et al. Comparative immunogenomics of canine natural killer cells as immunotherapy target. *Front Immunol.* (2021) 12:670309. doi: 10.3389/fimmu.2021.670309

18. Denman CJ, Senyukov VV, Somanchi SS, Phatarpekar PV, Kopp LM, Johnson JL, et al. Membrane-bound IL-21 promotes sustained ex vivo proliferation of human natural killer cells. *PLoS One*. (2012) 7:e30264. doi: 10.1371/journal.pone.0030264
19. Park JS, Withers SS, Modiano JF, Kent MS, Chen M, Luna JI, et al. Canine cancer immunotherapy studies: linking mouse and human. *J Immunother Cancer*. (2016) 4:97. doi: 10.1186/s40425-016-0200-7
20. Canter RJ, Grossenbacher SK, Foltz JA, Sturgill IR, Park JS, Luna JI, et al. Radiotherapy enhances natural killer cell cytotoxicity and localization in pre-clinical canine sarcomas and first-in-dog clinical trial. *J Immunother Cancer*. (2017) 5:98. doi: 10.1186/s40425-017-0305-7
21. Somanchi SS, Senyukov VV, Denman CJ, Lee DA. Expansion, purification, and functional assessment of human peripheral blood NK cells. *J Vis Exp*. (2011) 48:2540. doi: 10.3791/2540
22. Judge SJ, Darrow MA, Thorpe SW, Gingrich AA, O'Donnell EF, Bellini AR, et al. Analysis of tumor-infiltrating NK and T cells highlights IL-15 stimulation and TIGIT blockade as a combination immunotherapy strategy for soft tissue sarcomas. *J Immunother Cancer*. (2020) 8:e001355. doi: 10.1136/jitc-2020-001355.
23. Sivori S, Della Chiesa M, Carlomagno S, Quatrini L, Munari E, Vacca P, et al. Inhibitory receptors and checkpoints in human NK cells, implications for the immunotherapy of Cancer. *Front Immunol*. (2020) 11:2156. doi: 10.3389/fimmu.2020.02156
24. Martín-Carrasco C, Delgado-Bonet P, Tomeo-Martín BD, Pastor J, de la Riva C, Palau-Concejo P, et al. Safety and efficacy of an oncolytic adenovirus as an immunotherapy for canine cancer patients. *Vet Sci*. (2022) 9:327. doi: 10.3390/vetsci9070327
25. Chambers MR, Foote JB, Bentley RT, Botta D, Crossman DK, Della Manna DL, et al. Evaluation of immunologic parameters in canine glioma patients treated with an oncolytic herpes virus. *J Transl Genet Genom*. (2021) 5:423–42. doi: 10.20517/jtgg.2021.31

26. Danaher P, Warren S, Dennis L, D'Amico L, White A, Disis ML, et al. Gene expression markers of tumor infiltrating leukocytes. *J Immunother Cancer*. (2017) 5:18. doi: 10.1186/s40425-017-0215-8
27. Barreno L, Sevane N, Valdivia G, Alonso-Miguel D, Suarez-Redondo M, AlonsoDiez A, et al. Transcriptomics of canine inflammatory mammary cancer treated with empty cowpea mosaic virus implicates neutrophils in anti-tumor immunity. *Int J Mol Sci*. (2023) 24:14034. doi: 10.3390/ijms241814034
28. Judge SJ, Murphy WJ, Canter RJ. Characterizing the dysfunctional NK cell: assessing the clinical relevance of exhaustion, anergy, and senescence. *Front Cell Infect Microbiol*. (2020) 10:49. doi: 10.3389/fcimb.2020.00049
29. Nolan MW, Kent MS, Boss MK. Emerging translational opportunities in comparative oncology with companion canine cancers: radiation oncology. *Front Oncol*. (2019) 9:1291. doi: 10.3389/fonc.2019.01291
30. Judge SJ, Yanagisawa M, Sturgill IR, Bateni SB, Gingrich AA, Foltz JA, et al. Blood and tissue biomarker analysis in dogs with osteosarcoma treated with palliative radiation and intratumoral autologous natural killer cell transfer. *PLoS One*. (2020) 15:e0224775. doi: 10.1371/journal.pone.0224775
31. Rebhun RB, York D, Cruz SM, Judge SJ, Razmara AM, Farley LE, et al. Inhaled recombinant human IL-15 in dogs with naturally occurring pulmonary metastases from osteosarcoma or melanoma: a phase 1 study of clinical activity and correlates of response. *J Immunother Cancer*. (2022) 10:e004493. doi: 10.1136/jitc-2022-004493
32. Maskalenko NA, Zhigarev D, Campbell KS. Harnessing natural killer cells for cancer immunotherapy: dispatching the first responders. *Nat Rev Drug Discov*. (2022) 21:559–77. doi: 10.1038/s41573-022-00413-7
33. Valdivia G, Alonso-Miguel D, Perez-Alenza MD, Zimmermann ABE, Schaafsma E, Kolling FW, et al. Neoadjuvant intratumoral immunotherapy with cowpea mosaic virus induces local and

- systemic antitumor efficacy in canine mammary cancer patients. *Cell*. (2023) 12:2241. doi: 10.3390/cells12182241
34. Cejalvo T, Perisé-Barrios AJ, Del Portillo I, Laborda E, Rodríguez-Milla MA, Cubillo I, et al. Remission of spontaneous canine tumors after systemic cellular viroimmunotherapy. *Cancer Res*. (2018) 78:4891–901. doi: 10.1158/0008-5472.CAN-17-3754
35. Cloquell A, Mateo I, Gambera S, Pumarola M, Alemany R, García-Castro J, et al. Systemic cellular viroimmunotherapy for canine high-grade gliomas. *J Immunother Cancer*. (2022) 10:e005669. doi: 10.1136/jitc-2022-005669
36. Klingemann H. Immunotherapy for dogs: still running behind humans. *Front Immunol*. (2021) 12:665784. doi: 10.3389/fimmu.2021.665784
37. Magee K, Marsh IR, Turek MM, Grudzinski J, Aluicio-Sarduy E, Engle JW, et al. Safety and feasibility of an in situ vaccination and immunomodulatory targeted radionuclide combination immuno-radiotherapy approach in a comparative (companion dog) setting. *PLoS One*. (2021) 16:e0255798. doi: 10.1371/journal.pone.0255798
38. Dittrich K, Yıldız-Altay Ü, Qutab F, Kwong DA, Rao Z, Nieves-Lozano SA, et al. Baseline tumor gene expression signatures correlate with chemoimmunotherapy treatment responsiveness in canine B cell lymphoma. *PLoS One*. (2023) 18:e0290428. doi: 10.1371/journal.pone.0290428
39. Maekawa N, Konnai S, Asano Y, Sajiki Y, Deguchi T, Okagawa T, et al. Exploration of serum biomarkers in dogs with malignant melanoma receiving anti-PD-L1 therapy and potential of COX-2 inhibition for combination therapy. *Sci Rep*. (2022) 12:9265. doi: 10.1038/s41598-022-13484-8
40. Maekawa N, Konnai S, Okagawa T, Nishimori A, Ikebuchi R, Izumi Y, et al. Immunohistochemical analysis of PD-L1 expression in canine malignant cancers and PD-1 expression on lymphocytes in canine oral melanoma. *PLoS One*. (2016) 11:e0157176. doi: 10.1371/journal.pone.0157176

41. Maekawa N, Konnai S, Takagi S, Kagawa Y, Okagawa T, Nishimori A, et al. A canine chimeric monoclonal antibody targeting PD-L1 and its clinical efficacy in canine oral malignant melanoma or undifferentiated sarcoma. *Sci Rep.* (2017) 7:8951. doi: 10.1038/s41598-017-09444-2
42. Maekawa N, Konnai S, Nishimura M, Kagawa Y, Takagi S, Hosoya K, et al. PD-L1 immunohistochemistry for canine cancers and clinical benefit of anti-PD-L1 antibody in dogs with pulmonary metastatic oral malignant melanoma. *NPJ Precis Oncol.* (2021) 5:10. doi: 10.1038/s41698-021-00147-6
43. Dong W, Wu X, Ma S, Wang Y, Nalin AP, Zhu Z, et al. The mechanism of antiPD-L1 antibody efficacy against PD-L1-negative tumors identifies NK cells expressing PD-L1 as a cytolytic effector. *Cancer Discov.* (2019) 9:1422–37. doi: 10.1158/2159-8290. CD-18-1259
44. Hullsiek R, Li Y, Snyder KM, Wang S, Di D, Borgatti A, et al. Examination of IgG Fc receptor CD16A and CD64 expression by canine leukocytes and their ADCC activity in engineered NK cells. *Front Immunol.* (2022) 13:841859. doi: 10.3389/ fimmu.2022.841859
45. Foltz JA, Moseman JE, Thakkar A, Chakravarti N, Lee DA. TGF β imprinting during activation promotes natural killer cell cytokine hypersecretion. *Cancers.* (2018) 10:423. doi: 10.3390/cancers10110423

2. Pre-clinical evaluation and first-in-dog clinical trials of PBMC-expanded natural killer cells for adoptive immunotherapy in dogs with cancer

2.1 Background

The discovery of immune checkpoint inhibitors (ICI) and other T cell-based immunotherapies has immensely impacted the treatment of an ever-growing number of cancers¹. Though successes with these immunotherapies have been significant, there are lingering barriers regarding toxicity and strategies to increase responses. Natural killer (NK) cells are innate cytotoxic and cytokine-producing lymphoid cells with a crucial role in anti-viral and anti-tumor responses. Their capacity to recognize heterogeneous cancer cell targets without prior sensitization or priming makes them exciting prospects for cellular immunotherapy. However, despite evidence for activity in hematologic malignancies such as acute myeloid leukemia², NK cell-based immunotherapies have yielded inconsistent responses in solid tumors to date^{3, 4, 5}. With only 10% of therapies that show promise in murine studies successfully showing efficacy in human clinical trials, canine models of spontaneous cancer are an important link to study and improve immunotherapies across species⁶⁻⁸. Dogs are an outbred species with an intact immune system that develop cancers strikingly similar to humans⁹⁻¹¹. And, like humans, there is an urgent unmet need for novel cancer therapies in dogs. Despite the clear benefits of dogs as a comparative immune-oncology (IO) model, gaps in knowledge concerning canine immune populations have limited canine immunotherapy success, especially for NK biology¹². These knowledge gaps are further compounded by significant differences in NK biology between mice and humans, making data interpretation challenging. Our group recently completed one of the first detailed analyses of canine NK cell transcriptomics, revealing that canine NK cells share significant homology with their human counterparts and appear closer phylogenetically to human than mouse NK cells^{13, 14}. Nevertheless, questions remain regarding the optimal characterization of dog NK populations as they expand and their differentiation status prior to

adoptive transfer, which is highly relevant to the longevity of NK cells in vivo and their application in the clinic as adoptive immunotherapy^{4, 13}. Given these ongoing knowledge gaps regarding canine NK immunobiology, additional in-depth characterization is needed to identify factors that impact in vivo efficacy and persistence, especially in the context of clinical trials. In contrast to humans, canine NK cells lack expression of CD56, a standard marker of human NK cells, but the depletion of CD5, a marker expressed at high levels in canine T cells, enriches for a CD5^{dim} population which has been shown to harbor key features of NK cells^{13, 15, 16}. Multiple groups have used low expression of CD5 or CD5^{dim} to identify dog NK cells by flow cytometry¹⁵. Previously, CD5 depletion of peripheral blood mononuclear cells (PBMCs) using magnetic separation has also been used in dogs to isolate or enrich for a CD5^{dim}-expressing NK subset prior to co-culture and expansion with an irradiated feeder line such as the genetically-modified human erythroleukemia line K562 clone 9^{14, 17-19}. However, this method using CD5 depletion can limit the yield of the final NK product needed for transfer.

To address the limitations of current canine NK expansion approaches, we sought to characterize the phenotype, function, and preliminary clinical activity of canine NK cells in first-in-dog clinical trials using unmanipulated PBMCs to generate our NK cell product. We aimed to compare bulk PBMC-derived NK cells versus NK cells expanded from CD5-depleted PBMCs, and then evaluate clinical and genomic characteristics of PBMC-expanded dog NK cells using both autologous and allogeneic NK products in first-in-dog clinical trials in dogs with cancer. The results from this study will enable us to understand optimal NK isolation and expansion techniques for adoptive transfer of canine NK cells for further clinical translation. Given the limitations of canine flow cytometry at this time, our findings will also fill critical knowledge gaps in the transcriptional characterization of canine NK cells and provide a foundation for future immunotherapy trials.

2.2 Methods

2.2.1 PBMC isolation and CD5 depletion of canine cells

Whole blood was collected from 11 healthy, farm-bred beagles (Ridglan Farms, Inc., Mt. Horeb, WI) using EDTA tubes diluted with sterile PBS. PBMCs were isolated from whole blood using a density gradient centrifugation (Lymphocyte Separation Medium, Corning Life Sciences) and red blood cell lysis with RBC lysis buffer for five minutes at 4°C. A subset of PBMCs underwent CD5 depletion using the Easy Sep PE Positive Selection Kit (Stem Cell Technologies, Vancouver, BC) and PE-conjugated anti-canine CD5 (Invitrogen, clone YKIX322.3) to select for CD5^{bright} cells and enrich the CD5^{dim} fraction for further processing and analysis.

2.2.2 PBMC isolation and NK purification of human cells

The collection of whole blood from 3 human patients undergoing resection of benign lesions was approved by the IRB at the University of California, Davis (Protocol # 218204). PBMCs were isolated from whole blood as described previously²⁰. A subset of PBMCs underwent NK isolation using the Rosette Sep Human NK Isolation Kit according to the manufacturer's specifications (Stem Cell Technologies, Vancouver, BC).

2.2.3 NK expansion of canine and human cells

Starting populations of CD5-depleted canine cells or NK isolated human cells, and respective PBMCs were co-cultured with K562 human feeder cells transduced with 4-1BBL (CD137L) and membrane-bound rh-IL21 (K562C9IL21, kind gift of Dr. Dean Lee, Nationwide Children's Hospital, Columbus, Ohio), and supplemented with rh-IL2. Flasks underwent media changes and addition of fresh feeder cells as previously described^{14, 17-19, 21}. Cell count and viability were assessed on co-culture days 0, 7, and 14.

2.2.4 Flow cytometry and killing assays

Cells were washed with PBS, incubated with Fc receptor blocking solution (Canine Fc Receptor Binding Inhibitor, Invitrogen #14-9162-42), then stained with the following fluorochrome-conjugated monoclonal antibodies: rat anti-canine CD5 on PerCP-eFluor 710 (clone YKIX322.3 Thermo Fisher #46-5050-42), mouse anti-dog CD3-FITC (clone CA17.2A12, BioRad #MCA1774F), unconjugated NKp46 (clone 48A, kind gift of Dr. Dean Lee) which was conjugated secondarily with PE, and live/dead staining using Fixable Viability Dye 780 (eBioscience #65-0865-14). Staining of canine $\gamma\delta$ T cells was completed using a mouse anti-dog TCR $\gamma\delta$ (clone CA20.8H1, IgG2a, kind gift of Dr. Peter F. Moore²²) primary antibody followed by a goat anti-mouse IgG (H+L) cross-adsorbed secondary antibody-AF647 (cat. A-21235). All flow cytometry results were acquired using a BD Fortessa flow cytometer (Becton Dickinson, San Jose, California, USA) equipped with BD FACSDiva software and analyzed using FlowJo Software (TreeStar, Ashland, OR).

For killing assays, canine osteosarcoma (OSA) and melanoma tumor cell lines (OSCA-78 and M5, respectively) were thawed labeled with carboxyfluorescein succinimidyl ester (CFSE, Invitrogen #C34554) for 5 min at room temperature at a final concentration of 1.25 μ M. After overnight incubation of effector and target cells, staining was performed with Fixable Viability Dye 780 prior to analysis by flow cytometry. Cytotoxicity was calculated according to the following formula: $[\text{CFSE+FVD780}^+ / (\text{CFSE+FVD780}^+ + \text{CFSE+FVD780}^-)] \times 100^{20}$.

2.2.4 Cytokines

Analytes were measured in cell culture supernatant by using the Eve Technologies Corp (Calgary, Alberta) Canine Cytokine 13-Plex Discovery Assay (MilliporeSigma, Burlington, Massachusetts, USA) performed on the Luminex 200 system (Luminex, Austin, Texas, USA). The 13 included markers were GM-CSF, IFN γ , IL-2, IL-6, IL-7, IL-8/CXCL8, IL-10, IL-15, IL-18, IP-10/ CXCL10, KC-like, MCP-1/CCL2, and TNF α ²³.

2.2.5 RNA sequencing

Samples from NK co-culture and PBMCs from four healthy donors and canine patients receiving immunotherapy underwent RNA extraction using RNeasy Mini kits (Qiagen) followed by sequencing using a 3'-Tag-RNA-Seq protocol for gene profiling completed by the UC Davis Genome Center²⁴. Data were only included for samples with sufficient RNA quantity and quality for analysis. Publicly available sequencing data for healthy day 0 and day 14 co-culture samples were utilized from a previous study by our laboratory (BioProject accession number PRJNA987155)²⁵. Quality assessment of all raw fastq files was performed using *multiqc*, *bbduk_qc* was used to trim the first 12 bases and carry out quality trimming²⁶, and *bbduk_find_ribo* was used to identify and select non-ribosomal RNA²⁶. Reads were indexed to a canine reference transcriptome (ROS_Cfam_1.0) or human reference transcriptome (GrCh38), and counts were generated by salmon²⁷. Count files were transported to R using *tximport*²⁸ and downstream analyses were completed in R using the *DESeq2* and *ggplot2* packages. For scRNA-Seq, PBMC-expanded NK cells after 14-day were quality checked to determine a cell concentration and adequate viability. Single-cell suspension of 700-1200 cells/ μ l in at least 40 μ l of PBS/0.5% BSA suspension buffer was submitted to the UC Davis Genome Center. Library preparation and sequencing using the 10X Chromium Next GEM Single-Cell 3' v3.1 Gene Expression protocol were completed by the UC Davis Genome Center. Single cell fastq files were processed using the *cellranger count* pipeline with generation of and alignment to a *Canis lupis familiaris* reference genome (CanFam3.1) using the *cellranger mkgtf* and *cellranger mkref* pipelines. Further preprocessing was completed in R using the *Seurat* package and data integration and visualization using R packages, *Seurat* and *ggplot2*.

2.2.6 Autologous NK immunotherapy in dogs with metastatic osteosarcoma and melanoma

This clinical trial was approved by the UC Davis School of Veterinary Medicine Clinical Trials Review Board and IACUC (protocol #21461). Based on our prior work showing safety and evidence for clinical activity using inhaled IL-15 in dogs with gross pulmonary metastases, we enrolled client-owned pet dogs with naturally occurring metastatic OSA or melanoma on a clinical trial combining IV autologous adoptive NK cell transfer. Treatment of inhaled IL-15 was given through a fitted nebulizer twice daily for 14 days at a dose level of 50 µg as previously described²³. Entry criteria included histologic confirmation of malignant melanoma or OSA, documented metastatic disease to the lungs (based on three-view thoracic radiographs), adequate end-organ function, and weight of 10kg or greater. Informed consent was obtained from all owners prior to enrollment. PBMCs were isolated from the patient's whole blood and co-cultured with irradiated feeder cells and rhIL-2 for 14 days to expand autologous cells for two scheduled NK cell infusions. NK cell preparations were confirmed as endotoxin and mycoplasma negative before injection on days 0 and 7 of a two-week twice daily inhaled IL-15 regimen. 7.5×10^6 NK cells/kg IV (with 5 ng/mL rhIL-15 in 50mL solution of 0.9% NaCl) were given for each injection by slow bolus through an IV catheter using a closed chemotherapy system. Response was assessed based on the Response Evaluation Criteria for Solid Tumors in Dogs (RECIST V.1.0) and evaluated by a boarded radiologist (EGJ)²⁹. Imaging was performed on day 28 and day 42 after treatment initiation followed by every four weeks. Patients had to have a minimum of 28 days to imaging to meet criteria for response assessment.

2.2.6 Allogeneic NK Immunotherapy in Dogs with Malignant Melanoma

We also performed a first-in-dog trial utilizing allogeneic NK cells in dogs with locally advanced, unresectable oral melanoma receiving palliative radiotherapy (RT). This trial was also approved by the UC Davis School of Veterinary Medicine Clinical Trials Review Board and IACUC (protocol # 21620). Patients were included based on a histologic diagnosis of malignant melanoma, adequate end-organ function, a weight of 10kg or greater, and a plan to undergo

palliative RT for disease control. Palliative RT is the standard of care for canine malignant melanoma and consists of four weekly treatments at a dose of 9 Gy administered to the primary tumor¹⁸. Blood was obtained from healthy, farm-bred beagles aged 2-8 years old of both sexes two weeks prior to scheduled NK cell infusion in canine patients. PBMCs were isolated from the healthy donor whole blood and co-cultured with irradiated feeder cells and rhIL-2 for 14 days to expand allogeneic cells. NK cell preparations were confirmed as endotoxin and mycoplasma negative before a single injection at a dose of 7.5×10^6 NK cells/kg IV (with 5 ng/mL rhIL-15 in 50 mL solution of 0.9% NaCl) on the day of the fourth and final session of RT. Cells were given by slow bolus through an IV catheter using a closed chemotherapy system, and dogs were administered 3 mcg/kg rhIL-15 SQ directly after NK cell infusion and then 20-30 hours post-infusion. Blood draws for complete blood counts (CBCs) and genomic analysis were completed at specified timepoints^{14, 23}.

2.2.7 Statistics

Graphs and statistical analyses for cell counts, viability, cytotoxicity, and cytokine secretion were completed using Prism software (GraphPad Software). Line graphs are expressed as mean and SEM with significant differences between groups determined by mixed-effects analysis. Bar graphs represent the mean with significant differences between groups determined by Mann-Whitney test. Rstudio V.4.3.2 (R Foundation for Statistical Computing, Vienna, Austria) was used for statistical analysis of bulk RNA-seq data, specifically the DESeq2 package in R which employs the Wald test and adjusts for multiple testing using the Benjamini-Hochberg procedure. $p \leq 0.05$ was considered statistically significant across all analyses unless otherwise noted.

2.3 Results

2.3.1 Canine NK Expansions in Vitro

Using PBMCs from healthy donor beagles, we compared the yield, viability and functional characteristics of NK cells expanded from unmanipulated bulk PBMCs versus those derived from CD5-depleted starting populations, using irradiated human feeder cells as we and others have done previously^{14, 18, 21} (**FIGURE 1A**). To validate the CD5-depleted cell population prior to co-culture, we performed flow phenotyping on both the positively and negatively selected populations, demonstrating successful magnetic separation of CD5 bright and CD5^{dim}/ negative subsets (**FIGURE 1B**). Cell count and viability data were collected for five time points up to day 14 (**FIGURE 1C**). A mixed-effects model analysis showed no statistical difference in calculated cell counts and viability between PBMC-derived and CD5-depleted NK cells. Viability decreased and reached a minimum at day 10 before stabilizing at day 14 in both groups¹⁵. PBMC-derived NK cells reached a higher mean overall expansion than CD5-depleted cells at day 14, peaking at a mean of 677 million cells from 5 million PBMCs at day 0 compared to 537 million from 5 million starting CD5-depleted cells ($P>0.05$, **FIGURE 1C**). We next assessed NK frequency at multiple time points using flow cytometry, demonstrating high percentages of CD3+NKp46- T cells and low percentages of CD3-NKp46+ NK cells in the resting PBMC populations compared to low percentages of CD3+NKp46- T cells and high percentages of CD3-NKp46+ NK cells by day 14 (**FIGURE 1D**). Due to the similarities between NK cells and gamma-delta ($\gamma\delta$) T lymphocytes as well as existing literature showing the expansion of $\gamma\delta$ T cells in a distinct but partially overlapping co-culture protocol³⁰, we sought to confirm the purity of the day 14 NK product. The proportion of CD3+ $\gamma\delta$ TCR+ cells remained low, below 4% as assessed by flow cytometry, in the day 14 NK product (**Figure 1E**), aligning with previous reports of minimal TCR $\gamma\delta$ + cells in canine peripheral blood³¹.

2.3.2 Genomic analysis of CD5 depleted and bulk PMBC-expanded canine NK cells

Given our phenotypic data validating the use of unmanipulated PBMCs to expand purified NK cells, we then aimed to characterize the differential gene expression (DGE) profiles of these

respective canine NK products using RNA sequencing (RNA-seq). First, PBMC-expanded NK cells were compared to unmanipulated PBMCs using scRNA-seq to validate our findings and confirm the populations present following expansion. PBMC-expanded NK cells were sequenced and assessed in relation to a previously published single-cell data set of PBMCs from a healthy donor which served as an unmanipulated control²⁵. The two datasets were integrated to enable comparison and the clusters present in unmanipulated PBMCs were visualized in a uMAP plot (**Figure 2A**). Differential gene expression testing was used to determine the genes that distinguished each cluster from remaining clusters in order match the clusters to cell types based on canonical cell markers. A subset of genes used to confirm cell cluster identities is visualized by dot plot (**Figure 2B**). Overlapping of the resting PBMCs and day 14 NK cells in a single uMAP plot shows the overall changes in clustering due to the expansion (**Figure 2C**). The changes in the resting and expanded populations are further explored in a series of uMAPs visualizing the expression of relevant genes along with the proportion of total cells expressing that gene (**Figure 2D**). Expression of CD3E and CD3D at day 0 was seen in 53.8% and 48.0% of cells, respectively, which dropped to less than 4% of the cells present at day 14. Similar decreases were seen in cells expressing additional T cell markers, CD4, CD5, and CD8A, as well as cells expressing myeloid markers, CD86, and B cell markers, CD22. In contrast, the percent of cells expressing NK cell markers NKp30 (NCR3) and NKG2D (KLRK1), and GZMB increased substantially from day 0 to day 14.

Next, PBMC-expanded NK cells were compared to NK cells expanded from CD5-depleted PBMCs using bulk RNA-seq of cells from four healthy donors. Principal Component Analysis (PCA) of PBMC-expanded and expanded CD5-depleted cells at day 0, day 7, and day 14 showed that expansion timepoint was the primary driving force for variance of PC1, with clustering also based on donor. We observed greater variances between bulk and CD5-depleted populations at day 0 than day 14 which were tightly clustered (**FIGURE 3A**). These

results suggest that PBMCs and CD5-depleted populations are distinct at rest, but then converge to form nearly identical NK populations by day 14 of co-culture. This is further substantiated in MA (ratio intensity) plots of PBMC-derived and CD5-depleted cells at day 14 of co-culture versus their respective populations at day 0, showing 3961 and 3107 DGEs, respectively (**FIGURE 3B-3C**), while comparison of both groups at D14 demonstrated high similarity with no DGEs (**FIGURE 3D**). To ensure that DEGs cannot be solely contributed to the loss of non-NK cells, we then specifically highlighted the log fold changes of genes associated with NK cell signatures at day 14 versus day 0 (**FIGURE 3E-3F**). Notably, IFNG, GZMB, and GZMA (canonical NK functional gene products) had the largest positive fold change, while CD16 showed the largest negative fold change in both groups. There were examples of specific genes, notably KLRB1 and KLRA1, which showed statistically significant DGE at day 14 in PBMC-derived but not CD5-depleted expanded NK cells compared to their resting counterparts. Next, the normalized counts of genes highly associated with NK function, including CD16, KLRB1, NKG2D/KLRK1, and GZMB, were extracted for each group (**FIGURE 3G**). Interestingly, both bulk PBMCs and CD5-depleted cells had virtually no expression of classic NK genes at rest (timepoint 0), with the exception of CD16. Notably, after co-culture, we observed DGE changes consistent with shedding of CD16 following activation, mirroring the human situation for this critical NK marker³², as well as increases in other important markers, such as KLRB1 and GZMB.

2.3.3 Functional assessment of expanded NK cells

We then performed killing assays and multiplex ELISA to determine the cytotoxicity and cytokine secretion capabilities of both subsets of NK cells at day 14-17. Representative flow gating demonstrates the effector and target cell populations using CFSE labeling (**FIGURE 4A**). Overall, we observed a clear dose-response in cytotoxicity for expanded NK cells against both OSA and melanoma targets (**FIGURE 4A, B**). Although PBMC-expanded NK cells

demonstrated increased cytotoxicity compared to expanded CD5-depleted NK cells at all E:T ratios, these differences were not statistically significant (**FIGURE 4B**). Additionally, we observed donor variability in NK killing against OSA and melanoma targets consistent with other published studies²³ (**FIGURE 4C**). We then performed multiplex analysis to analyze cytokines in the culture supernatant (**FIGURE 4D**). Importantly, secretion of GM-CSF and IFN- γ was significantly greater in PBMC-expanded NK cells compared to expanded CD5-depleted NK cells, while MCP-1 was significantly lower ($P < 0.05$). No significant differences were observed between NK cells expanded from bulk PBMCs compared to those expanded from CD5-depleted cells in any of the other 9 cytokines investigated.

2.3.4 Genomic analysis of magnetic bead purified and bulk PBMC-expanded human NK cells

To provide comparative context to information gleaned from sequencing canine cells, we used RNA-seq to characterize human NK cells expanded from both magnetic bead purified and bulk PBMC starting populations. Studies using human cells have the advantage of well-defined NK markers and well-characterized antibodies and purification protocols, thereby providing a necessary controlled setting to corroborate canine gene expression patterns. At rest, purified human NK cells showed clear differences compared to bulk PBMCs. The normalized counts of genes associated with NK function were higher in purified NK cells than bulk PBMCs, with significantly greater CD56 expression as expected following isolation of the NK population (**FIGURE 5A**). Genes related to T and B cells similarly followed expected trajectories, with little to no expression in the purified NK population and increased expression in PBMCs (**FIGURE 5B**). The differences in normalized counts between NK-isolated cells and bulk PBMCs at day 0 are then clearly visualized using an MA plot showing 1739 DGEs between the two groups (**FIGURE 5C**). The significant differences at day 0 provide the framework to emphasize the lack of differences between the two populations at day 14 co-culture, where an MA plot shows only 4

DGEs between the two groups (**FIGURE 5D**). This convergence of gene expression profiles is plainly illustrated using a PCA plot, and the addition of day 7 samples suggests that the majority of the convergence occurs in the first half of the co-culture timeline (**FIGURE 5E**). To further compare canine and human co-culture expression signatures, we again highlighted the log fold changes of genes associated with NK cell signatures at day 14 versus day 0 (**FIGURE 5F**). Similar to canine data, IFNG and GZMA had the largest positive fold changes in human cell expansions. However, human cells notably differed in respect to CD16, which had insignificant changes, and KLRG1, which had the largest negative fold change in both groups. The merging of distinct NK and bulk populations into a nearly identical activated NK phenotype, with significant changes in NK functional genes at day 14 versus day 0, aligns biologically with equivalent canine data for CD5-depleted and bulk populations.

2.3.5 First-in-dog clinical trial of adoptive transfer of autologous canine NK cells

Together, these phenotypic, functional and transcriptomic study results aligned with our hypothesis that NK cells expanded from bulk PBMC starting populations produce an equivalent or superior cellular product compared to NK cells expanded from CD5-depleted cells. Previously, we completed a first-in-dog trial combining palliative RT and intra-tumoral autologous NK cell transfer in dogs with unresectable, non-metastatic OSA¹⁸ where we used NK cells expanded from CD5-depleted cells as our starting source material. While intra-tumoral injections have the advantage of bypassing the constraints of NK homing from the systemic circulation and potentially avoiding toxicity, not all tumors are accessible for injection and the efficacy of intra-tumoral administration is limited in patients with disseminated disease. We therefore conducted a first-in-dog trial using IV injection of autologous NK cells expanded from bulk PBMCs in dogs with pulmonary metastases from OSA and melanoma. This was combined with inhaled IL-15 to support in vivo persistence and activation of endogenous and exogenous NK cells based on our previous work establishing a maximum tolerated dose and suggesting

potential clinical activity of inhaled IL-15 as a monotherapy in dogs with lung metastases from OSA and melanoma²³ (**FIGURE 6A**). Cytokine immunotherapy using IL-15 effectively activates NK cells and the inhaled route appears to stimulate anti-tumor efficacy against gross metastasis without the toxicities of systemic administration. Although autologous NK cells have been characterized as hypofunctional in human NK trials^{33, 34}, we designed this trial with primary considerations of safety given that systemic NK immunotherapy had never previously been performed in dogs. Nine dogs with naturally occurring melanoma (n=4) or OSA (n=5) were enrolled (**FIGURE 6B**).²⁹ One dog demonstrated a partial response and one dog demonstrating stable disease based on RECIST criteria (**FIGURE 6C**). To assess the expansion ability of PBMCs derived from cancer bearing dogs compared to healthy dogs, we obtained cell count, fold change, and viability data for both expansions from each of the nine patients compared to expansions from beagle donors (**FIGURE 6D**). Viability was similar between cancer-bearing and healthy donors ($P>0.05$). Absolute cell counts were numerically higher but not statistically significant, while overall fold change was significantly higher in PBMC-expanded NK cells from healthy beagle donors compared to cancer patients ($P<0.05$). Taken together, this study established the feasibility of obtaining therapeutic amounts of clinical grade dog NK cells from patient derived PBMCs along with the safety of adoptively transferring those cells in dogs with advanced cancer, providing a framework for subsequent trials to improve efficacy.

2.3.6 First-in-dog clinical trial of adoptive transfer of allogeneic canine NK cells

A key advantage of NK cells in cancer immunotherapy centers on the ability to use allogeneic sources for off-the-shelf treatment with decreased risk of AEs^{33, 34}. NK cells can also be made readily available for canine cancer patients in the clinic, which is highly valuable in the context of rapidly progressing cancers and in patients experiencing immune suppression, since time delays for cell manufacturing and adequacy of bone marrow reserve can be problematic when using autologous sources for cellular immunotherapy. Therefore, we next evaluated the

combination of palliative RT with the first-in-dog use of allogeneic NK cells from unmanipulated PBMC starting populations from healthy beagle donors for dogs with unresectable oral melanoma (**FIGURE 7A, 7B**). Standard palliative RT was administered weekly in four fractions followed by infusion of intravenous allogeneic NK cells (7.5×10^6 cells/kg) on the day of the final RT treatment³⁵. We observed no serious AEs related to NK cell injections. While the small sample size limits conclusions regarding efficacy, we did observe a median survival of 145 days in this cohort with one dog surviving 445 days, a particularly promising response given the poor prognosis of canine malignant melanoma^{35, 36}. With standard of care treatment, 85% of dogs diagnosed with malignant oral melanoma will develop metastatic disease within 6 months, and the large majority will die within 1 year of diagnosis^{35, 36}. We then performed RNA-seq on patient PBMCs using a 3'-Tag-RNA-Seq protocol for gene profiling. PCA showed individual dogs as the driving force for variance of PC1, and samples clustered based on patient rather than treatment timepoint (**FIGURE 7C**). Notably, the dog that lived the longest (ID5) clustered separately from the rest of the dogs. We then analyzed the relative gene expression of patient samples across timepoints and across dogs using a heatmap highlighting genes related to NK activation and function (**FIGURE 7D**). We observed variability in NK gene expression between dogs, with the exception of CD16 and IFNGR2 which had consistently high relative gene expression in all patients. To interrogate absolute changes in response to treatment, we then analyzed normalized counts of key NK genes as a composite of patient samples for each timepoint (**FIGURE 7E**). Most striking was a peak in CD16 expression one day following NK transfer, while KLRB1 increased moderately from one to fourteen days after NK transfer. Interestingly, the inhibitory marker TIGIT, a key NK exhaustion marker^{37, 38}, increased substantially during the course of RT but subsequently decreased following NK adoptive immunotherapy, suggesting marked fluctuations in NK phenotype over the course of multimodality therapy. To address potential gene signatures in relation to outcome, we analyzed NK DGE signatures from the dog with the longest survival (ID5) to those from the dog with the shortest survival (ID1). Genes that

were significantly different from dog ID5 to dog ID1 were visualized by GO analysis and showed enrichment of several diverse pathways, including cell cycle and viral-related pathways (**FIGURE 7F**). Taken together, this proof-of-concept trial provides notable baseline data validating the canine model for investigating allogeneic adoptive NK cell transfer alone or in combination with other therapies and reinforces the value of high throughput sequencing in hypothesis generation and uncovering mechanisms of therapeutic response and resistance.

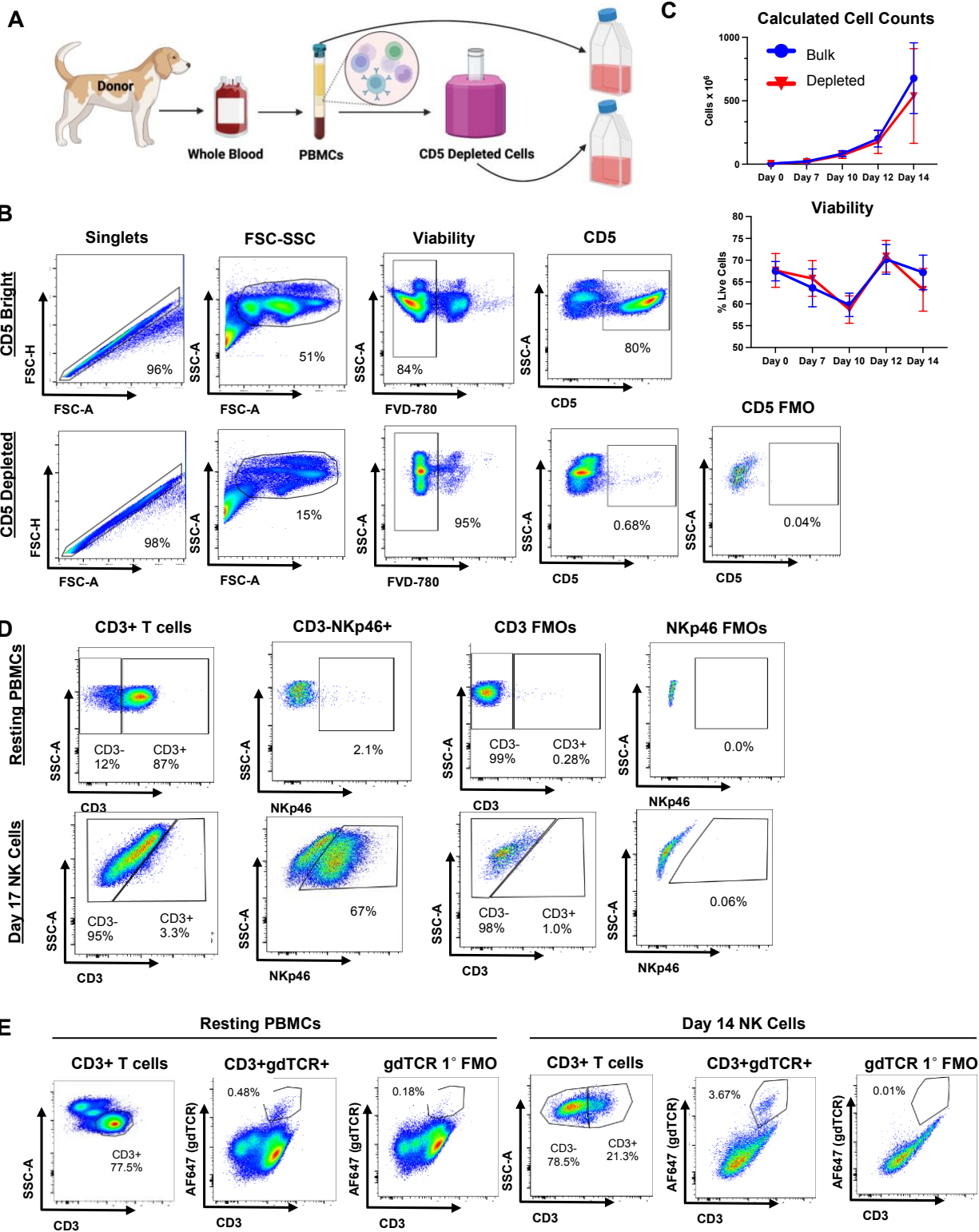


Figure 1. Expansion of canine NK cells in vitro. (A) Schema of experimental strategy expanding NK cells from PBMC and CD5-depleted starting populations. After processing, respective cell populations were co-cultured with irradiated K562 clone 9 feeder cells and 100 mIU/mL rhIL-2 for 14 days. (B) Representative flow cytometry gating of cells prior to co-culture and following magnetic bead separation using CD5 depletion. Depleted cells showed virtually no CD5 expression in contrast to positively selected CD5+ cells, confirming the efficacy of magnetic separation and phenotype of CD5-depleted cells as a starting population. (C) Cell counts and viability were calculated on days 0, 7, 10, 12, and 14 of the 14-day co-culture using bulk PBMCs (blue) and CD5-depleted cells (red) as starting populations. Mean and SEM for 11 healthy donor dogs are plotted against time. (D) Representative flow cytometry gating of bulk PBMCs before and after 14-day co-culture, corroborating the expansion of NKp46+ NK cells from PBMCs without preceding NK-isolation. NK cells were identified as CD3-NKp46+, reaching a majority at day 14 with minimal CD3+ T cell infiltrate. PBMC, peripheral blood mononuclear cells. (E) Flow cytometry gating of PBMCs at rest and following 14-day co-culture

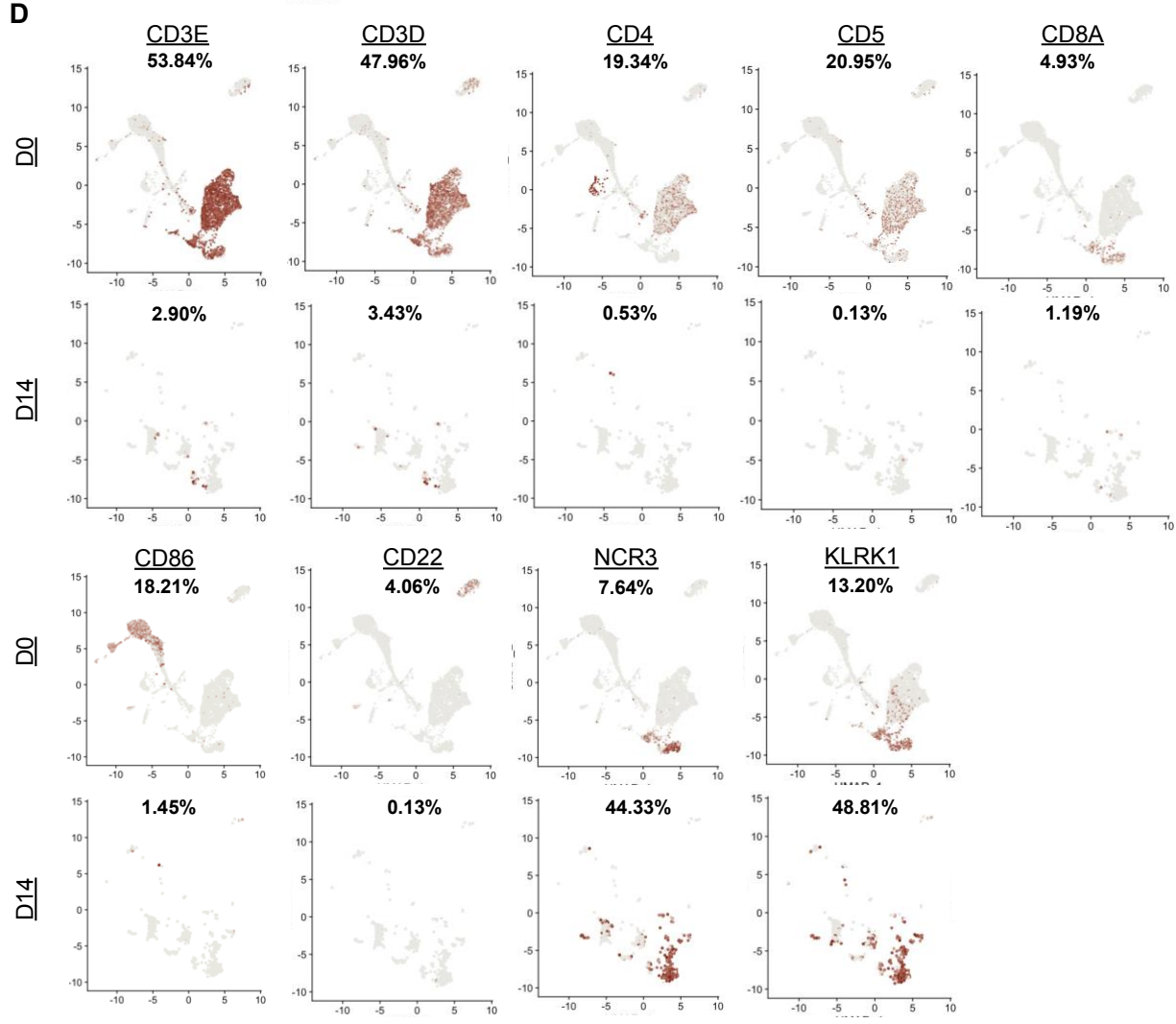
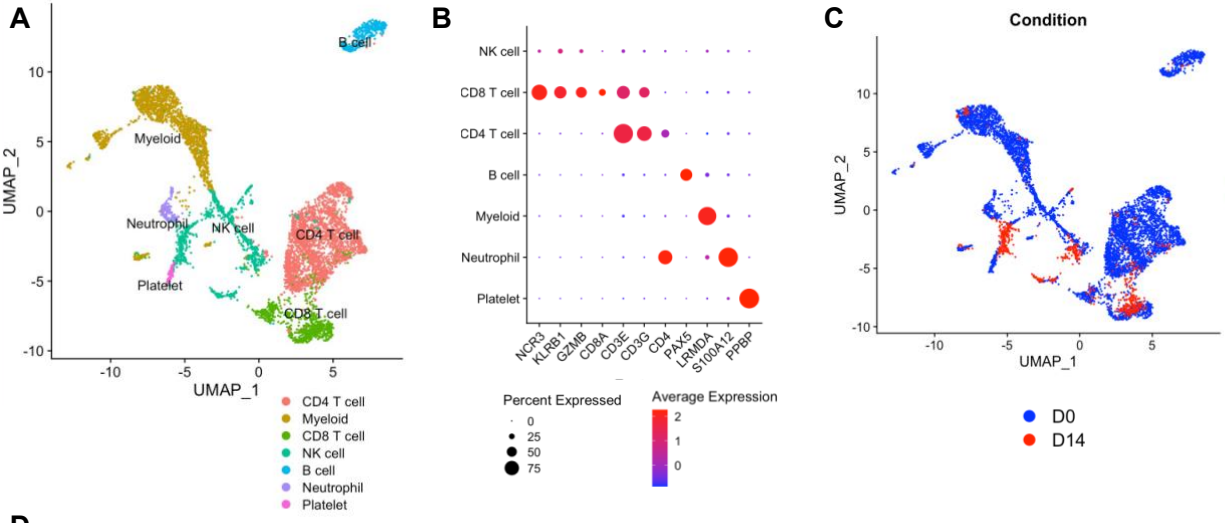


Figure 2. Genomic analysis of expanded NK cells by scRNA-seq. Cells from PBMC-expanded NK cells at day 14 were collected and scRNA-seq was completed. The resulting dataset was integrated with a dataset for resting PBMCs. (A) Uniform Manifold Approximation and Projection (uMAP) plot of clusters present in resting PBMCs color-coded by cell type. Cell identities were determined by analysis of differentially expressed genes that distinguished each cluster from all other clusters. (B) Dot plot visualizing a selection of gene markers used to annotate the cells present. Dot size represents the percent of cells expressing the gene while color correlates with average expression within a cell. (C) uMAP of overlapping datasets included within the integration, showing the differences in resting PBMCs (D0, blue) and PBMC-expanded NK cells (D14, red). (D) uMAPs showing distribution and percent of cells expressing various genes associated with cell types in the integrated conditions, D0 (above) and D14 (below). Percentages are calculated as the percent of cells with expression of the specified gene out of the total cells present. The threshold for gene expression is set at 0.

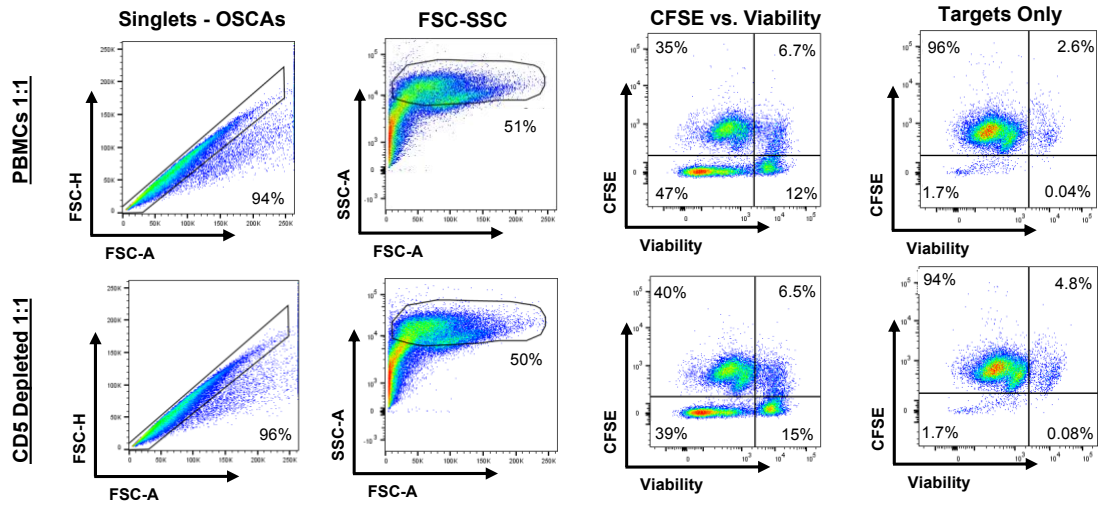
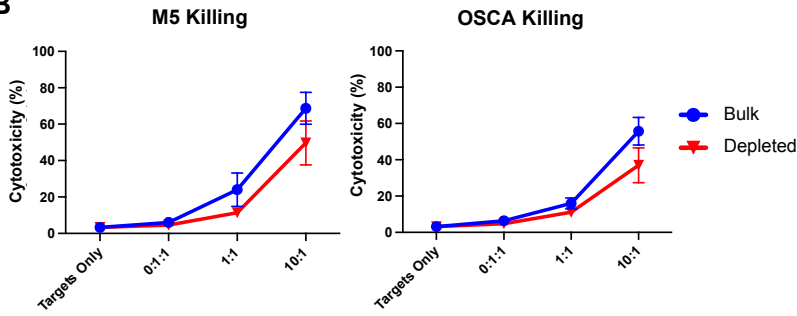
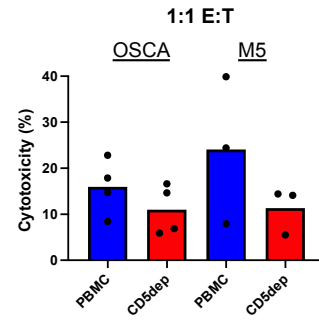
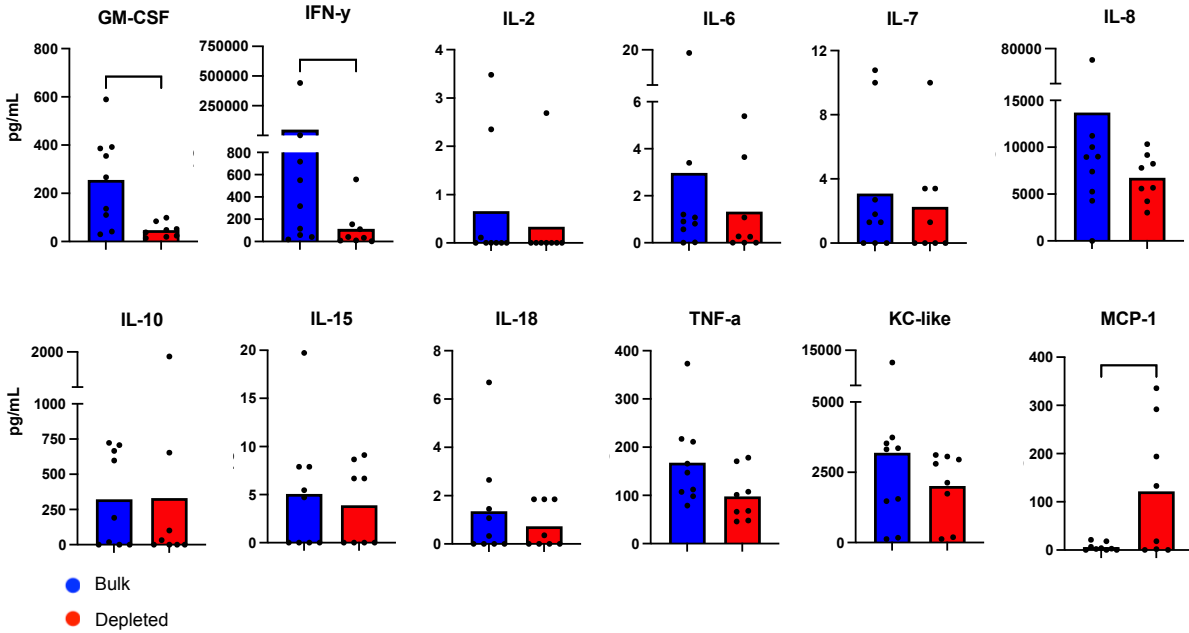
A**B****C****D**

Figure 3. Genomic analysis of expanded NK cells by bulk RNA-seq. Cells from bulk PBMC and CD5-depleted cell starting populations were collected at days 0, 7 and 14 of the 14-day co-culture from four separate healthy beagle donors and 3'-Tag-RNA-Seq was performed. (A) Principal component analysis (PCA) of cells color-coded by donor dog (left) or starting population (right) demonstrated variability at days 0 (squares) and 7 (triangles) of co-culture with convergence of cell signatures at day 14 (circles). Certain samples from donor 3 did not meet RNA quantity standards and were excluded, including day 0 depleted, day 14 depleted, and day 14 bulk. MA plots, using a $p < 0.05$ significance threshold, corroborate PCA plot patterns with (B) 3961 differentially expressed genes (DGEs, blue) between PBMCs at day 14 versus day 0 of co-culture, (C) 3107 DGEs between CD5-depleted cells at day 14 versus day 0 of co-culture, and (D) zero DGEs between bulk PBMCs and CD5-depleted cells at day 14 co-culture. The log fold change of NK cell-related gene expression was assessed between day 14 and day 0 co-culture in (E) the bulk PBMC group and (F) the CD5-depleted cell group. Several key genes were significantly different following co-culture compared to day 0 (bold, green). P values were determined using the DESeq2 package in R. (G) Absolute normalized counts for CD16, KLRB1, NKG2D, and GZMB were visualized for CD5-depleted cells at day 0 co-culture (Dep 0) and day 14 co-culture (Dep 14) as well as PBMCs at day 0 co-culture (Bulk 0) and day 14 co-culture (Bulk 14). Bars show median of normalized counts for donor dogs and P values were determined using the DESeq2 package in R, * $P < 0.05$, ** $P < 0.01$, *** $P < 0.001$.

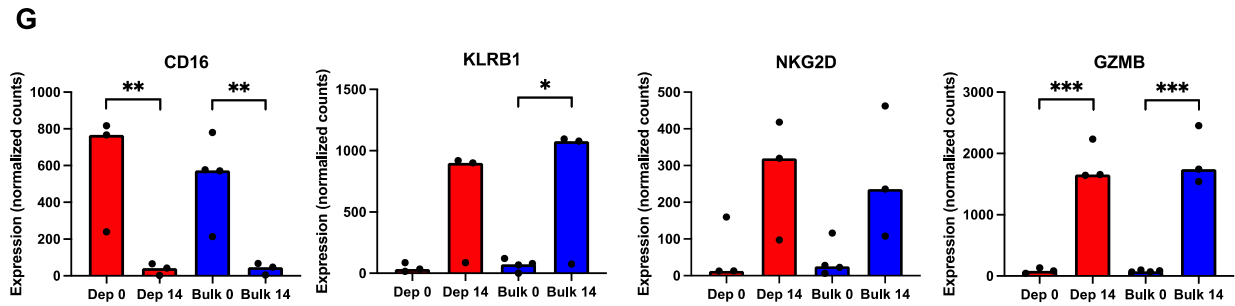
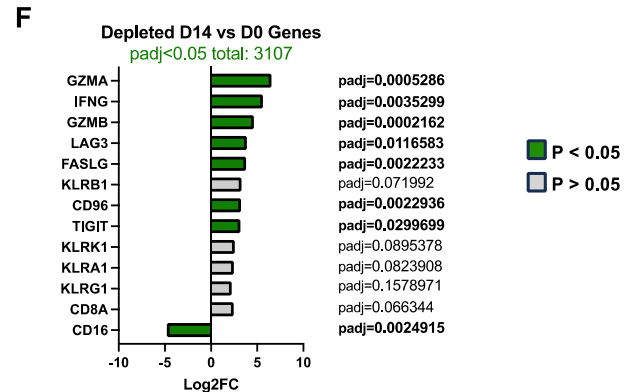
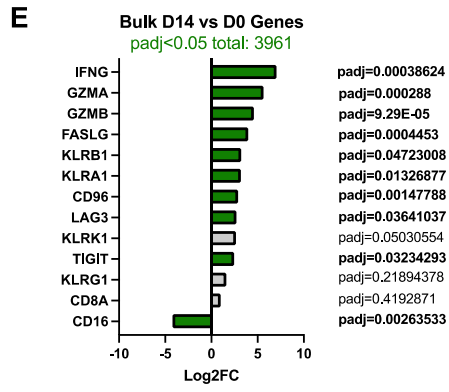
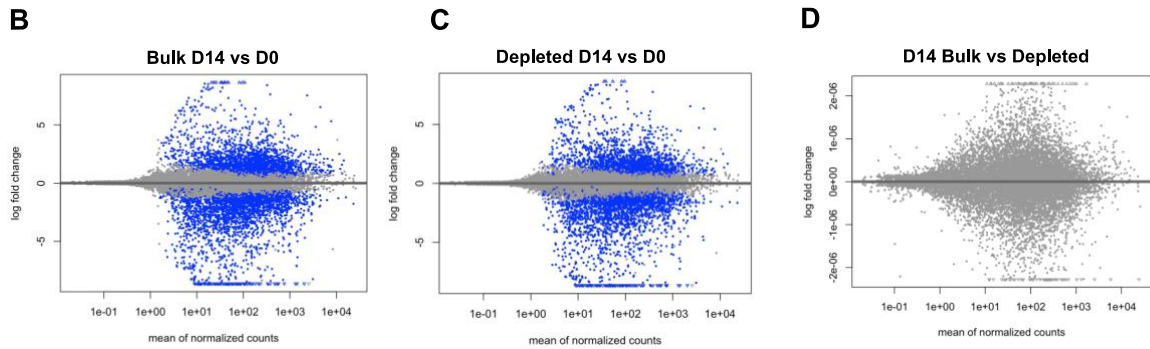
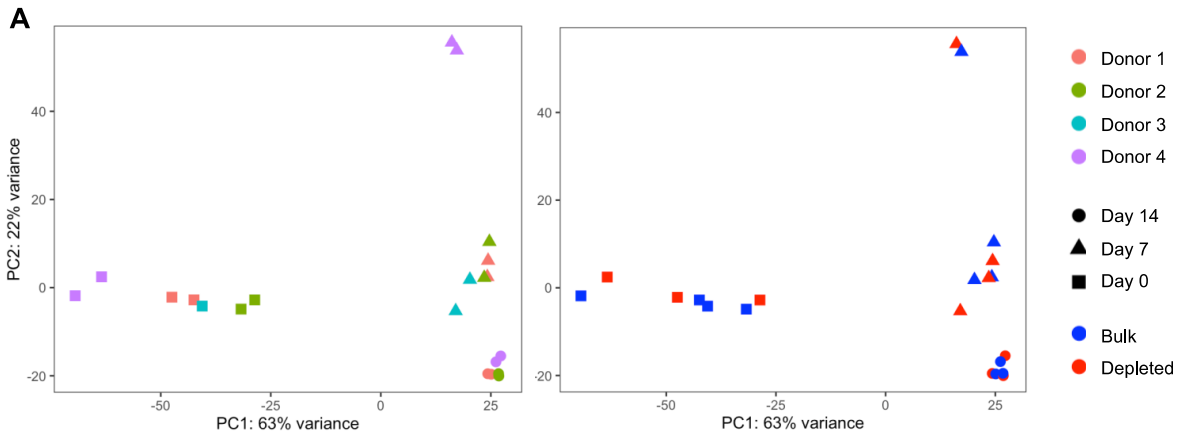


Figure 4. Functional assessment of expanded NK cells. (A) Representative flow cytometry showing gating strategy for NK killing assays using PBMC and CD5-depleted expanded NK cells against osteosarcoma cell line targets (OSCA) at a 1:1 effector to target (E:T) ratio. Target cells were identified from effector cells by CFSE+ labelling with separate viability dye staining to identify dead cells. (B) Mean cytotoxicity (\pm SEM) of NK cells at day 14 from four donor dogs at increasing E:T ratios from bulk PBMC (blue) and CD5-depleted (red) starting populations against melanoma (M5, left) and osteosarcoma (OSCA, right) targets. (C) At the 1:1 E:T ratio, mean cytotoxicity of expanded NK cell effectors varied against osteosarcoma and melanoma targets, with increased PBMC-expanded NK cell killing against melanoma targets compared to osteosarcoma ($p = ns$). (D) Supernatant cytokine levels were measured by canine Luminex assay. Bars depict mean values of eight or nine healthy donor dogs for PBMC (blue) and CD5-depleted cells (red) following 14-day co-culture. GM-CSF and IFN- γ concentrations were significantly greater in the PBMC group, while MCP-1 was significantly greater in the CD5-depleted group. P values were determined using the Mann-Whitney test, * $P < 0.05$, ** $P < 0.01$.

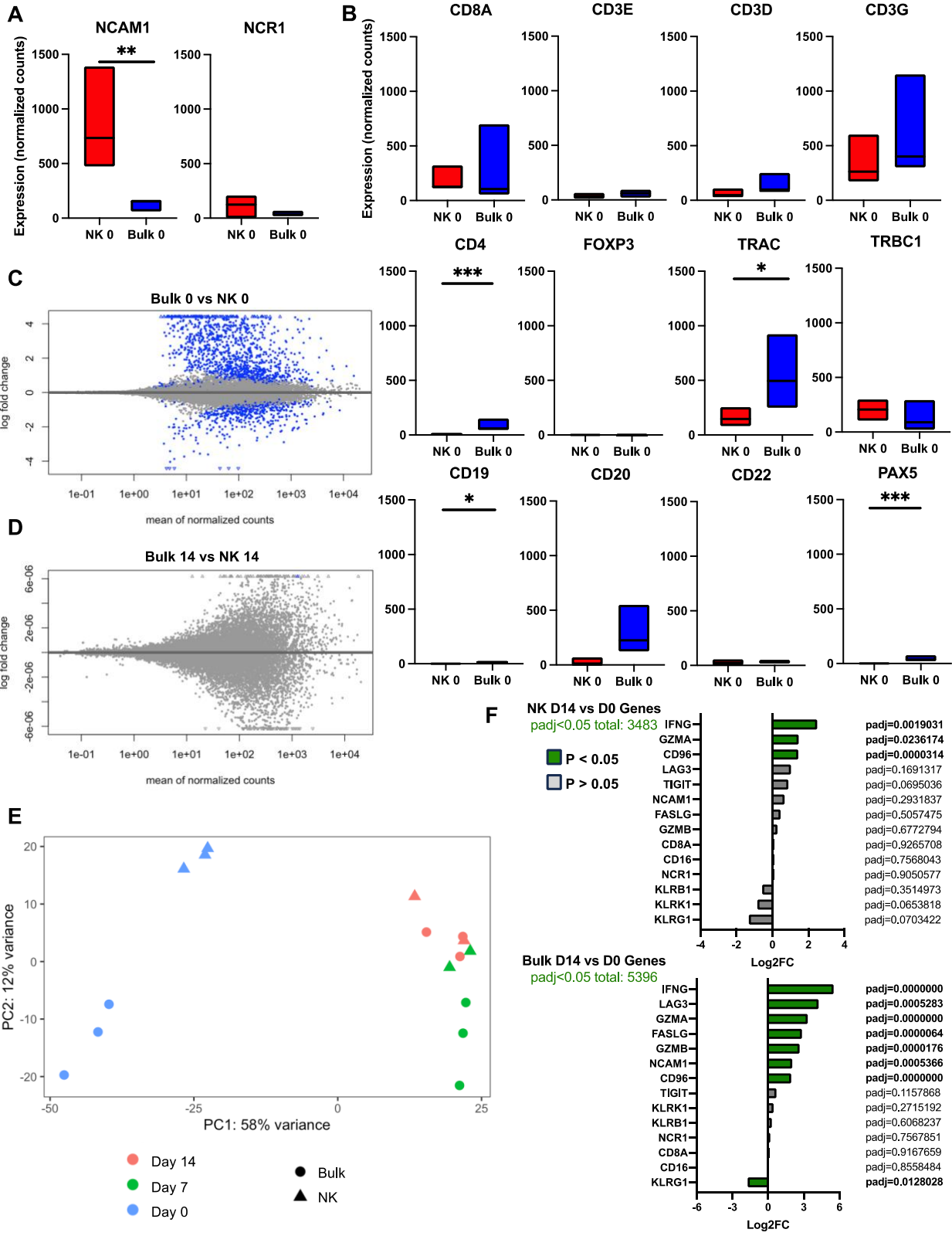
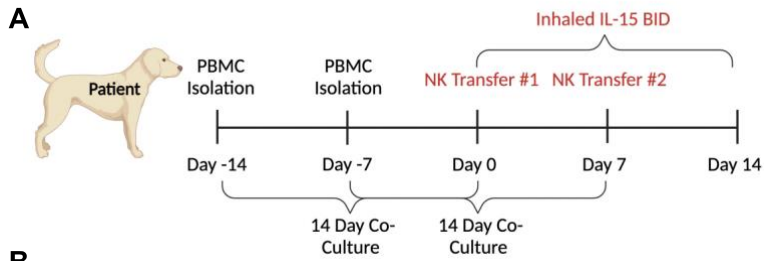


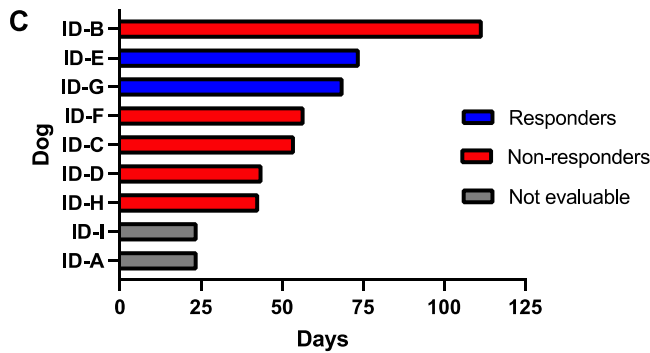
Figure 5. Genomic analysis of human bulk PBMCs versus purified NK cells. Human cells from bulk PBMC and purified NK cell starting populations were collected at days 0, 7, and 14 of 14-day co-culture from three separate human donors and 3'Tag-RNA-Seq was performed. Absolute normalized counts for (A) NCAM1/CD56 and NCR1/NKp46 and (B) T and B cell-related genes were visualized for purified NK cells (NK 0) and PBMCs (Bulk 0) at day 0 co-culture. Certain samples from did not meet RNA quantity standards and were excluded, including day 7 NK isolated and day 14 NK isolated. Floated bars show minimum to maximum of normalized counts for human cells and P values were determined using the DESeq2 package in R, * P<0.05, ** P<0.01, *** P<0.001. MA plots, using a p<0.05 significance threshold, reveal starting populations that are distinct at rest, with (C) 1739 DGEs between bulk PBMCs and purified NK cells at day 0, but converge when activated, with (D) only four DGEs between bulk PBMCs and purified NK cells at day 14 co-culture. (E) Principal component analysis (PCA) of cells aligns with MA plot patterns with high variability at day 0 (blue) and concentration of cell signatures at day 7 (green) and furthermore at day 14 (peach) of co-culture. (F) The log fold change of NK cell-related gene expression was assessed between day 14 and day 0 co-culture from purified NK cells (top) and bulk PBMCs (bottom). Several key genes were significantly different following co-culture compared to day 0 (bold, green). P values were determined using the DESeq2 package in R.



B

Characteristics of autologous NK + IL-15 trial cohort

Dog ID	Weight (kg)	Age (yrs)	Sex	Breed	Diagnosis	Response	Survival (days)
A	42	12	MC	Labrador Retriever	OSA	NE	24
B	35.3	12.1	MC	Swiss Mountain	MEL	PD	112
C	18.8	13.7	FS	German Shepherd	MEL	PD	54
D	25	10.3	MC	Golden Retriever	OSA	PD	44
E	30	7.5	FS	Golden Retriever	OSA	SD	74
F	41	8.2	FS	Labrador Retriever	OSA	PD	57
G	38.5	7.6	FS	Bouvier Des Flandres	OSA	PR	69
H	25.4	13.7	MC	Portugese Water Dog	MEL	PD	43
I	13.1	9	FS	Jack Russel Terrier mix	MEL	NE	24



D

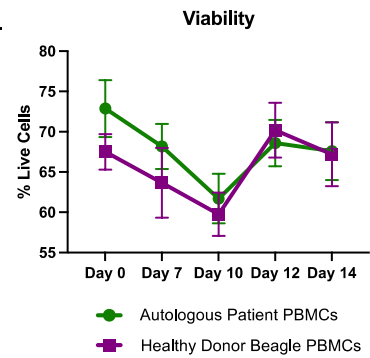
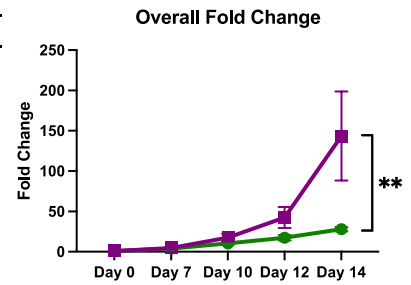
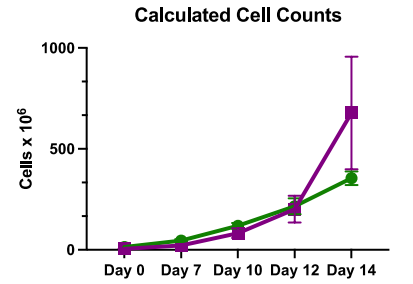


Figure 6. First-in-dog clinical trial of adoptive transfer of autologous canine NK cells. (A)

Schema of trial design combining adoptive transfer of PBMC-expanded autologous NK cells with inhaled IL-15. PBMCs were isolated from whole blood drawn from patient dogs 14 and 7 days before the start of treatment for the 14-day expansion of autologous NK cells. Dogs received IV injection of autologous NK cells at a dose of 7.5 million cells/kg times two.

Additionally, on day 0, dogs began twice daily treatments with inhaled rhIL-15 continuing for 14

days total. (B) Characteristics of the nine total dogs with pulmonary metastatic melanoma (MEL) or osteosarcoma (OSA) that met entry criteria and were enrolled in the trial. Response was determined by RECIST criteria defining Partial Response (PR), Stable Disease (SD),

Progressive Disease (PD), and Not Evaluable (NE). Survival was calculated from initiation of treatment to death or humane euthanasia. (C) Survival plotted as bars color-coded by RECIST

criteria defining responders (PR and SD, blue), non-responders (PD, red), and not evaluable

(NE, grey). (D) Cell counts, fold change, and viability were calculated on days 0, 7, 10, 12, and

14 of the 14-day co-culture for autologous PBMCs isolated from patient blood (green) compared

to PBMCs isolated from healthy beagle blood (purple). Mean (\pm SEM) for expansions of both

injections of PBMC-expanded autologous NK cells were compared to healthy donor PBMC

expansions and plotted over time. P values were determined by mixed effects model, * $P < 0.05$,

** $P < 0.01$.

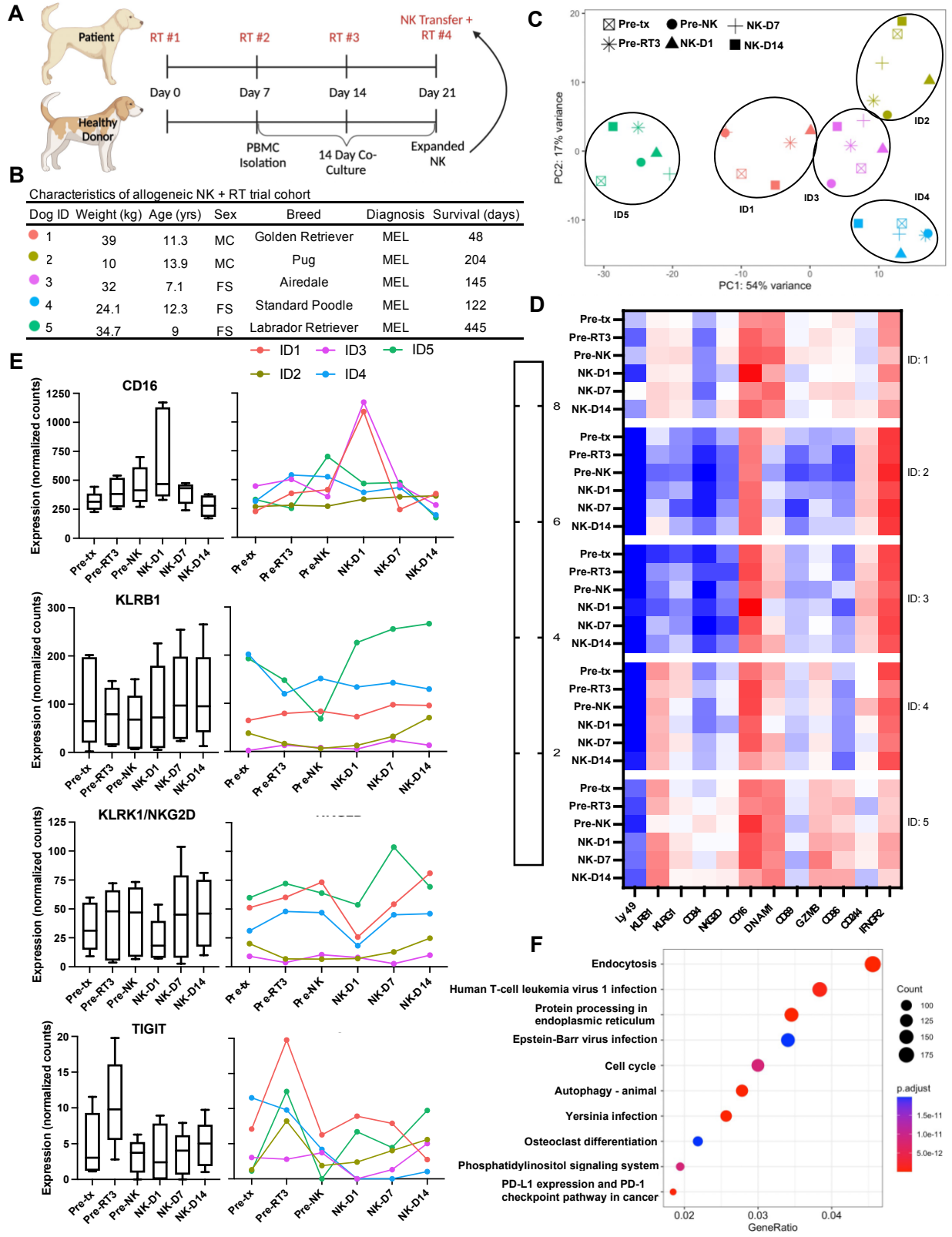


Figure 7. First-in-dog clinical trial of adoptive transfer of allogeneic canine NK cells. (A) Schema of trial design combining adoptive transfer of PBMC-expanded allogeneic NK cells with palliative radiotherapy (RT). PBMCs were isolated from healthy donor beagle blood 14 days before the scheduled NK cell infusion for each patient. Donor PBMC-expanded NK cells at a dose of 7.5 million cells/kg were injected IV in patients upon completion of RT. (B) Characteristics of the five total dogs with malignant melanoma that met entry criteria and were enrolled in the trial. Dogs ID 1, 4, and 5 had known lymph node metastasis on enrollment and dog ID 4 had pulmonary metastasis on enrollment. Survival was calculated from initiation of RT to death or humane euthanasia. PBMCs were isolated from patients' whole blood at 6 time-point and submitted for 3'-Tag-RNA-Seq. (C) Principal component analysis (PCA) of cells color-coded by patient and symbols distinguishing time-point, demonstrated PBMCs clustered based on the dog they originated from rather than time point of treatment. (D) A heatmap depicting log Counts Per Million (logCPM) transformed expression of key NK-related genes shows variation across both patients and treatment. (E) Absolute normalized counts for CD16, KLRB1, NKG2D, and TIGIT were visualized as an aggregate of all patients at each time-point (box and whiskers, left) and individual values by patient (right). While distinct peaks and trends in expression were recognized, changes between time-points were not significant for the genes assessed. (F) Samples across time-points were combined based on donor and compared between the dog with the longest (ID5) and the dog with the shortest (ID1) survival. Induced gene pathways in the dog with the highest survival are depicted as a dot plot of gene ontology (GO) analysis.

2.4 Discussion

Our study compared the trajectory of phenotypic, functional, and genomic changes during the 14-day expansion and activation of canine NK cells derived from both bulk PBMC and CD5-depleted starting populations. Overall, we observed that bulk PBMC-expanded canine NK cells were equivalent, if not superior, to CD5-depleted starting populations. Capitalizing on the practical and clinical-trial enabling aspects of this approach, we performed first-in-dog clinical trials using autologous (N=9) and allogeneic (N=5) NK cells for dogs with malignant melanoma and OSA. These first-in-dog clinical trials showed no serious AEs and preliminary efficacy data for canine cancers with extremely poor prognoses.

The ability to achieve sufficient expansions was a fundamental objective in our study. Concerns regarding expanding adequate cell numbers for cellular immunotherapy are not limited to dogs; studies expanding human NK cells have also been restricted by low cell numbers collected after CD3-selection, reducing the cell numbers available to administer to patients³⁹. Our results show higher average cell counts at day 14 in expanded PBMCs (677 million) compared to expanded CD5-depleted cells (537 million), which although not statistically significant, remains relevant in the clinic, where doses are based on patient weight and can influence whether dogs receive their full treatment. Previously, MHC-low K562 feeder cells with membrane bound IL-21 and cytokine support successfully enriched for NK cells from human PBMCs but had over 21% contamination of T cells at day 21 co-culture⁴⁰. These concerns necessitated our extensive characterization of PBMC-expanded NK cells where we saw minimal CD3+ cells present at day 14 co-culture as assessed by flow cytometry and confirmed by genomic analysis. Flow cytometric analysis of PBMC-expanded day 14 product showed 67% CD3-NKp46+ cells compared to 40.4% in our lab's previous analysis of NK cells expanded from CD5-depleted cells¹⁸. The variability of CD3+ cells in the day 14 product as assessed by flow cytometry and the potential influence of non-specific staining necessitated the need for thorough validation through both bulk and single-cell RNA sequencing. Potential T cell contamination is particularly

relevant in the context of allogeneic transfer, where donor T cells are capable of recognizing healthy recipient tissue as foreign and mounting a response culminating in graft versus host disease. Resting PBMCs analyzed by scRNA-seq were used as a positive control to establish the presence of expected cell types and their proportions prior to expansion. PBMC-expanded NK cells at day 14 confirmed the loss of all cell types except for NK cells. The lack of T cell, B cell, and myeloid gene expression in scRNA-seq and the convergence of distinct PBMC and CD5-depleted resting populations into a near identical NK population at day 14 by bulk RNA-seq, affirmed the ability of the expansion protocol to support the survival of NK cells specifically. This echoes previous work by Gingrich et al., where FACS sorted CD3-NKp46⁺ and CD5^{dim} populations became essentially identical by day 14 of co-culture following the same expansion technique used here¹⁴. This is especially useful in the context of ongoing efforts for better characterization of the phenotype of canine NK cells. Defining canine NK cells has been notoriously difficult, as neither CD5^{dim} nor CD3-NKp46⁺ expression appears to satisfactorily identify all canine NK cells at rest^{14, 41}. This implies that NK selection prior to co-culture could not only limit cell counts but potentially exclude certain NK subsets altogether, depending on the marker used, with implications for function and engraftment of the NK product. This highlights the utility of using human sequencing data to confirm the convergence of distinct cells at day 14 of co-culture, since human NK cells are reliably identified by a CD3-CD56⁺ phenotype and can be reproducibly isolated with available protocols. We used several functional assays to confirm the cytotoxic and cytokine secreting capabilities of our expanded NK cell products. A curious finding was the wide range of cytokine secretion detected by multiplex assay in co-cultured NK cells, particularly IFN- γ . NK cells are known to produce abundant cytokines in response to stimulation. However, RNA-seq results showed significant upregulation of IFNG transcription, aligning with expected functional features of NK cells. RNA-seq also validated this activated phenotype of expanded cells with increased number of cells expression NKG2D and GZMB in scRNA-seq and significant upregulation of KLRB1 and granzyme B along with

downregulation of CD16 in bulk RNA-seq. The loss of CD16 in canine NK cells in response to activation is particularly relevant for comparative oncology immunotherapy studies since it is observed in human NK cells following feeder line co-culture, where it is caused by activation of matrix metalloproteases (MMPs) through target cell contact^{42, 43}. However, cleavage by MMPs is post-translational in nature which would not sufficiently explain the downregulation we observed by RNAseq. Though this transcriptional downregulation was not altogether unexpected since the pattern was similarly reported in a genomic analysis of NK cells expanded from CD5-depleted PBMCs¹⁴. CD16 in this analysis refers to the low affinity immunoglobulin gamma Fc region receptor III (FCGR3A, Locus 478984), which allows for ADCC in NK cells, and lack of CD16 has been shown to impact NK regulation and cytotoxicity^{32, 44}. In our study, expanded PBMCs maintained high percent killing in the context of CD16 transcription downregulation, suggesting that killing is primarily occurring through non-ADCC methods, such as death receptors and perforin and granzyme granules. CD16 is extremely relevant for combinatorial strategies, and our data suggest that CD16 regulation is highly complex in canine NK cells and that dogs with spontaneous cancer may be an informative model interrogating changes in CD16 on NK cells in the future.

While the primary aim in our small cohort using IV adoptive transfer of autologous canine NK cells was to establish feasibility, it is important to note that we observed only modest clinical activity, even with the addition of inhaled IL-15 to support NK engraftment where we did previously observe evidence of clinically meaningful responses²³. Allogeneic NK cells in human trials have demonstrated superior oncologic benefits compared to autologous NK cells, primarily for hematologic malignancies^{2, 5, 45}. This is due, at least in part, to the advantage of MHC mismatch in allogeneic donor cells, where the mismatch between donor KIRs and recipient MHC-I ligands contributes an additional activating signal that promotes activation in favor of NK antitumor response^{46, 47}.

To potentially improve efficacy from autologous transfer, we also piloted a first-in-dog trial using allogeneic NK cells. Since patient-specific immune signatures at baseline and after therapy may ultimately predict outcomes, as has been shown in human immunotherapy trials, we also evaluated DGE signatures from the blood of dogs on therapy⁴⁸. In our canine allogeneic NK recipients, PCA depicted distinct clusters for each patient and reduced variance between patients with similar survival. The intriguing distinctive signatures found within our small patient cohort were further analyzed by comparing gene signatures from PBMCs across treatments between the longest and shortest surviving dogs. The enrichment of pathways associated with response to viral infections suggests an anticipated involvement of NK cells, which are critical in antiviral immunity. However, we observed the highest DGE enrichment for endocytosis pathways, suggesting the influence of non-NK, myeloid populations in shaping differences between gene signatures of these two patients. The assessment of CD16 shedding in NK cells expanded from PBMCs also shapes our interpretation of gene expression patterns in PBMCs from dogs receiving allogeneic NK cells, where CD16 expression peaked one day following NK cell transfer. Beyond CD16, we generally did not see clear, consistent NK signature patterns across patients in response to either RT or NK transfer, highlighting the importance of evaluating larger patient cohorts to better define genomic biomarkers of response and resistance to NK immunotherapy, especially given limitations related to longitudinal access to tumor specimens.

NK cells for human immunotherapy have experienced a steep increase in interest with rapid innovation over the past two decades^{49, 50}. Sources of NK cells for adoptive transfer now include umbilical cord blood stem cells, iPSCs, NK-92 cell line in addition to peripheral blood⁵¹. Like T cells, NK cells can also be genetically engineered to increase specificity and longevity⁵². Imai et al published one of the first successful applications of CAR NKs, determining the ideal expansion of PB NK cells with feeder cells and cytokine support before testing the CAR transduction using the superior expansion method⁵³. Similarly, our study is a crucial first step in

the forward momentum of immunotherapies in dogs, from which we may begin to develop genetically engineering products and novel NK sources. Dogs are a readily available resource for developing new combinations of therapies, which can then inform the most promising paths for improving immunotherapy across species¹³. Future studies will further contextualize dog NK cells compared to human, and the resulting data can be the framework for advancing NK immunotherapy and improving the prognosis for both dogs and humans with aggressive cancers.

In summary, our findings support the use of unmanipulated PBMCs plus feeder line co-culture for adoptive immunotherapy in dogs with cancer. Overall, our pre-clinical and clinical data highlight the safety and feasibility of this technique as a novel platform for optimizing NK immunotherapy in dogs. Our work also demonstrates the strength of the dog model to address practical, clinically relevant questions regarding optimization of novel immunotherapy approaches. Ultimately, teaming rapid and innovative clinical trials with robust genomic characterization is anticipated to advance the field of NK immunotherapy across the bench-to-bedside continuum.

REFERENCES

1. Houot R, Schultz LM, Marabelle A, Kohrt H. T-cell-based Immunotherapy: Adoptive Cell Transfer and Checkpoint Inhibition. *Cancer Immunol Res.* 2015;3(10):1115-22. doi: 10.1158/2326-6066.CIR-15-0190. PubMed PMID: 26438444.
2. Miller JS, Soignier Y, Panoskaltsis-Mortari A, McNearney SA, Yun GH, Fautsch SK, McKenna D, Le C, Defor TE, Burns LJ, Orchard PJ, Blazar BR, Wagner JE, Slungaard A, Weisdorf DJ, Okazaki IJ, McGlave PB. Successful adoptive transfer and in vivo expansion of human haploidentical NK cells in patients with cancer. *Blood.* 2005;105(8):3051-7. Epub 20050104. doi: 10.1182/blood-2004-07-2974. PubMed PMID: 15632206.
3. Gras Navarro A, Björklund AT, Chekenya M. Therapeutic potential and challenges of natural killer cells in treatment of solid tumors. *Front Immunol.* 2015;6:202. Epub 20150429. doi: 10.3389/fimmu.2015.00202. PubMed PMID: 25972872; PMCID: PMC4413815.
4. Rezvani K, Rouce RH. The Application of Natural Killer Cell Immunotherapy for the Treatment of Cancer. *Front Immunol.* 2015;6:578. Epub 20151117. doi: 10.3389/fimmu.2015.00578. PubMed PMID: 26635792; PMCID: PMC4648067.
5. Lupo KB, Matosevic S. Natural Killer Cells as Allogeneic Effectors in Adoptive Cancer Immunotherapy. *Cancers (Basel).* 2019;11(6). Epub 20190603. doi: 10.3390/cancers11060769. PubMed PMID: 31163679; PMCID: PMC6628161.
6. Park JS, Withers SS, Modiano JF, Kent MS, Chen M, Luna JI, Culp WTN, Sparger EE, Rebhun RB, Monjazeb AM, Murphy WJ, Canter RJ. Canine cancer immunotherapy studies: linking mouse and human. *J Immunother Cancer.* 2016;4:97. Epub 20161220. doi: 10.1186/s40425-016-0200-7. PubMed PMID: 28031824; PMCID: PMC5171656.

7. LeBlanc AK, Mazcko CN. Improving human cancer therapy through the evaluation of pet dogs. *Nat Rev Cancer*. 2020;20(12):727-42. Epub 20200915. doi: 10.1038/s41568-020-0297-3. PubMed PMID: 32934365.
8. Dow S. A Role for Dogs in Advancing Cancer Immunotherapy Research. *Front Immunol*. 2019;10:2935. Epub 20200117. doi: 10.3389/fimmu.2019.02935. PubMed PMID: 32010120; PMCID: PMC6979257.
9. Prouteau A, André C. Canine Melanomas as Models for Human Melanomas: Clinical, Histological, and Genetic Comparison. *Genes (Basel)*. 2019;10(7). Epub 2019/06/30. doi: 10.3390/genes10070501. PubMed PMID: 31262050; PMCID: PMC6678806.
10. Hernandez B, Adissu HA, Wei BR, Michael HT, Merlino G, Simpson RM. Naturally Occurring Canine Melanoma as a Predictive Comparative Oncology Model for Human Mucosal and Other Triple Wild-Type Melanomas. *Int J Mol Sci*. 2018;19(2). Epub 2018/01/30. doi: 10.3390/ijms19020394. PubMed PMID: 29385676; PMCID: PMC5855616.
11. Fenger JM, London CA, Kisseberth WC. Canine osteosarcoma: a naturally occurring disease to inform pediatric oncology. *ILAR J*. 2014;55(1):69-85. doi: 10.1093/ilar/ilu009. PubMed PMID: 24936031.
12. Addissie S, Klingemann H. Cellular Immunotherapy of Canine Cancer. *Vet Sci*. 2018;5(4). Epub 20181206. doi: 10.3390/vetsci5040100. PubMed PMID: 30563208; PMCID: PMC6313932.
13. Gingrich AA, Modiano JF, Canter RJ. Characterization and Potential Applications of Dog Natural Killer Cells in Cancer Immunotherapy. *J Clin Med*. 2019;8(11). Epub 2019/10/27. doi: 10.3390/jcm8111802. PubMed PMID: 31717876; PMCID: PMC6912828.

14. Gingrich AA, Reiter TE, Judge SJ, York D, Yanagisawa M, Razmara A, Sturgill I, Basmaci UN, Brady RV, Stoffel K, Murphy WJ, Rebhun RB, Brown CT, Canter RJ. Comparative Immunogenomics of Canine Natural Killer Cells as Immunotherapy Target. *Front Immunol.* 2021;12:670309. Epub 20210914. doi: 10.3389/fimmu.2021.670309. PubMed PMID: 34594320; PMCID: PMC8476892.
15. Michael HT, Ito D, McCullar V, Zhang B, Miller JS, Modiano JF. Isolation and characterization of canine natural killer cells. *Vet Immunol Immunopathol.* 2013;155(3):211-7. Epub 20130628. doi: 10.1016/j.vetimm.2013.06.013. PubMed PMID: 23876304; PMCID: PMC4019669.
16. Huang YC, Hung SW, Jan TR, Liao KW, Cheng CH, Wang YS, Chu RM. CD5-low expression lymphocytes in canine peripheral blood show characteristics of natural killer cells. *J Leukoc Biol.* 2008;84(6):1501-10. Epub 20080815. doi: 10.1189/jlb.0408255. PubMed PMID: 18708592.
17. Somanchi SS, Senyukov VV, Denman CJ, Lee DA. Expansion, purification, and functional assessment of human peripheral blood NK cells. *J Vis Exp.* 2011(48). Epub 20110202. doi: 10.3791/2540. PubMed PMID: 21339714; PMCID: PMC3180743.
18. Canter RJ, Grossenbacher SK, Foltz JA, Sturgill IR, Park JS, Luna JI, Kent MS, Culp WTN, Chen M, Modiano JF, Monjazeb AM, Lee DA, Murphy WJ. Radiotherapy enhances natural killer cell cytotoxicity and localization in pre-clinical canine sarcomas and first-in-dog clinical trial. *J Immunother Cancer.* 2017;5(1):98. Epub 20171219. doi: 10.1186/s40425-017-0305-7. PubMed PMID: 29254507; PMCID: PMC5735903.
19. Judge SJ, Yanagisawa M, Sturgill IR, Bateni SB, Gingrich AA, Foltz JA, Lee DA, Modiano JF, Monjazeb AM, Culp WTN, Rebhun RB, Murphy WJ, Kent MS, Canter RJ. Blood and tissue

- biomarker analysis in dogs with osteosarcoma treated with palliative radiation and intra-tumoral autologous natural killer cell transfer. *PLoS One*. 2020;15(2):e0224775. Epub 20200221. doi: 10.1371/journal.pone.0224775. PubMed PMID: 32084139; PMCID: PMC7034869.
20. Judge SJ, Darrow MA, Thorpe SW, Gingrich AA, O'Donnell EF, Bellini AR, Sturgill IR, Vick LV, Dunai C, Stoffel KM, Lyu Y, Chen S, Cho M, Rebhun RB, Monjazeb AM, Murphy WJ, Canter RJ. Analysis of tumor-infiltrating NK and T cells highlights IL-15 stimulation and TIGIT blockade as a combination immunotherapy strategy for soft tissue sarcomas. *J Immunother Cancer*. 2020;8(2). doi: 10.1136/jitc-2020-001355. PubMed PMID: 33158916; PMCID: PMC7651745.
21. Foltz JA, Somanchi SS, Yang Y, Aquino-Lopez A, Bishop EE, Lee DA. NCR1 Expression Identifies Canine Natural Killer Cell Subsets with Phenotypic Similarity to Human Natural Killer Cells. *Front Immunol*. 2016;7:521. Epub 20161123. doi: 10.3389/fimmu.2016.00521. PubMed PMID: 27933061; PMCID: PMC5120128.
22. PF M, Rossitto PV, T O. Development of monoclonal antibodies to canine T cell receptor-1 (TCR- $\gamma\delta$) and their utilization in the diagnosis of epidermotropic cutaneous T cell lymphoma. *Veterinary Pathology*1994. p. 597.
23. Rebhun RB, York D, Cruz SM, Judge SJ, Razmara AM, Farley LE, Brady RV, Johnson EG, Burton JH, Willcox J, Wittenburg LA, Woolard K, Dunai C, Stewart SL, Sparger EE, Withers SS, Gingrich AA, Skorupski KA, Al-Nadaf S, LeJeune AT, Culp WT, Murphy WJ, Kent MS, Canter RJ. Inhaled recombinant human IL-15 in dogs with naturally occurring pulmonary metastases from osteosarcoma or melanoma: a phase 1 study of clinical activity and correlates of response. *J Immunother Cancer*. 2022;10(6). doi: 10.1136/jitc-2022-004493. PubMed PMID: 35680383; PMCID: PMC9174838.

24. Morrissy AS, Morin RD, Delaney A, Zeng T, McDonald H, Jones S, Zhao Y, Hirst M, Marra MA. Next-generation tag sequencing for cancer gene expression profiling. *Genome Res.* 2009;19(10):1825-35. Epub 20090618. doi: 10.1101/gr.094482.109. PubMed PMID: 19541910; PMCID: PMC2765282.
25. Gingrich AA, Razmara AM, Gingrich PW, Rebhun RB, Murphy WJ, Kent MS, Brown CT, Siegel JB, Canter RJ. Missing a "Missing Self" Mechanism: Modeling and Detection of Ly49 Expression in Canine NK Cells. *Immunohorizons.* 2023;7(11):760-70. doi: 10.4049/immunohorizons.2300092. PubMed PMID: 37971282; PMCID: PMC10696421.
26. Bushnell B, Rood J, Singer E. BBMerge - Accurate paired shotgun read merging via overlap. *PLoS One.* 2017;12(10):e0185056. Epub 20171026. doi: 10.1371/journal.pone.0185056. PubMed PMID: 29073143; PMCID: PMC5657622.
27. Patro R, Duggal G, Love MI, Irizarry RA, Kingsford C. Salmon provides fast and bias-aware quantification of transcript expression. *Nat Methods.* 2017;14(4):417-9. Epub 20170306. doi: 10.1038/nmeth.4197. PubMed PMID: 28263959; PMCID: PMC5600148.
28. Sonesson C, Love MI, Robinson MD. Differential analyses for RNA-seq: transcript-level estimates improve gene-level inferences. *F1000Res.* 2015;4:1521. Epub 20151230. doi: 10.12688/f1000research.7563.2. PubMed PMID: 26925227; PMCID: PMC4712774.
29. LeBlanc AK, Atherton M, Bentley RT, Boudreau CE, Burton JH, Curran KM, Dow S, Giuffrida MA, Kellihan HB, Mason NJ, Oblak M, Selmic LE, Selting KA, Singh A, Tjostheim S, Vail DM, Weishaar KM, Berger EP, Rossmeisl JH, Mazcko C. Veterinary Cooperative Oncology Group-Common Terminology Criteria for Adverse Events (VCOG-CTCAE v2) following investigational

- therapy in dogs and cats. *Vet Comp Oncol.* 2021;19(2):311-52. Epub 20210218. doi: 10.1111/vco.12677. PubMed PMID: 33427378; PMCID: PMC8248125.
30. Deniger DC, Maiti SN, Mi T, Switzer KC, Ramachandran V, Hurton LV, Ang S, Olivares S, Rabinovich BA, Huls MH, Lee DA, Bast RC, Champlin RE, Cooper LJ. Activating and propagating polyclonal gamma delta T cells with broad specificity for malignancies. *Clin Cancer Res.* 2014;20(22):5708-19. Epub 20140515. doi: 10.1158/1078-0432.CCR-13-3451. PubMed PMID: 24833662; PMCID: PMC4233015.
31. Marchetti C, Borghetti P, Cacchioli A, Ferrari L, Armando F, Corradi A, Cantoni AM. Profile of gamma-delta ($\gamma\delta$) T lymphocytes in the peripheral blood of crossbreed dogs during stages of life and implication in aging. *BMC Vet Res.* 2020;16(1):278. Epub 20200808. doi: 10.1186/s12917-020-02504-2. PubMed PMID: 32771003; PMCID: PMC7414535.
32. Romee R, Foley B, Lenvik T, Wang Y, Zhang B, Ankarlo D, Luo X, Cooley S, Verneris M, Walcheck B, Miller J. NK cell CD16 surface expression and function is regulated by a disintegrin and metalloprotease-17 (ADAM17). *Blood.* 2013;121(18):3599-608. Epub 20130313. doi: 10.1182/blood-2012-04-425397. PubMed PMID: 23487023; PMCID: PMC3643761.
33. Myers JA, Miller JS. Exploring the NK cell platform for cancer immunotherapy. *Nat Rev Clin Oncol.* 2020. Epub 2020/09/15. doi: 10.1038/s41571-020-0426-7. PubMed PMID: 32934330.
34. Klingemann HG. Natural killer cell-based immunotherapeutic strategies. *Cytotherapy.* 2005;7(1):16-22. doi: 10.1080/14653240510018000. PubMed PMID: 16040380.
35. Bergman PJ. Canine oral melanoma. *Clin Tech Small Anim Pract.* 2007;22(2):55-60. doi: 10.1053/j.ctsap.2007.03.004. PubMed PMID: 17591290.

36. Proulx DR, Ruslander DM, Dodge RK, Hauck ML, Williams LE, Horn B, Price GS, Thrall DE. A retrospective analysis of 140 dogs with oral melanoma treated with external beam radiation. *Vet Radiol Ultrasound*. 2003;44(3):352-9. doi: 10.1111/j.1740-8261.2003.tb00468.x. PubMed PMID: 12816381.
37. Zhang Q, Bi J, Zheng X, Chen Y, Wang H, Wu W, Wang Z, Wu Q, Peng H, Wei H, Sun R, Tian Z. Blockade of the checkpoint receptor TIGIT prevents NK cell exhaustion and elicits potent anti-tumor immunity. *Nat Immunol*. 2018;19(7):723-32. Epub 2018/06/18. doi: 10.1038/s41590-018-0132-0. PubMed PMID: 29915296.
38. Judge SJ, Dunai C, Aguilar EG, Vick SC, Sturgill IR, Khuat LT, Stoffel KM, Van Dyke J, Longo DL, Darrow MA, Anderson SK, Blazar BR, Monjazebe AM, Serody JS, Canter RJ, Murphy WJ. Minimal PD-1 expression in mouse and human NK cells under diverse conditions. *J Clin Invest*. 2020;130(6):3051-68. doi: 10.1172/JCI133353. PubMed PMID: 32134744; PMCID: PMC7260004.
39. Lee DA, Denman CJ, Rondon G, Woodworth G, Chen J, Fisher T, Kaur I, Fernandez-Vina M, Cao K, Ciurea S, Shpall EJ, Champlin RE. Haploidentical Natural Killer Cells Infused before Allogeneic Stem Cell Transplantation for Myeloid Malignancies: A Phase I Trial. *Biol Blood Marrow Transplant*. 2016;22(7):1290-8. Epub 20160416. doi: 10.1016/j.bbmt.2016.04.009. PubMed PMID: 27090958; PMCID: PMC4905771.
40. Denman CJ, Senyukov VV, Somanchi SS, Phatarpekar PV, Kopp LM, Johnson JL, Singh H, Hurton L, Maiti SN, Huls MH, Champlin RE, Cooper LJ, Lee DA. Membrane-bound IL-21 promotes sustained ex vivo proliferation of human natural killer cells. *PLoS One*. 2012;7(1):e30264. Epub

20120118. doi: 10.1371/journal.pone.0030264. PubMed PMID: 22279576; PMCID: PMC3261192.

41. Grøndahl-Rosado C, Boysen P, Johansen GM, Brun-Hansen H, Storset AK. NCR1 is an activating receptor expressed on a subset of canine NK cells. *Vet Immunol Immunopathol.* 2016;177:7-15. Epub 20160524. doi: 10.1016/j.vetimm.2016.05.001. PubMed PMID: 27436439.
42. Harrison D, Phillips JH, Lanier LL. Involvement of a metalloprotease in spontaneous and phorbol ester-induced release of natural killer cell-associated Fc gamma RIII (CD16-II). *J Immunol.* 1991;147(10):3459-65. PubMed PMID: 1834741.
43. Grzywacz B, Kataria N, Verneris MR. CD56(dim)CD16(+) NK cells downregulate CD16 following target cell induced activation of matrix metalloproteinases. *Leukemia.* 2007;21(2):356-9; author reply 9. doi: 10.1038/sj.leu.2404499. PubMed PMID: 17251901.
44. Srpan K, Ambrose A, Karampatzakis A, Saeed M, Cartwright ANR, Guldevall K, De Matos GDSC, Önfelt B, Davis DM. Shedding of CD16 disassembles the NK cell immune synapse and boosts serial engagement of target cells. *J Cell Biol.* 2018;217(9):3267-83. Epub 20180702. doi: 10.1083/jcb.201712085. PubMed PMID: 29967280; PMCID: PMC6122987.
45. Lamb MG, Rangarajan HG, Tullius BP, Lee DA. Natural killer cell therapy for hematologic malignancies: successes, challenges, and the future. *Stem Cell Res Ther.* 2021;12(1):211. Epub 20210325. doi: 10.1186/s13287-021-02277-x. PubMed PMID: 33766099; PMCID: PMC7992329.
46. Oh S, Lee JH, Kwack K, Choi SW. Natural Killer Cell Therapy: A New Treatment Paradigm for Solid Tumors. *Cancers (Basel).* 2019;11(10). Epub 20191011. doi: 10.3390/cancers11101534. PubMed PMID: 31614472; PMCID: PMC6826624.

47. Liang S, Xu K, Niu L, Wang X, Liang Y, Zhang M, Chen J, Lin M. Comparison of autogeneic and allogeneic natural killer cells immunotherapy on the clinical outcome of recurrent breast cancer. *Onco Targets Ther.* 2017;10:4273-81. Epub 20170828. doi: 10.2147/OTT.S139986. PubMed PMID: 28894383; PMCID: PMC5584889.
48. Kovács SA, Fekete JT, Gyórfy B. Predictive biomarkers of immunotherapy response with pharmacological applications in solid tumors. *Acta Pharmacol Sin.* 2023. Epub 20230413. doi: 10.1038/s41401-023-01079-6. PubMed PMID: 37055532.
49. Piccinelli S, Romee R, Shapiro RM. The natural killer cell immunotherapy platform: An overview of the landscape of clinical trials in liquid and solid tumors. *Semin Hematol.* 2023;60(1):42-51. Epub 20230305. doi: 10.1053/j.seminhematol.2023.02.002. PubMed PMID: 37080710.
50. Kundu S, Gurney M, O'Dwyer M. Generating natural killer cells for adoptive transfer: expanding horizons. *Cytotherapy.* 2021;23(7):559-66. Epub 20210108. doi: 10.1016/j.jcyt.2020.12.002. PubMed PMID: 33431318.
51. Laskowski TJ, Biederstädt A, Rezvani K. Natural killer cells in antitumour adoptive cell immunotherapy. *Nat Rev Cancer.* 2022;22(10):557-75. Epub 20220725. doi: 10.1038/s41568-022-00491-0. PubMed PMID: 35879429; PMCID: PMC9309992.
52. Schmidt P, Raftery MJ, Pecher G. Engineering NK Cells for CAR Therapy-Recent Advances in Gene Transfer Methodology. *Front Immunol.* 2020;11:611163. Epub 20210107. doi: 10.3389/fimmu.2020.611163. PubMed PMID: 33488617; PMCID: PMC7817882.
53. Imai C, Iwamoto S, Campana D. Genetic modification of primary natural killer cells overcomes inhibitory signals and induces specific killing of leukemic cells. *Blood.*

2005;106(1):376-83. Epub 20050308. doi: 10.1182/blood-2004-12-4797. PubMed PMID:
15755898; PMCID: PMC1895123.

3 Single Cell Atlas of Canine Natural Killer (NK) Cells Identifies Distinct Tissue Resident and Tumor-Infiltrating Profiles with Candidate Genomic Biomarkers from First-in-Dog NK Immunotherapy Trials

3.1 Introduction

Natural Killer (NK) cells are enigmatic innate lymphoid cells that uniquely blur the boundaries of innate and adaptive immunity due to their ability to recognize targets without sensitization while still possessing memory-like and tissue resident features¹⁻³. Equipped with an extensive array of inhibitory and activating receptors, NK cells use the dynamic engagements of these receptors to mediate effective antiviral and anticancer responses along with comparable tolerance to healthy cells and tissues. These features have made NK cells attractive candidates for cancer immunotherapy given their ability to spontaneously target diverse cancer cells that have evaded other immune recognition strategies and their modest association with toxicity. NK cell therapies, including recent advances in CAR NK cells, have led to significant improvements in the outcomes of patients with leukemias and lymphomas^{4, 5}. However, the complex tumor microenvironment (TME) of solid tumors introduces additional challenges in cancer immunotherapy, and further work is needed to achieve consistent success of NK cells in the treatment of these cancers.

Comparative oncology takes advantage of the similarities shared across species to identify and optimize treatments that are projected to have success in clinical trials⁶⁻⁸. Although extensive studies have been completed in mice to advance NK immunotherapy, murine and human NK cells have significant differences in phenotype and function (intriguingly more than T cells) which have impaired clinical translation^{9, 10}. Of note, recent transcriptomic analyses have revealed greater homology between human and dog NK cells than human and mouse NK cells¹¹. Importantly, beyond NK cell-specific similarities between dogs and humans, dogs are also an outbred species that develop cancers spontaneously in the context of an intact immune system,

further supporting their strength as a valuable model of human malignancy. This is especially true given the genotypic and phenotypic resemblance of spontaneous canine cancers to human cancers including immunoediting and immune surveillance with data showing homology between dog and human lymphoma, osteosarcoma, mammary tumors, melanoma, and high grade gliomas. Consequently, the canine model is actively being leveraged to inform human cancer treatments, including novel immunotherapy combination trials for osteosarcoma and melanoma¹²⁻¹⁴.

Numerous studies have highlighted the heterogeneity of NK cells, including diverse subsets of NK cells across tissue compartments in humans and mice. In humans, classical NK subsets include putative immature, CD56^{bright}CD16^{dim} cytokine-secreting NK cells that predominate in lymph nodes versus mature cytotoxic CD56^{dim}CD16^{bright} NK cell subsets that predominate in the blood¹⁵. Additional subsets include terminally differentiated NK cells found frequently in the lung¹⁶, mixed maturation state NK subpopulations in the liver¹⁷, and exhausted NK cells in the TME¹⁸. However, identification of equivalent NK subsets in dogs has not been delineated. While spontaneous cancer in dogs presents a readily available, high fidelity model for translation to human cancers, studies are limited due to the gap in knowledge regarding NK subsets present in the dog. Additionally, it's paramount to address the differences between circulating and tissue NK cells in order to interpret tissue-specific responses in cancer, which can vary from those seen in the blood. Fortunately, high-quality canine reference genomes have been assembled allowing for the use of single-cell RNA sequencing (scRNAseq) to bypass limitations and investigate canine NK cells at the individual level with extensive markers for accurate identification and characterization.

To uncover the heterogeneity of NK cells throughout body compartments and identify potential targets for immunotherapy or potential sources and modifications for adoptive NK transfer, we created a transcriptomic atlas of canine NK cells across blood, multiple tissues, and soft tissue sarcoma in dogs with a comparative analysis of human tissues for cross-species validation.

Taking advantage of access to patient samples from three first-in-dog canine immunotherapy trials, we also performed single cell analysis of circulating NK cells from dogs in these trials. We observed unique signatures across organs consistent with activated, stem-like, and conventional/regulatory NK cells in the lung, placenta, and liver, respectively. We observed considerable overlap of canine tissue resident NK subsets with known subsets in humans with both tissue and tumor-unique profiles conserved across species. Finally, we demonstrate that dogs with favorable response to NK targeted immunotherapy treatments have significant upregulation of NK activation genes with implications for outcomes on human sarcoma patients. Together, our data establish a landscape for evaluating NK cell tissue and tumor adaptation and maladaptation in dogs, inform the development and compartmentalization of NK cells in dogs, and begin to unravel the mechanics underpinning NK plasticity and heterogeneity in healthy and cancer-bearing dogs with relevance to humans.

3.2 Materials and methods

3.2.1 Sample acquisition and processing

For canine samples, lung, liver, spleen, and placenta samples were obtained from patients undergoing surgical procedures at the UC Davis VMTH. When applicable, only visually unaffected, non-tumor bearing tissue was used. Processing of spleen and placenta consisted of mechanical digestion followed by incubation with RBC lysis buffer for five minutes at 4°C. Liver processing included mechanical digestion followed by a cell separation step using Percoll and PBS+3% FBS before RBC lysis¹⁹. Lung processing included mechanical digestion followed by enzymatic digestion using DNase and collagenase²⁰. PBMCs were collected from whole blood from healthy beagle donors or dogs undergoing immunotherapy treatments as indicated. Processing was performed as described previously^{11, 21, 22}.

For human samples, the collection of blood and tissue Specimens was approved by the IRB at the University of California, Davis (Protocol #218204 UC Davis Pathology Biorepository -

Tissue, Blood, Urine and Other Biological Material). Human samples were processed as described previously^{11, 21, 22}.

3.2.2 Fluorescence-activated Cell Sorting

After processing, dog lung, liver, placenta and tumor cells were washed with PBS and staining buffer. Canine cells were incubated with Fc receptor blocking solution (Canine Fc Receptor Binding Inhibitor, Invitrogen #14-9162-42), and stained with rat anti-dog monoclonal antibody CD45-EF450 (clone YKIX716.13, Invitrogen #48-5450-42). Human cells were incubated with Human TruStain Fc receptor blocking solution (BioLegend, #422302), and stained with mouse anti-human monoclonal antibody CD45-BV510 (clone HI30, BioLegend). Live/dead discrimination was performed using Fixable Viability Dye 780. Cell sorting for live CD45+ cells was performed using the Becton Dickinson “Aria II” Cell Sorter (Becton Dickinson, San Jose, California, USA).

3.2.3 Single-Cell RNA Sequencing and Analysis

Single-cell suspensions of 700–1200 cells/ μ L with a minimum of 40 μ L of PBS/0.5% bovine serum albumin suspension buffer were submitted for library preparation and sequencing using the 10X Chromium Next GEM Single-Cell 3' V.3.1 Gene Expression protocol performed by the UC Davis Genome Center as previously described²¹. Human (GRCh38) and canine (CanFam3.1) reference genomes were created using the *cellranger mkgtf* and *cellranger mkref* pipelines. Raw fastq files were aligned to the relevant reference genome and feature-barcode matrices were created using CellRanger v.7.1.0 (10x Genomics). The feature-barcode matrices were uploaded in Rstudio and analyzed using Seurat. Seurat objects were created with a minimum cell threshold of 3 and minimum features of 200. Only cells with $\leq 15\%$ of mitochondrial counts and unique feature counts ≥ 200 and $\leq 5,000$ -6,000 were filtered for analysis. For the canine tumor sample, cells also had additional filtering for $PTPRC > 0$. Data then underwent standard Seurat processing workflow which included normalization, identification of highly variable features (2,000), and scaling. Cells were then clustered through a standard workflow

that included linear dimensional reduction, determination of the k-nearest neighbor (KNN) using the top PCs based on the generation and interpretation of an elbow plot, and then implementation using a resolution of 0.5 after testing of multiple PCs and resolutions. Doublets were then identified and removed using DoubletFinder before the cell clustering workflow was repeated with doublets and unwanted cells removed.

For merged analyses, samples were integrated using Harmony²³. Layers were joined and cells clustered using 50 PCs and resolution of 2. For subset datasets, cells identified as NK cells were subset followed by normalization, identification of variable features, scaling, PCA, clustering and generation of UMAP. Differential gene expression testing was performed using the FindAllMarkers function in the Seurat R package to identify differences between two identified groups using the Wilcoxon Rank Sum test. Genes were only considered significant if the adjusted p-value, using Bonferroni correction, was $p < 0.05$.

Tissue signatures were developed by determining significantly different genes between NK cell within one tissue compared to NK cells in all remaining tissues. The list of DEGs was then filtered to include only include genes that had an adjusted p-value < 0.05 , average fold change > 1.0 , and had expression in at least 20% of NK cells. Representative genes were selected and categorized by associations obtained from public databases (EnrichR, Uniprot, and NCBI).

Correlations were determined by extracting the scaled gene expression from merged NK cell datasets, then the Cor function was used to find pairwise correlation coefficients and create a correlation matrix. The correlation matrix was then visualized using CorrPlot with hierarchical clustering to order the variables. To infer cell-cell interactions across all tissues as well as within individual tissues, CellChat was used²⁴. The strengths and weights of interactions were based on the CellChat ligand-receptor interaction database. Pseudotime analysis was completed using Monocle3 with clustering using a resolution parameter set to 1×10^{-3} and the root set based on visualizations of cluster IDs, partition assignments, and tissue of origin.

3.2.4 Publicly available data

Data analyzing single cell composition of the human soft tissue sarcoma tumor microenvironment previously published by Subramanian et al. were downloaded from GEO under accession code GSE53844²⁵. Barcodes, features, and matrix files for sample ID SRC141 were available after data processing and read alignment by the authors using CellRanger v6.0.0 (10x Genomics) and human genome assembly GRCh38. These files were uploaded to R and used to create a Seurat object subject to the same workflow used for canine tumor.

3.3 Results

3.3.1 Canine NK cells vary in abundance and immune interactions across tissues

To understand canine NK cell heterogeneity, activation, and maturation states, we created a transcriptomic atlas of canine NK cells across tissues and peripheral blood. We began by obtaining two samples each of canine placenta, spleen, liver, and lung in addition to a single blood sample from a healthy beagle donor and sorting for CD45+ immune cells to perform scRNAseq (Figure 1A, **Figure S1A**). After quality control and processing, samples were integrated for a dataset of approximately 50,000 high-quality cells available for analysis. We used harmony integration to remove batch effects and allow for cell grouping based on cell type rather than donor or tissue²³, as demonstrated in uniform manifold approximant and projection (UMAP) plots color coded by tissue or cell type (**Figure 1B and 1C**). Immune populations, including NK cells, varied across tissues (**Figure 1C and 1D**) with the largest proportion of NK cells found in the liver, making up nearly 45% of CD45+ cells. Proportions of other cell types also matched known cell distributions in tissues including large populations of myeloid cells in the lung and B cells in the spleen (**Figures 1D and 1E**). Immune cell identities were determined by interrogation of cluster-specific gene markers against canonical immune cell type markers. Canine NK cells were confirmed as expressing NCR3 and KLRK1 but lacking the CD3 expression seen in CD4 and CD8 T cells (**Figure 1F**), previously identified as a transcriptomic

signature of canine NK cells in the blood²⁶. Since cell-to-cell communications and cues vary based on maturation and activation states, we used CellChat to further predict cell interactions within tissues²⁴. NK cells in the lung had the strongest interactions with myeloid cells, which is particularly relevant due to the immunoregulatory interactions between NK and myeloid cells in tumor microenvironments (**Figure 1G**). Meanwhile, NK cells in the spleen had minimal interaction with myeloid cells and stronger interactions with neutrophils. The combined tissue circle plot depicts a complex network of cell interactions across all cell types. These interactions were further elucidated by determination of all significant ligand receptor interactions between NK cells and other cell types (**Figure 1H**). The SELL-SELPLG interaction between NK cells and other NK cells, B cells, neutrophils and myeloid cells was previously appreciated in treatment naive canine osteosarcoma between NK cells and mature regulatory dendritic cells²⁷. The two interactions with the highest probability were PTPRC-MRC1 in myeloid cells in the lung and CLEC2D-KLRB1 with other NK cells in the liver (**Figure 1H**). The CLEC2D-KLRB1 interaction has been noted between myeloid and NK cells in human neuroblastoma and between tumor and CD8 T cells in human rhabdomyosarcoma^{28, 29}, pointing to the presence of immunosuppressive communications in the liver.

3.3.2 Canine NK cells demonstrate tissue-specific gene signatures

To better understand the characteristics of canine NK cells and their diversity across tissues, we then analyzed the NK cell clusters from the integrated dataset and performed unsupervised clustering for higher resolution analysis of these cells. The majority of these cells were from liver (n=6,643) (**Figure 2A, 2B**). NK cells across tissues expressed genes associated with a conventional NK cell signature, including NCR3, KLRK1, and GZMA (**Figure 2C**). The topmost significant genes of tissue-specific NK cells when compared to all remaining NK cells were interrogated to elucidate the heterogeneity of NK gene expression (**Figure 2D**). Liver NK cells had increased expression of conventional NK genes including IL12RB2 and GZMA, the latter

being identified as one of seven genes that drive human NK cell subpopulations³⁰. Additionally, NK cells in the lung expressed CXCL8 which is induced in activated NK cells leading to the migration and activation of other cell types such as dendritic cells³¹. We then combed through these significant gene sets to determine signatures that represented each tissue. Within NK cells in the placenta, this included genes associated with differentiation and signaling (**Figure 2E**). The involvement of RUNX1 and TCF7 in NK cell maturation has been well-documented^{17, 32, 33}, and TCF7 expression has been inversely correlated with lymphocyte exhaustion in human breast cancer³⁴. Genes associated with activation and migration were significantly enriched in lung NK cells (**Figure 2F**). Of note, we observed upregulation of multiple immune recruitment associated genes, CXCR4, CCL4, and CCL5, implicating lung NK cells in the orchestration of coordinated multi-cellular immune responses. The expression of these genes, particularly CCL4, have often associated with the activated and mature, effector CD56^{dim} classification in human NK cells^{15, 30, 32, 35-37}. Interestingly, NK cells in the liver expressed a mixed signature with genes associated with immunoregulation in combination with genes associated with activation and differentiation (**Figure 2G**). One of the most recognized inhibitory receptors in NK cells, CD96, was upregulated simultaneously with cytotoxicity receptors GZMA and FASLG, indicative of the sensitive balance of opposing receptors that culminate in NK responses. We also observed expression of the activation marker, CD160, known to be enriched in NK cells identified in hepatocellular carcinoma³⁶, but also potentially a marker of early, tissue-resident ILC1 cells¹⁷. Like the placenta, the liver also had increased expression of RUNX3 and IL12RB2, both associated with NK precursors and differentiation^{38, 39}. Due to the overlapping characterization of liver NK cells with both placenta and lung NK cells, we determined the key differences between these organs with direct comparisons of liver and lung NK cells and liver and placenta NK cells (**Figures 2H, 2I**). In both lung and placenta NK comparisons, genes in liver NK cells had relatively reduced significance and log2FC. We also observed upregulation of AUTS2 and TXK in liver NK cells, both of which been associated with poor prognosis and

malignant progression in multiple human cancers^{40, 41}. Additional differentiation-related genes were confirmed in placenta NK cells, such as IL1R1 which has been shown to play a role in precursor commitment to the NK cell lineage⁴². These data demonstrate that canine NK cells have tissue-specific gene signatures despite moderate functional overlap and underscore the plasticity of NK cells across tissue and organs related to maturation and activation states.

3.3.3 Canine tissue and peripheral NK cells can be categorized into distinct subsets

Given the known diversity of human NK cells across peripheral blood and tissue, we then evaluated for comparable cross-species heterogeneity in canine NK cells. NK clusters with overlapping genes were combined into 6 dog NK clusters labeled d1-6 (**Figure 3A**). Using pseudotime analysis, we determined that clusters d1 and d6 were furthest along the inferred trajectory (**Figure 3B**). The pseudotime trajectory could then be contextualized by classification of subclusters by genes that were best able to distinguish one cluster from another. These classifications included cytotoxicity, signaling, regulation, differentiation, proliferation and trafficking, and inflammation/migration (**Figure 3C, 3D**). The determination of a mature, cytotoxic subset, d1, showed high alignment with the CD56^{dim}CD16^{bright} subset of human NK cells based on its effector functions and predominance in PBMCs (**Figure 3E**). Generally, genes defining clusters d1, d2, and d3 were expressed in multiple clusters with high expression of conventional NK genes, while genes in d4, d5, and d6 had comparably unique gene expression with higher fold change in gene expression compared to other clusters (**Figures 3D, 3F, 3G**). All subclusters were present across tissues except for d6, which clustered farthest along the pseudotime trajectory, was absent in PBMCs, and showed only minimal presence in liver NK cells. Notably, this cluster was most abundant in lung NK cells, consistent with genes associated with inflammatory response and infiltration, including CXCL8 which was one of the top five significant genes in lung NK cells, suggesting a highly specialized function in lung mucosal immunology. Genes involved in proliferation and trafficking were representative of cluster d5,

and these clusters were most abundant in lung and placenta NK cells. This included CD52 and IL7R, markers of CD56^{bright} NK cells in humans^{15, 35, 43}. As expected, the cluster associated with differentiation, d4, was largely found in the placenta as well as in liver NK cells. Genes in cluster d4 have also been associated with CD56^{bright} features, like LEF1, but also include genes specific to stem cells, such as NOTCH2 found in human decidual NK cells⁴⁴. Overall, the dog NK clusters demonstrated significant heterogeneity consistent with human NK heterogeneity^{32, 45-47}, coincident with gene signatures that aligned with our distinct canine tissue-specific NK signatures and also overlapped with established NK subtypes in humans.

3.3.4 Canine sarcoma infiltrating NK cells are heterogeneous with unique activation and exhaustion features

Interpreting the unique characteristics of immune cells of the TME is critical for understanding potential targets and improving cancer immunotherapy. To place our tissue-specific canine NK signatures in the context of tumor-resident immune cells, we next analyzed immune cells from a canine soft tissue sarcoma. The dissociated tumor sample was sorted for CD45+ immune cells and analyzed by scRNAseq to identify cell types and their proportions (**Figure 4A, 4B, 4C**). A total of 6,514 high quality cells were available for analysis. Similar to our blood and tissue samples, NK cells were primarily distinguished by NCR3 and KLRK1 with concurrent lack of CD3 expression. NK cells comprised 15% of the total CD45+ cells, which was the largest proportion of NK cells in any of our investigated tissues except for liver (**Figure 4C**). We then subset the NK cells in the tumor and integrated them with NK cells from other canine tissues and blood (**Figure 4D**). This new integrated dataset was utilized to conduct further comparisons of tumor NK cells to those in other tissue compartments. The top genes significantly upregulated in tumor NK cells compared to NK cells in all other samples included genes with a variety of functions, including PLXNA4, known to be upregulated in NK cells that have been reprogrammed after exposure to malignant cells⁴⁸ (**Figure 4E**). Tumor NK cells downregulated

canonical NK activation markers, such as FASLG, GZMB, and KLRD1, the latter being a marker of favorable prognosis in human cancers if present in either the serum or tumor^{49, 50} (**Figure 4F**). Conversely, canonical NK inhibitory markers were significantly upregulated in canine intra-tumoral NK cells, aligning with previous reports of the inverse relationship between inhibitory genes CD96 and KLRB1 and cytotoxicity signatures in NK cells in human tumors²⁸. The genes upregulated in canine tumor NK cells compared to all other NK cells were evaluated to determine a canine STS NK signature (**Figure 4G**). The most common were genes associated with chronic activation and cancer pathways, but we also observed significant upregulation of genes associated with adhesion and migration, differentiation and proliferation, and signaling (**Figure 4H**). This pattern was further confirmed when tumor NK cells were enriched for the d2 and d3 dog NK subclusters, classified by signaling and regulation respectively. Notably, there was clear overlap in expression characteristics between dog sarcoma and liver NK cells, suggesting potential mixed immunoregulatory and cytotoxic programs in canine sarcoma NK cells consistent with our liver scRNAseq data. Tumor NK cells were enriched for the d2 and d3 dog NK subclusters which were positively correlated to liver NK cells (**Figure 4I**). These results appear to corroborate the exhausted phenotype of intra-tumor NK cells seen in human cancers⁵¹. Though tumor-resident NK cells had unique gene signatures in the dog, certain overlapping characteristics with tissue-resident NK cells implies the malleability of NK cell states rather than strict or static functional groups.

3.3.5 Human NK cells mirror dog NK cells in abundance and immune interactions across tissues

The insights gained from the characterization of canine NK cells can improve the comparative model and help advance NK immunotherapy across species. To validate the results of our canine NK data, we created an equivalent transcriptomic atlas of human NK cells across tissues and peripheral blood. We acquired samples of placenta, spleen, liver, lung, and blood from

healthy/ non-cancer bearing human patients. The tissues were dissociated into single cell suspension and sorted for CD45+ immune cells before submitting for scRNAseq. After stringent quality control, processing, and integration to remove batch effects, approximately 34,000 cells were available for analysis and visualized by UMAP (**Figure 5A, 5B**). Expected cell types were found across the tissues, including a NKT cell cluster that was not apparent in our canine analysis and was particularly evident in human placenta (**Figure 5B, 5C**). Similar to our canine samples, the largest human NK proportion was found in the liver, making up 36% of CD45+ cells, compared to the 44% found in canine liver. In contrast, the proportions of NK cells in other tissues were greater in the human tissues compared to dog (**Figure 5C, 5D**). The identity of human cell types was confirmed by known canonical markers, with the advantage of human NK cells having unique expression of CD56 (NCAM1) not expressed in canine NK cells (**Figure 5E**). Once cell identities were annotated, we used CellChat to interrogate the inferred interactions between cell types across tissues, highlighting distinct interactions with NK cells (**Figure 5F**). Overall, human NK cells had particularly strong interactions with CD8 T cells, likely representative of their coordinated roles in immune surveillance and anti-tumor/ anti-viral responses^{52, 53}, with additional notable interactions between NK cells and both myeloid and NKT cells in the lung. Canine NK cells had noticeably stronger interactions with myeloid cells in the lung compared to human, but the total interactions depict a similarly complex network of cell interactions in both species. We then queried the ligand-receptor interactions that were significant within the cell communication network to discern the states of the NK cells based on their outgoing signals. There were greater numbers of significant NK receptor-ligand interactions in human than in canine tissues with 65 and 29, respectively (**Figure 5G**). However, certain conserved patterns emerged across species, including the interaction of PTPRC-MRC1 between myeloid and NK cells in the lung, which was highly frequent in both human and dog. We also observed high probability of interaction of CLEC2D-KLRB1 between NK cells and CD8 T cells across all tissues in both human and dog. The multiple HLA-dependent interactions

between NK cells and CD8 T cells were particularly striking in our human data, with the greatest probability occurring between classical HLA class I molecules on NK cells and CD8A/B on CD8 T cells in the peripheral blood. Our results suggest notable cross-species similarities in NK proportions and cell interactions further underlining the homology in the immunogenomics of human and canine NK cells, especially when compared to murine counterparts¹¹.

3.3.6 Canine and human NK cells show homology across blood, tissue, and tumor compartments

To recapitulate our canine NK analysis, we then subset the identified NK cells cluster in the integrated human dataset and performed unsupervised clustering to confirm the presence of 5,491 NK cells across tissues (**Figure 6A, 6B**). Similar to previous, the largest number of NK cells were identified in the liver (n=1,985), followed by the lung (n=1514), and then PBMC, placenta, and spleen with an average of 664 cells each. To more directly compare human and canine NK cells, we integrated the NK cell clusters including NK cells from the liver, lung, PBMC, placenta, and spleen which clustered distinctly based on species (**Figure 6C**). To determine the similarities in tissue-specific genes in NK cells across species, we analyzed the genes that were significantly upregulated in each tissue in dog and human separately, and then identified the overlapping DEGs. There were 98 upregulated genes that overlapped across species in lung NK cells, 18 upregulated genes in placenta NK cells and 15 upregulated genes in liver NK cells (**Figure 6D, 6E, 6F**). Notable genes included CCL4 and CXCR4, which were part of the dog lung NK activation signature and similarly upregulated in human lung. Likewise, ZNF683 and IGF2BP3 were part of the dog placenta NK differentiation signature and also upregulated in human placenta. The activating NK receptor CD160, associated with canine liver NK cells, was similarly upregulated in human liver NK cells. Given these similarities, we then directly compared tissue resident NK cells across species to understand what genes were different (**Figures G, H, I**). Notably, dog placenta NK cells had increased expression of

activation and signaling markers, BCL2A1 and CRIP1, compared to human placenta NK cells. However, NK cells in the human placenta upregulated KLRD1 in comparison to dog placenta, a canonical NK marker which functions in NKG2 heterodimers to create either activating or inhibitory signals.

Ultimately, the maturation and activation states of NK cells in the peripheral blood and tissue are most relevant to translational analyses in the context of how these cells adjust within the tumor microenvironment. We therefore accessed a publicly available sample of human undifferentiated pleomorphic sarcoma (UPS)²⁵, which served as a comparable match for our canine sarcoma sample. The UPS sample of Subramanian et al. included 1658 CD45+ cells based on threshold of PTPRC>0. Only 4% of those cells were identified as NK cells, which we then integrated with our own human tissue and blood NK cell dataset (**Figure 6J**). The top significant genes in tumor NK cells were relatively distinct compared to the moderate overlap seen in top genes across other tissues and blood (**Figure 6K**). We next took our total tumor, tissue, and peripheral NK cells from human patients and integrated them with our equivalent canine dataset (**Figure 6L**). There were 172 genes shared between NK cells in canine and human tumor tissue that were significantly upregulated compared to their respective canine and human NK cells in other tissue samples (**Figure 6M**). We saw cross-species upregulation of immunoregulatory receptor, NRP1, often expressed in Treg cells but also in NK cells, with potential as a checkpoint target^{54, 55}. Additionally, COL1A1 and FBLN1 were previously used as markers for canine tumor or fibroblast cells²⁷, and MMP2 and DCN as markers of mesenchymal-like cells in human cancers^{29, 56}, with the latter also being a top differentially expressed gene in our canine STS sample (**Figure 4E**). Given that canine and human STS tumor samples had the largest overlap in shared upregulated genes against their respective tissue and blood samples, we used a direct contrast of the tumors to understand the biological relevance of top DEGs (**Figure 6N**). Human tumor NK cells had increased expression of EID1, one of the markers of the regulatory

canine NK subcluster d3, and ISG15, part of the differentiation signature in canine placenta NK cells (**Figures 2E, 3C**). Also, human sarcoma-infiltrating NK cells expressed, BST2, which has also been observed to be upregulated in blood cancer cell lines that were exposed to NK cells⁵⁷. On the other hand, canine tumor NK cells had increased expression of PTPRC/CD45, a hallmark present on all leukocytes, which had a high probability of interaction with MRC1 on myeloid cells in the canine lung (**Figure 1H**). STAT4, also significantly increased, is an epigenetic regulator NK cells involved in NK activation and IFN- γ production⁵⁸. Together, we observed subtle differences between NK cells in the TME across species that point to modifications in activation states with potential influence of neighboring cells. Nevertheless, the considerable similarities between tumor samples across species support the validity of the canine model in soft tissue sarcoma research, aligning with previous reports of conserved characteristics across canine and human cancers^{7, 59-64}.

3.3.7 NK proportions increase in response to treatment in good responders to first-in-dog immunotherapy regimens

Insights into blood, tissue, and tumor-infiltrating NK cells are most relevant in the larger scope of clinical data and how results that can be hypothesis generating to inform future clinical trials. We therefore obtained blood samples from dogs who were enrolled in three separate, NK-targeting trials. Dogs in UCD Trial #1 (UCD1) underwent palliative radiotherapy (RT) in addition to infusion of PBMC-derived allogeneic NK cells (**Figure 7A**). Dogs in UCD Trial #2 (UCD2) received two injections of autologous NK cells in combination with inhaled rhIL-15 (**Figure 7B**). These two trials were the first to employ systemic administration of PBMC-derived NK cells in dogs with naturally occurring cancer²¹. We also accessed samples from dogs in a third trial, the UW cohort, which treated dogs with low-dose molecular targeted radionuclide therapy (MTRT), external beam radiation therapy (EBRT) and intratumoral injection of IL-2 fusion cytokine (**Figure 7C**). These dogs were treated based on the results of a protocol cohort that

demonstrated safety and feasibility of the combination therapy⁶⁵. Together, PBMCs were available for six dogs, two from each trial representing a good responder and a poor responder. For each dog, a pre-treatment and post-treatment PBMC sample was obtained for a total of 12 PBMC samples which were submitted for single-cell RNA sequencing. Those samples were integrated, with an average of 5,425 cells per sample, and cell types identified by canonical cell markers (**Figure 7D**). Samples could then be assessed and compared based on trial, treatment timepoint, and response, which was assessed based on RECIST criteria and overall survival (**Figure 7E**). The poor responder from UCD1 did not live long enough to determine response and therefore was not evaluable. The good responder from UCD1 had a complete response and the longest survival of 445 days. Responses corresponded reliably with the fold change of NK cell proportion following treatment, with all three poor responders showing a negative fold change in response to treatment and all three good responders showing a positive fold change (**Figure 7F**). The proportions of NK cells were largest in UCD1, reaching a maximum of 13.7% of cells in good responders (**Figure 7G**). NK cells were between 1-2% of total cells in UCD2, but made up less than 1% of total cells in the UW poor responder (**Figures 7H, 7I**). We therefore report substantial variability of NK proportions in the peripheral blood of dogs diagnosed with cancer, but predictable changes that indicate dogs respond better to treatment when a positive fold change in NK cells is identified.

3.3.8 Good responders upregulate NK activation signatures after treatment while poor responders have minimal treatment-related changes

Due to the intriguing results indicating the distinct role of NK cells in treatment response, we then subset out the NK cell cluster to focus on their specific characteristics (**Figure 8A**). The NK cluster included over 2,000 cells across trials that met quality standards for analysis (**Figure 8B**). We completed DEG analysis comparing pre and post treatment samples in good responders and poor responders and compared good vs poor responders at both the pre and

post treatment timepoint in all trials (**Figures 8C, 8D, 8E**). We found that there were large differences in pre-treatment samples between poor and good responders in UCD1 but that the poor responder had no genes upregulated in response to treatment (**Figure 8C**). Samples from UCD2 had minimal changes, both in response to treatment and between responders (**Figure 8D**). This was in contrast to UW which had over 250 genes differentially expressed in their good responder and, similar to UCD1, had considerably fewer DEG changes in the poor responder (**Figure 8E**). We found that the majority of DEGs between pre and post treatment in good responders were significantly upregulated in response to treatment rather than downregulated (**Figure 8F**). Similarly, the majority of DEGs between poor and good responders at the pre-treatment had increased expression in poor responders (**Figure 8G**). These patterns necessitated further analysis of the specific genes that contributed to the changes assessed. A selection of genes that were upregulated post treatment in good responders and those upregulated pre-treatment in poor versus good responders are presented in a venn diagram, with specific emphasis on genes that were previously identified in tissue-specific signatures (**Figures 8H, 8I**). Most striking was the identification of CCL4, which was significantly upregulated in good responders from both UCD1 and UW and was also found in activated lung NK cells and shared with human lung cells. This corresponds with data from The Cancer Genome Atlas (TCGA), where CCL4 expression in UPS primary tumor samples was a significant prognostic biomarker (**Figure 8J**). This is contrary to FTH, a gene significantly upregulated in poor responders in both the UCD1 and UW trials, which was associated with worse overall survival in the UPS TCGA dataset, though not significant (**Figure 8K**). Although poor responders had minimal response to treatment overall, we did see that they expressed several activation genes at greater levels than good responders before the start of treatment, including BCL2A1, present in both UCD1 and UW trials. The overall pattern of our results points to the possibility that response to treatment may be a more meaningful biomarker than baseline gene expression in NK cells during cancer immunotherapy.

3.3.9 Figures

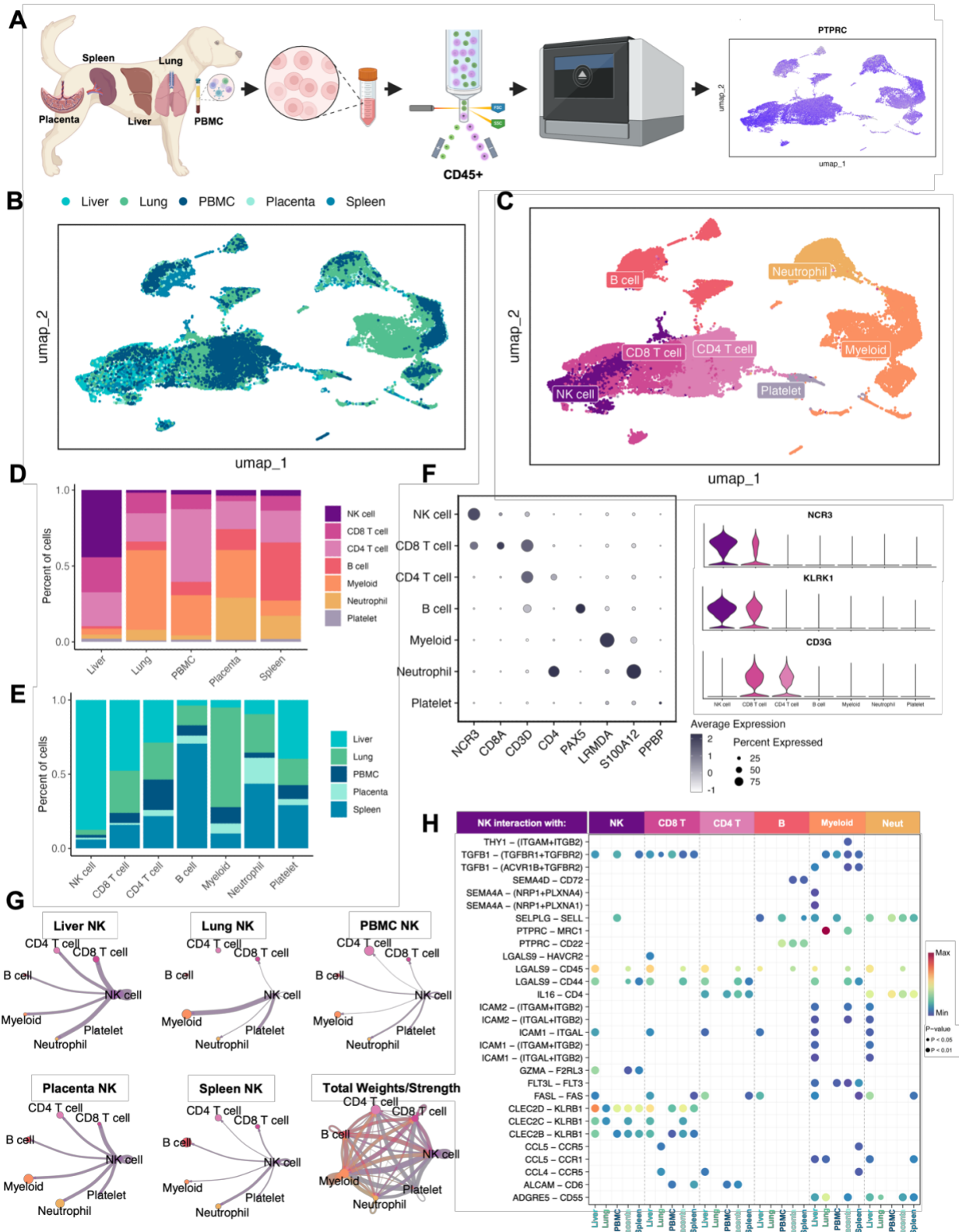


Figure 1: Canine NK cells vary in abundance and immune interactions across tissues

(A) Schema depicting the canine samples obtained and the study workflow.

(B and C) Uniform manifold approximation and projection (UMAP) visualizations of integrated samples encompassing nine total samples color coded by (B) tissue or (C) cell type.

(D and E) Bar plots depicting the percent of cells analyzed by (D) tissue compartment or (E) cell type.

(F) Left: Dotplot of representative canonical gene markers used to confirm cell types. Dot color represents average gene expression and dot size represents the percent of cells expressing the gene. Right: violin plot of key genes distinguishing NK cells from T lymphocytes.

(G) Circle plots constructed using CellChat visualizing predicted NK cell outgoing interactions separated by tissue. Lines represent the scaled weights or strength of the interaction. Total weights and strengths of ingoing and outgoing interactions between all cell types across all tissues visualized in the bottom right panel.

(H) Bubbleplot of significant predicted ligand receptor interactions between NK cells and other cell types, separated by tissue. Color of dot represents the probability of the interaction, and size of the dot corresponds to p-value. Only interactions expressed in a minimum of 10 cells were retained in the analysis.

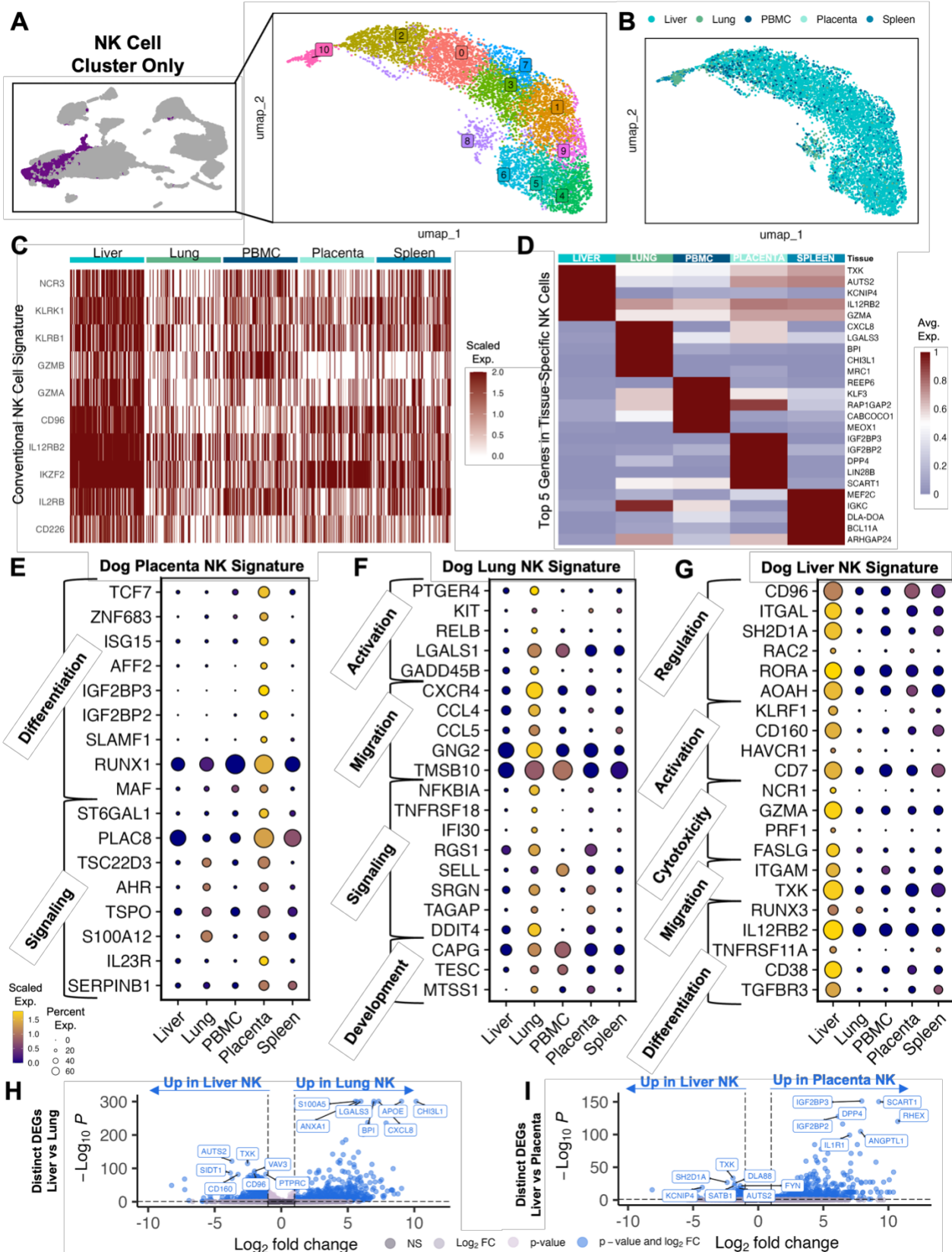


Figure 2: Canine NK cells demonstrate tissue-specific gene signatures

(A) UMAP representation of NK cells subset from the integrated dataset with 11 clusters identified by unsupervised clustering.

(B) UMAP visualization of NK cells color coded by tissue.

(C) Heatmap of conventional NK cell markers in NK cells analyzed by tissues. Columns represent cells and rows represent genes. Gene expression data for all features/genes were scaled and a random downsample of 100 NK cells from each tissue were plotted for proportional visualization.

(D) Heatmap showing the average expression of the top five differentially expressed genes in NK cells from each tissue that distinguish them from NK cells in all other tissues.

(E-G) Dotplots showing expression of representative genes significantly upregulated in (E) placenta, (F) lung, and (G) liver NK cells compared to NK cells in all other tissues. Genes included were present in >20% of cells, with $\text{avg_log}_2\text{FC} > 1$ and adjusted $P < 0.05$. Gene category labels were determined by gene-set library and gene ontology annotations associated with each gene.

(H-I) Volcano plots with labels for the top seven significant genes that differentiate (H) liver vs lung NK cells and (I) liver vs placenta NK cells based on direct DEG comparison.

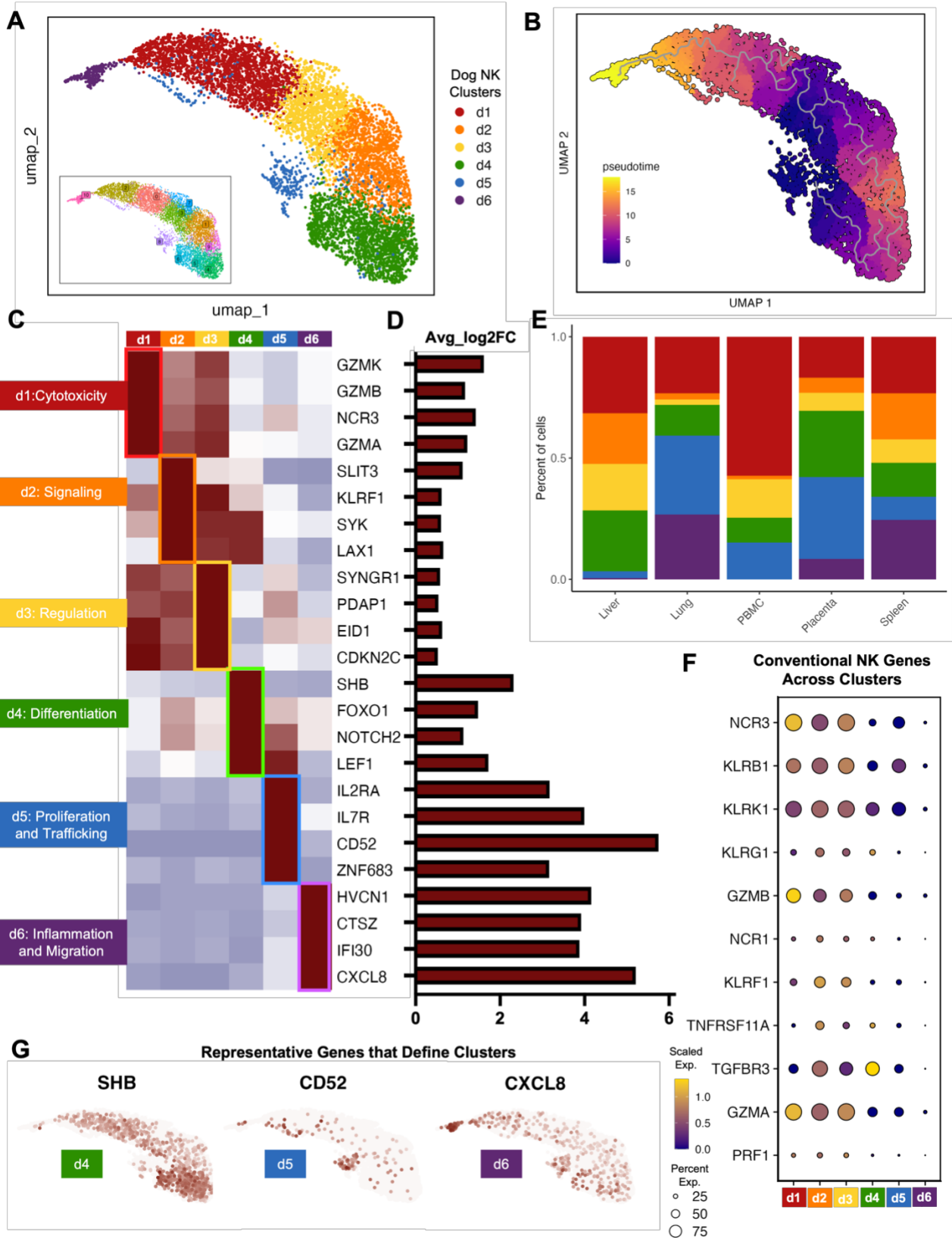


Figure 3: Canine tissue and peripheral NK cells can be categorized into distinct subsets

(A) Clusters resulting from unsupervised clustering were combined based on overlapping genes markers. The result was six canine NK cell clusters labeled d1-d6.

(B) Cell trajectories projected onto the UMAP and colored by pseudotime.

(C-D) Significant genes that distinguish each canine NK subcluster from the remaining subclusters visualized by (C) average expression heatmap and (D) average log2fold change bar plot.

(E) Bar plots depicting the percent of cells grouped by canine NK subcluster and split by tissue compartment.

(F) Dotplot of conventional NK cell markers and their expression within cells of each canine NK cell subcluster.

(G) Feature plots depicting expression and distribution of selected significant genes that differentiate clusters d4 (left), d5 (center), and d6 (right).

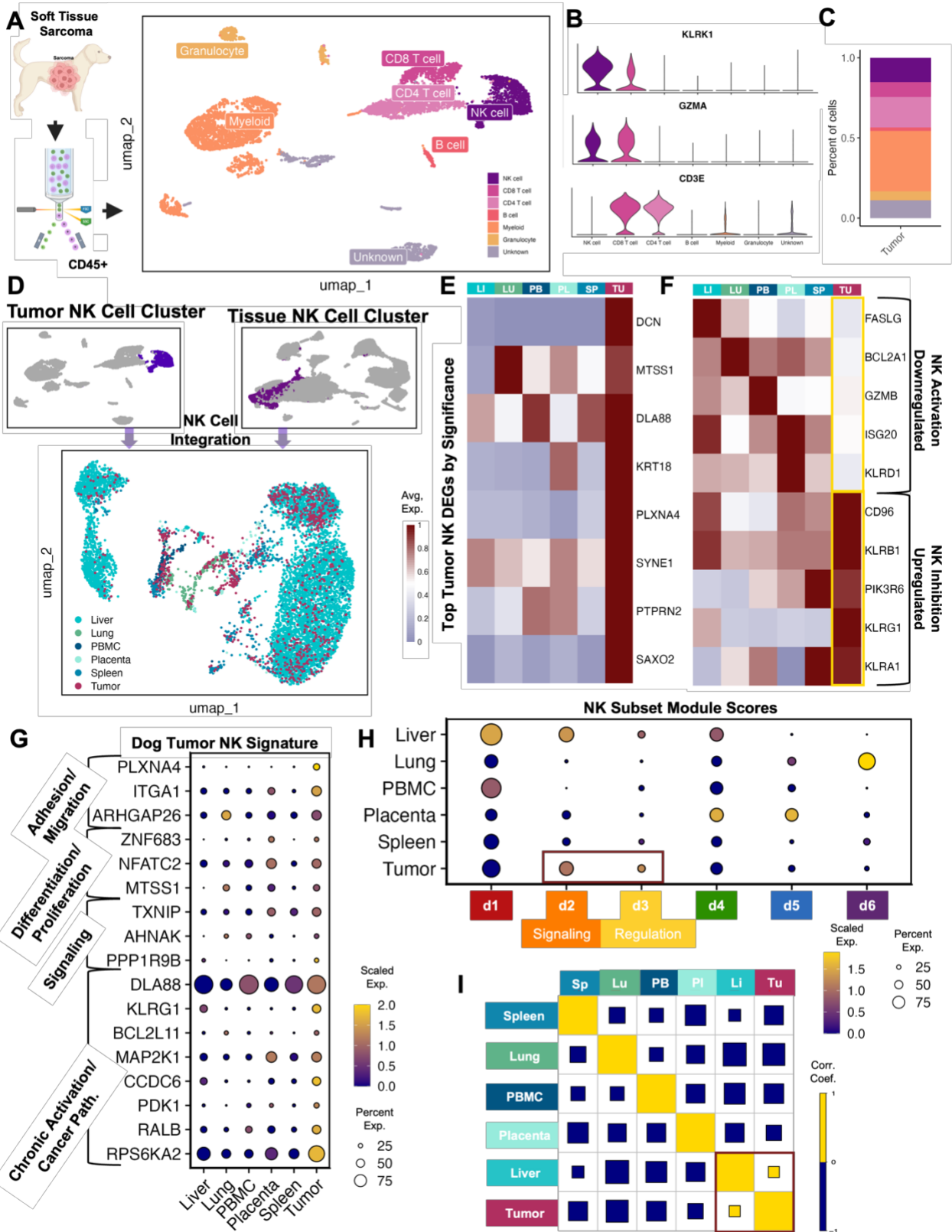


Figure 4: Canine sarcoma infiltrating NK cells are heterogeneous with unique activation and exhaustion features

(A) Schema depicting workflow for FACS sorting and sequencing of CD45+ canine spindle cell sarcoma cells with the cell types identified. A total of 6514 CD45+ immune cells were available for analysis.

(B) Violin plot of key genes identifying NK cells and distinguishing them from T lymphocytes.

(C) Bar plot showing the percent of each cell type in the tumor. NK cells represented 15.2% of all CD45+ tumor cells isolated.

(D) NK cells subset from the canine tumor sample and NK cells subset from the integrated liver lung, PBMC, placenta, and spleen dataset were integrated and visualized by UMAP color coded by tissue.

(E) Heatmap showing the average expression of the top differentially expressed genes in tumor NK cells that distinguish them from NK cells in all other tissues.

(F) Heatmap of conventional NK activating and inhibitory genes and their average expression in tissues. Tumor NK expression is outlined.

(G) Dotplot showing expression of representative genes significantly upregulated in tumor NK cells compared to NK cells in all other tissues. Genes included were present in >20% of cells, with $\text{avg_log2FC} > 1$ and adjusted $P < 0.05$. Gene category labels were determined by gene-set library and gene ontology annotations associated with each gene.

(H) Dotplot visualization of the scaled module score of tissue-specific NK cells scored with the top genes that defined each canine NK subcluster. Subclusters with the highest expression in tumor NK cells were outlined and labeled.

(I) Correlations across all tissue compartments. Yellow and blue squares represent positive and negative correlations respectively. Square size represents the absolute value of the correlation coefficient.

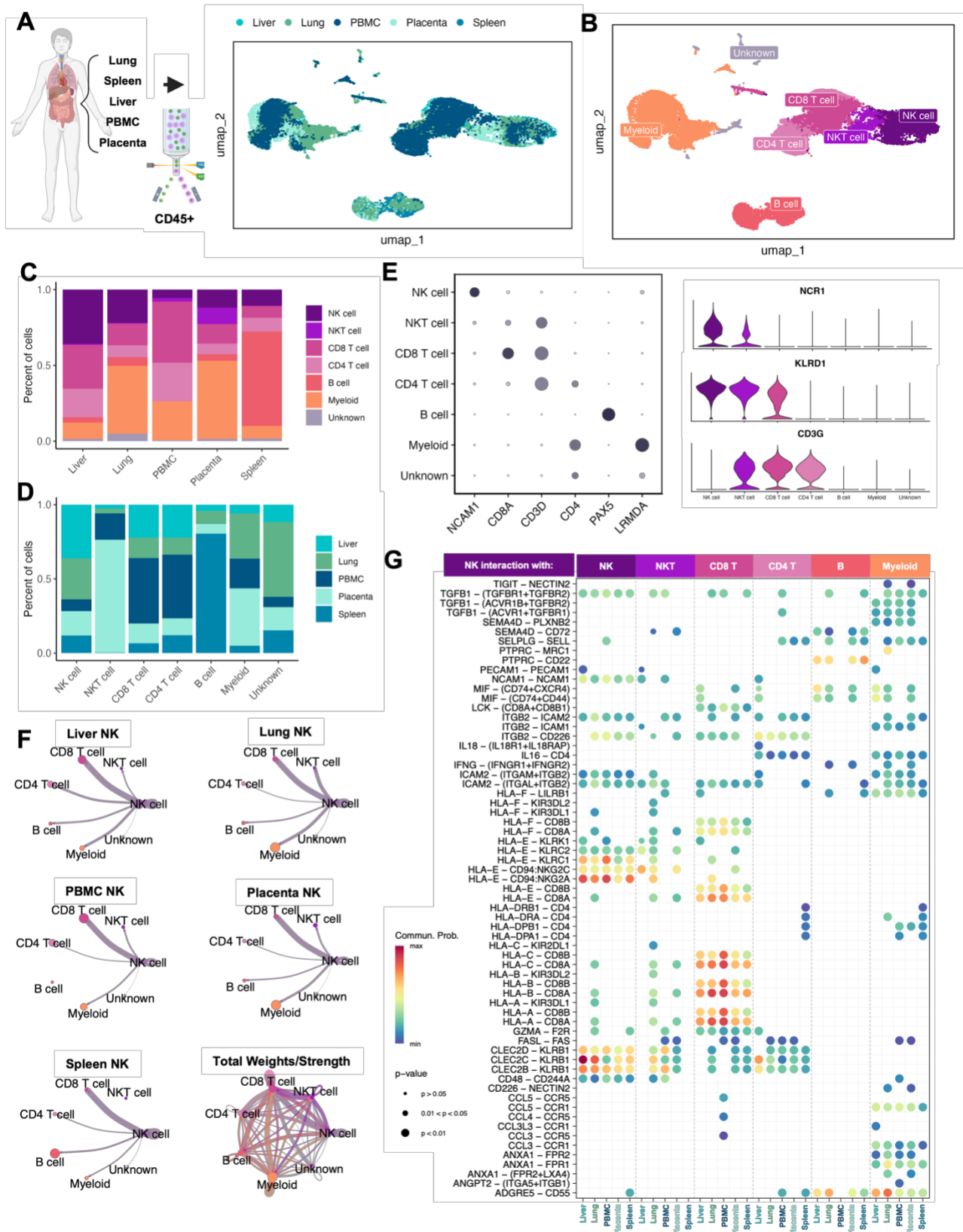


Figure 5: Human NK cells mirror dog NK cells in abundance and immune interactions across tissues

(A and B) Schema depicting the human samples obtained and the sorting and sequencing of CD45+ immune cells. Integration of five total samples were visualized by UMAP and color coded by (A) tissue or (B) cell type.

(C and D) Bar plots depicting the percent of cells split by (C) tissue compartment or (D) cell type.

(E) Left: Dotplot of representative canonical gene markers used to confirm cell types. Dot color represents average gene expression and dot size represents the percent of cells expressing the gene. Right: violin plot of additional genes distinguishing NK cells from T lymphocytes.

(F) Circle plots constructed using CellChat visualizing predicted NK cell outgoing interactions separated by tissue. Lines represent the scaled weights or strength of the interaction. Total weights and strengths of ingoing and outgoing interactions between all cell types across all tissues visualized in the bottom right panel.

(G) Bubbleplot of significant predicted ligand receptor interactions between NK cells and other cell types, separated by tissue. Color of dot represents the probability of the interaction, size of the dot represents p-value. Only interactions expressed in a minimum of 10 cells were retained in the analysis.

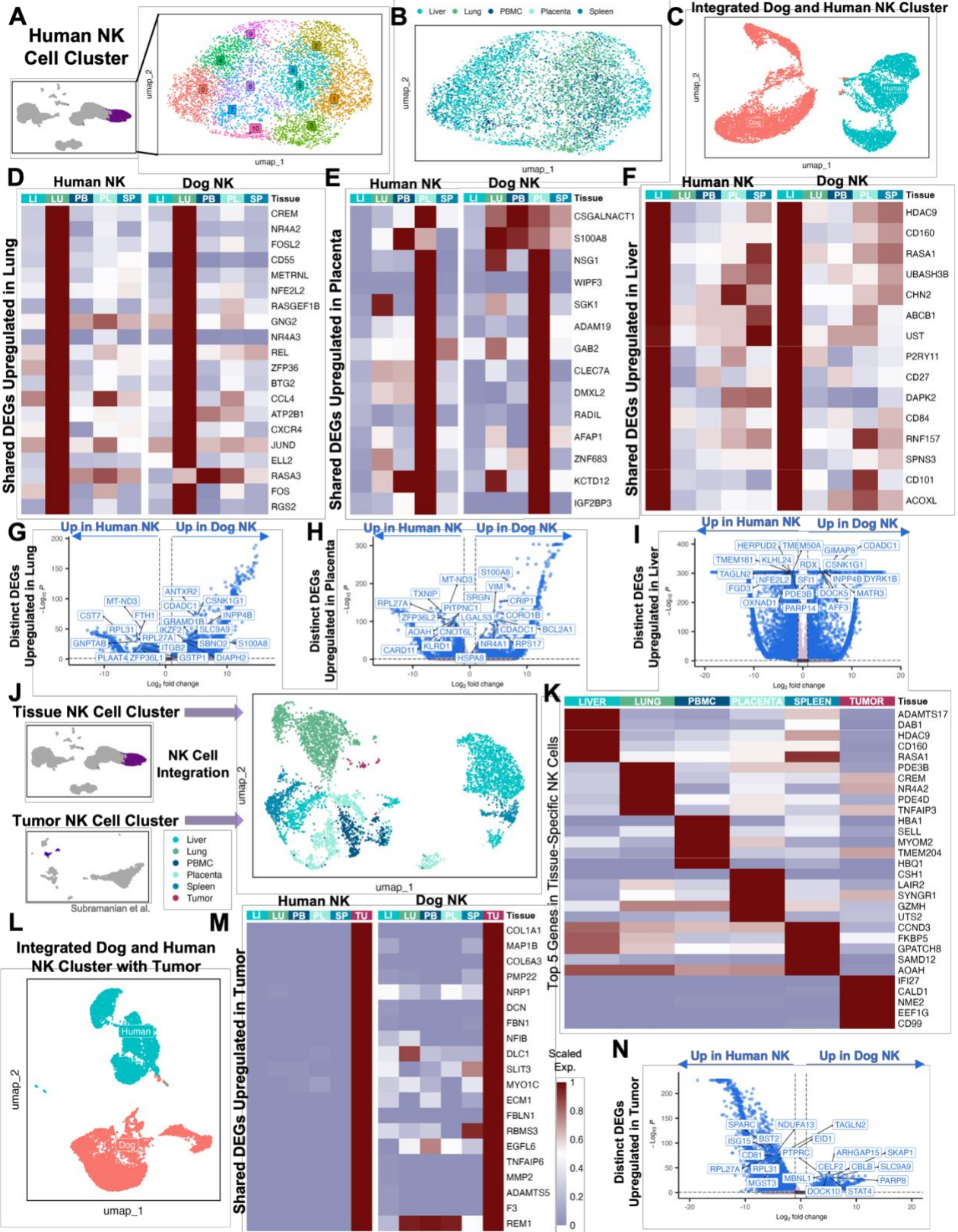


Figure 6: Canine and human NK cells show homology across blood, tissue, and tumor compartments

(A) UMAP representation of NK cells subset from the integrated liver, lung, placenta, and spleen dataset with 11 clusters identified by unsupervised clustering.

(B) UMAP visualization of NK cells color coded by tissue.

(C) NK cells from liver, lung, PBMC, placenta, and spleen tissue in both humans and dogs were integrated and visualized by UMAP, color coded by species.

(D, E, F) Genes that were significantly upregulated in NK cells within each tissue compared to NK cells in the remaining tissues within each species with adjusted p value <0.05 and average $\log_2FC >1$ were identified. The average expression of genes that were upregulated in both human and dog (D) lung, (E) placenta, and (F) liver NK cells were visualized by heatmap.

(G, H, I) Volcano plots with labels for the top ten significant genes that differentiate human and canine NK cells in the (G) lung, (H) placenta, and (I) liver based on direct DEG comparisons.

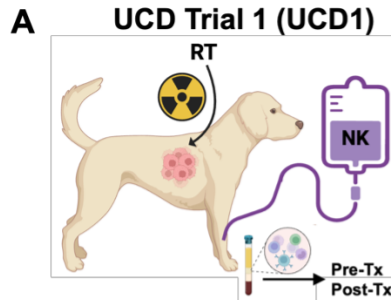
(J) NK cells subset from the integrated human tissue dataset and NK cells subset from a publicly available human UPS sample were integrated and visualized by UMAP color coded by tissue.

(K) Heatmap showing the average expression of the top differentially expressed genes in NK cells from each tissue that distinguish them from NK cells in all other tissues.

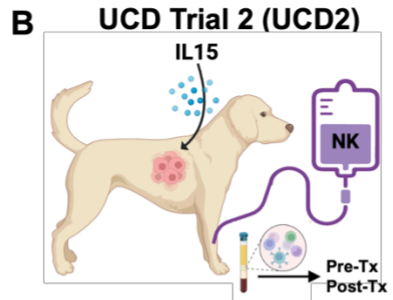
(L) NK cells from liver, lung, PBMC, placenta, spleen, and tumor tissue in both humans and dogs were integrated and visualized by UMAP, color coded by species.

(M) Genes that were significantly upregulated in tumor NK cells compared to the NK cells in the remaining tissues within each species with adjusted p value <0.05 and average FC >1 were identified. The average expression of genes that were upregulated in both human and dog tumor NK cells were visualized by heatmap.

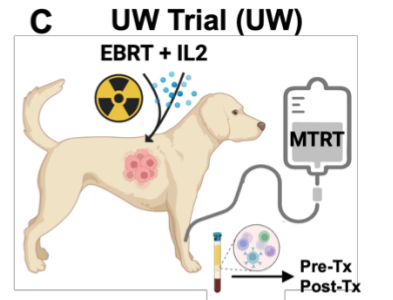
(N) Volcano plot with labels for the top ten significant genes that differentiate human and canine NK cells in tumor based on direct DEG comparisons.



Responder ID	Good	Poor
Age	9	11
Sex	FS	MN
Breed	Labrador Retriever	Golden Retriever
Disease	Oral Melanoma	Oral Melanoma
Metastasis	Lymph Node	Lymph Node
RECIST	CR	NE
OS (days)	445	48



Responder ID	Good	Poor
Age	7	8
Sex	FS	FS
Breed	Bouvier Des Flandres	Labrador Retriever
Disease	Oral Melanoma	Oral Melanoma
Metastasis	Distant	Distant
RECIST	PR	PD
OS (days)	69	57



Responder ID	Good	Poor
Age	9	8
Sex	MN	MN
Breed	Labrador Retriever	Cocker Spaniel
Disease	Oral Melanoma	Oral Melanoma
Metastasis	Distant	Distant
RECIST	PR	SD
OS (days)	71*	79

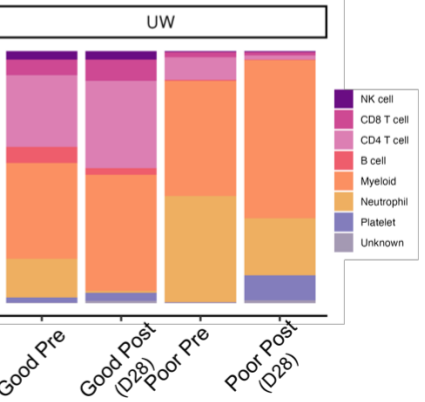
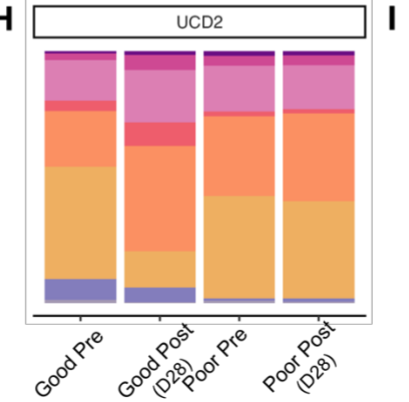
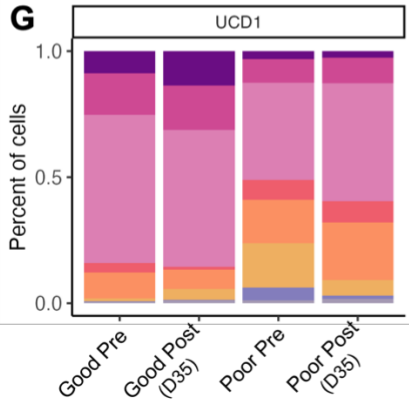
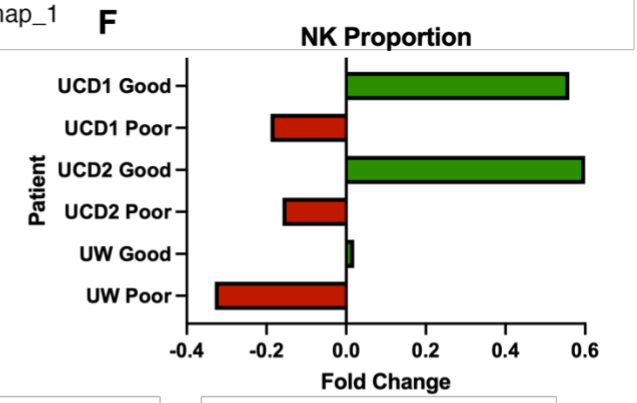
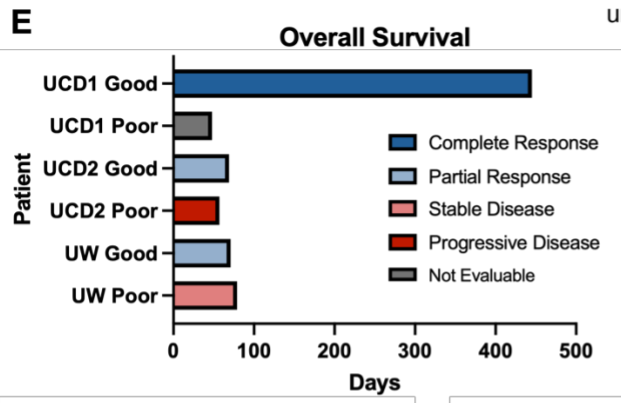
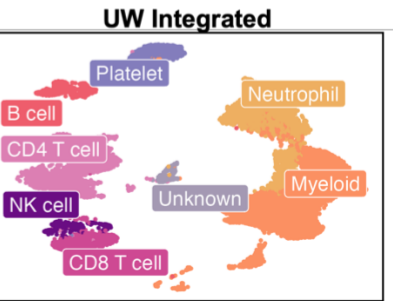
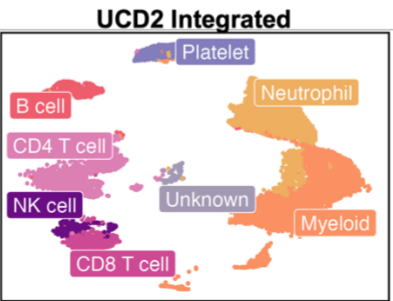
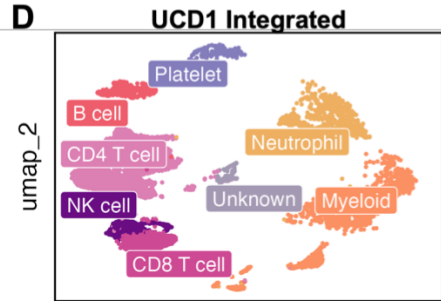


Figure 7: NK proportions increase in response to treatment in good responders to first-in-dog immunotherapy regimens

(A, B, C) Schema depicting clinical trial treatments and corresponding signalments and outcomes for dogs enrolled in (A) UCD trial 1 with combination of radiotherapy and allogeneic NK cell transfer, (B) UCD trial 2 with combination of inhaled IL-15 and autologous NK cell transfer, and (C) UW trial with combination molecular targeted radionuclide therapy (MTRT), IL-2 cytokine, and external beam radiation therapy (EBRT). Good and poor responders were determined based on RECIST criteria of the primary tumor and overall survival. PBMCs were collected pre and post treatment for each dog. The UCD1 Good responder did not survive long enough to determine response and was therefore considered not evaluable (NE). *UW good responder was lost to follow up at 71 days.

(D) UMAP visualizations of the twelve integrated PBMC samples split by trial and color coded by cell type.

(E) Bar plot depicting the overall survival or date or last follow up (UW Good) for each of the dogs included in the analysis. Bars are color coded by response based on RECIST criteria.

(F) Bar plot showing fold change of the NK cell proportion in each dog included in the analysis. Green and red bars represent positive and negative fold change respectively. Fold change of NK cell proportion was calculated by $(\text{Post-treatment} - \text{Pre-treatment}) / \text{Pre-treatment}$.

(G, H, I) Bar plots showing the percent of each cell type in each PBMC sample included in the analysis. Plots are split by trial and then further split by pre and post treatment sample for each dog. Post treatment samples were obtained (G) 35 days after the start of treatment in UCD trial 1, (H) 28 days after the start of treatment in UCD Trial 2, and (I) 28 days after the start of treatment in UW trial.

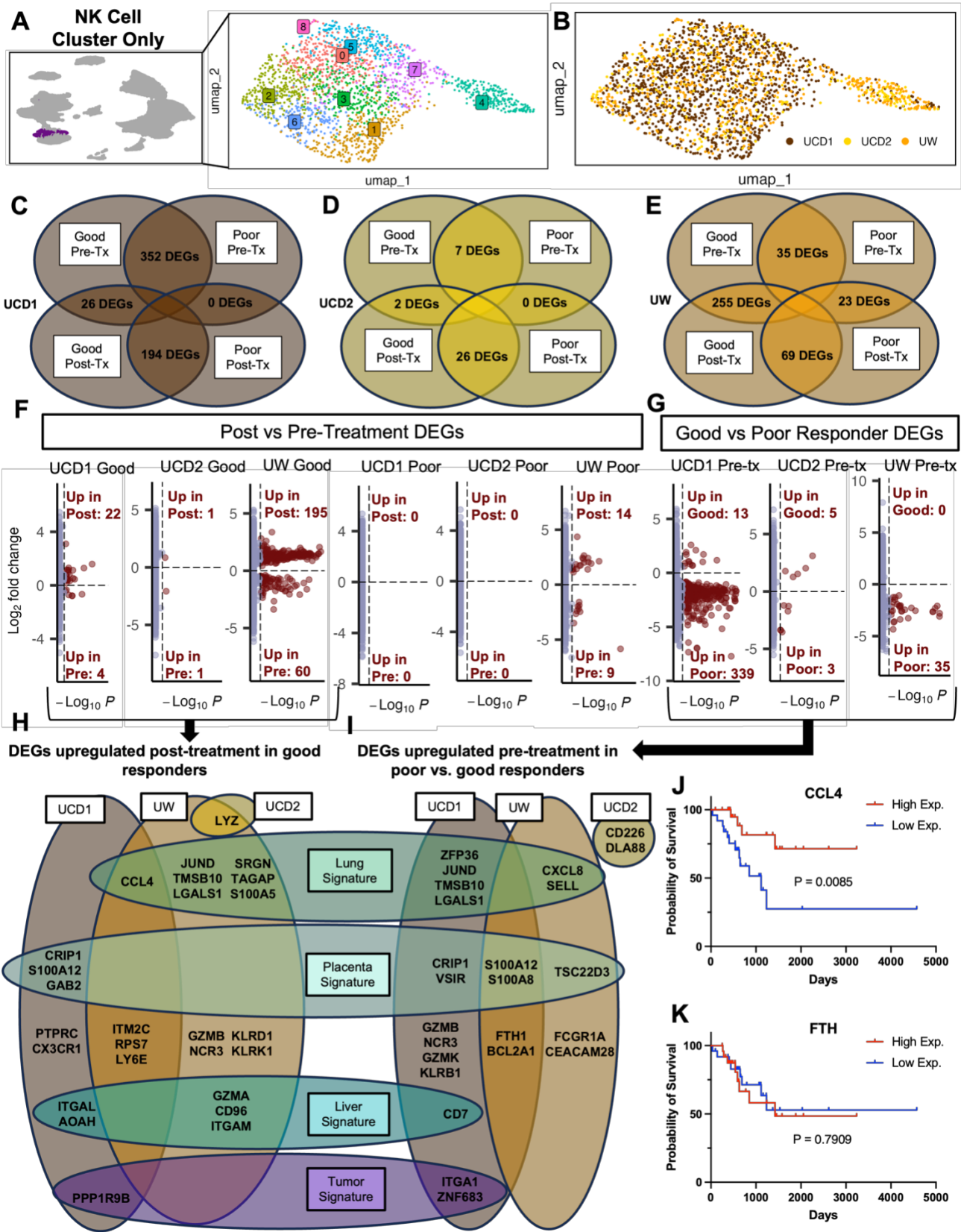


Figure 8: Good responders upregulate NK activation signatures after treatment while poor responders have minimal treatment-related changes

(A) UMAP representation of NK cells subset from the integrated PBMC samples across trials with 9 clusters identified by unsupervised clustering.

(B) UMAP visualization of NK cells color coded by trial.

(C, D, E) DEG analysis was completed between post and pre treatment for each dog and between good and poor responders for each timepoint. The number of genes with adjusted p-value < 0.05 in each comparison are depicted in venn diagrams for (C) UCD trial 1, (D) UCD trial 2, and (E) UW trial.

(F, G) Volcano plots distinguish the number of genes that were significantly upregulated or downregulated in (F) post vs pre-treatment and (G) good vs poor responders pre-treatment,

(H, I) Selected genes that were significantly upregulated (H) post-treatment in good responders and (I) pre-treatment in poor vs good responders were displayed in a venn diagram. All significant genes associated with tissue signatures were displayed.

(J, K) Kaplan–Meier survival curves showing the survival time of TCGA UPS patient samples with high and low expression of (J) CCL4, which was significantly upregulated both UCD1 and UW good responders in response to treatment in addition to the activated lung signature, and (K) FTH, which was significantly upregulated in both UCD1 and UW poor responders compared to their respective good responders pre-treatment.

Sample	Breed	Sex	Age	Status	Procedure
Lung	Beagle	FS	10	Pulmonary Adenoma	Lung Lobectomy
Lung	Australian Shepherd	FS	10	Pulmonary Adenocarcinoma	Lung Lobectomy
Liver	Pit Bull Terrier	FS	9	Poorly Differentiated Sarcoma	Liver Lobectomy
Liver	Pomeranian Mix	MN	10	Hematocellular Adenoma	Liver Lobectomy
Spleen	Bull Mastiff	FS	9	Lymphoma	Splenectomy
Spleen	Border Collie	FS	14	Hematoma	Splenectomy
Placenta	Danish-Swedish Farmdog	F	5	Healthy	C-section
Placenta	French Bulldog	F	4	Healthy	C-section
PBMC	Beagle	FS	6	Healthy	None

Supplemental Figure 1: Characteristics of canine sample donors.

3.4 Discussion

In this study, we present varying abundance and genomic profiles of NK cells across canine blood, spleen, liver, lung, placenta, and tumor. Most striking was the large population of NK cells in the canine liver and strong interactions between NK cells and myeloid cells in the canine lung. We identified canine NK subpopulations throughout tissue compartments with variations in markers associated with cytotoxicity, signaling, regulation, and maturation, similar to NK subpopulations seen in humans. We then found meaningful overlap in tissue-specific signatures using direct comparisons of blood and resident NK cells from humans and dogs. NK cells in the placenta upregulated markers associated with differentiation, NK cells in the lung upregulated activation and migration markers, and NK cells in the liver had a mixed signature with specific regulatory genes similarly seen in tumor-resident NK cells. Finally, we reveal changes in peripheral NK cell gene expression that align with response to NK-targeting canine immunotherapy trials. Notably, upregulation of CCL4 was a prevalent finding in activated NK cells, seen in human and canine lung NK signatures as well as in response to treatment in dogs that responded well to immunotherapy. Together, we present NK cells as key immune constituents of canine tissues that can serve as a valid model of human NK cells with translational relevance in immune-oncology research.

The heterogeneity of NK cells has been well-documented in humans, in both peripheral blood and tissue. We similarly see this variability in canine NK cells. We found distinct signatures that represent NK cells in the lung, placenta, and liver. Additionally, we determined six canine NK cell subsets that were present across tissues, implying the tunability of NK cells based on the tissue environment and cell signals present. This is especially apparent in the exhausted phenotype of NK cells in canine soft tissue sarcoma, representing the inhibitory signals present in the TME. Tumor NK cells corresponded most with hepatic NK cells, which expressed similar inhibitory markers, such as CD96. The population of inhibitory NK cells in the liver could potentially be part of typical and necessary regulation of immune responses in normal tissue that are exploited

during tumor progression. The various states or subsets of NK cells point to inherent malleability that can be harnessed to create NK cell-based targets or treatments.

Sources and modifications of NK cells for adoptive cell therapy have continued to advance in recent years. Numerous methods have been employed to enhance antitumor efficacy through mechanisms including blocking inhibitory receptors with monoclonal antibodies, amplifying activation with bi- and tri-specific killer engagers (BiKEs and TriKEs), and increasing persistence in cytokine support. NK cell sources include cell lines like NK-92, peripheral blood, umbilical cord blood (CB), and induced pluripotent stem cells (iPSCs). Cord blood-derived human NK cells are thought to have higher proliferative capabilities than those in the peripheral blood and, along with immature iPSC-derived NK cells, are more readily engineered to create consistent NK cell products. Following this line of reasoning, we characterize canine NK cells derived from the placenta as expressing markers corresponding with early development while maintaining indicators of signaling and activation. Therefore, canine stem-like NK cells could be promising candidates for expansion and transfer, particularly with the successful expansion of PBMC-derived canine NK cells and safety of allogeneic adoptive cell transfer. The clearer understanding of canine NK cells granted by this study set the foundation for future sources and targets in NK cell therapy.

Integrated analysis NK cells from patients enrolled in canine NK-targeting clinical trials showed distinct signatures with greater DGEs related to activation and recruitment post treatment in responders compared to non-responders. Good responders generally had less activation markers at baseline than poor responders but had dramatically greater responses to treatment. Numerous studies have shown that baseline gene expression can predict responses to immunotherapy in several human cancers. However, others have shown that predictive biomarkers of response are more distinct in post-treatment compared to pre-treatment samples⁶⁶. A potential explanation of this pattern is that NK cells with increased plasticity are more capable of adjusting their activity and effector functions in response to treatment, leading

to better responses. The flexibility of NK cells corresponds well with our own data regarding tissue and tumor-specific NK cells. This is also evidenced in human NK cells, for example, even the popular framework of CD56^{bright} NK cells maturing to CD56^{dim} has been shown to be bidirectional in certain contexts⁶⁷. Overall, the malleability of NK subsets seems to be a conserved characteristic between canine and human NK cells.

Accurate models of human NK cells and related immunotherapies is crucial for the forward momentum of the field, especially given the limitations of murine models. While companion dogs have been extensively used as valid models of human cancers, only recently have canine NK cells been thoroughly studied¹¹. Canine NK cells are notoriously difficult to identify, mostly due to their lack of CD56 expression. There has also been moderate success identifying canine NK cells by NKp46, the pan-mammalian NK cell marker, using flow cytometry. NKp46 is a transmembrane receptor encoded by the gene NCR1, part of a family of natural cytotoxicity receptors (NCRs) that include NKp44 and NKp30, encoded by NCR2 and NCR3 respectively. Interestingly, we find that in transcriptomic analysis, NCR3 is more highly expressed in canine NK cells than NCR1. This pattern was similar seen in an atlas of circulating leukocytes in healthy and cancer bearing dogs, where NCR3, rather than NCR1, was part of the transcriptional signature of canine NK cells²⁶. In contrast to NCR1, NCR3 is not expressed by NK cells in all mammals and has been identified as a pseudogene in most mouse species⁶⁸. Additionally, while NCR1 which is always activating, NCR3 can be activating or inhibitory based on the splice variants NKp30A, NKp30B or NKp30C. Though several studies associate NCR3 with increased activation. Human NK cells express both NCR1 and NCR3 at high levels³², and low expression of NCR3 specifically has been associated with poor prognosis⁶⁹. The expression of NCR3 represents an additional example of the overlap between human and canine NK cells, and additional work is needed to understand whether NCR3 has similar prognostic indications in dogs diagnosed with cancer.

Overall, this comprehensive genomic analysis provides insight into the canine NK profiles across tissues and in response to immunotherapy. Specifically, we shed light on the diverse heterogeneity of NK cells throughout the body with indications of adaptability that confirm the potential of these cells to be manipulated in cancer immunotherapy. This investigation increases our understanding of canine NK cells and can form the basis for advancing mechanistic investigations into novel therapeutic approaches.

3.5 References

1. Gang M, Wong P, Berrien-Elliott MM, Fehniger TA. Memory-like natural killer cells for cancer immunotherapy. *Semin Hematol.* 2020;57(4):185-93. Epub 20201117. doi: 10.1053/j.seminhematol.2020.11.003. PubMed PMID: 33256911; PMCID: PMC7810422.
2. Myers JA, Miller JS. Exploring the NK cell platform for cancer immunotherapy. *Nat Rev Clin Oncol.* 2021;18(2):85-100. Epub 20200915. doi: 10.1038/s41571-020-0426-7. PubMed PMID: 32934330; PMCID: PMC8316981.
3. Malmberg KJ, Carlsten M, Björklund A, Sohlberg E, Bryceson YT, Ljunggren HG. Natural killer cell-mediated immunosurveillance of human cancer. *Semin Immunol.* 2017;31:20-9. Epub 20170906. doi: 10.1016/j.smim.2017.08.002. PubMed PMID: 28888619.
4. Liu E, Marin D, Banerjee P, Macapinlac HA, Thompson P, Basar R, Nassif Kerbauy L, Overman B, Thall P, Kaplan M, Nandivada V, Kaur I, Nunez Cortes A, Cao K, Daher M, Hosing C, Cohen EN, Kebriaei P, Mehta R, Neelapu S, Nieto Y, Wang M, Wierda W, Keating M, Champlin R, Shpall EJ, Rezvani K. Use of CAR-Transduced Natural Killer Cells in CD19-Positive Lymphoid Tumors. *N Engl J Med.* 2020;382(6):545-53. doi: 10.1056/NEJMoa1910607. PubMed PMID: 32023374; PMCID: PMC7101242.
5. Li Y, Rezvani K, Rafei H. Next-generation chimeric antigen receptors for T- and natural killer-cell therapies against cancer. *Immunol Rev.* 2023;320(1):217-35. Epub 20230807. doi: 10.1111/imr.13255. PubMed PMID: 37548050; PMCID: PMC10841677.

6. Park JS, Withers SS, Modiano JF, Kent MS, Chen M, Luna JI, Culp WTN, Sparger EE, Rebhun RB, Monjazeb AM, Murphy WJ, Canter RJ. Canine cancer immunotherapy studies: linking mouse and human. *J Immunother Cancer*. 2016;4:97. Epub 20161220. doi: 10.1186/s40425-016-0200-7. PubMed PMID: 28031824; PMCID: PMC5171656.
7. LeBlanc AK, Mazcko CN. Improving human cancer therapy through the evaluation of pet dogs. *Nat Rev Cancer*. 2020;20(12):727-42. Epub 20200915. doi: 10.1038/s41568-020-0297-3. PubMed PMID: 32934365.
8. Schiffman JD, Breen M. Comparative oncology: what dogs and other species can teach us about humans with cancer. *Philos Trans R Soc Lond B Biol Sci*. 2015;370(1673). doi: 10.1098/rstb.2014.0231. PubMed PMID: 26056372; PMCID: PMC4581033.
9. Sungur CM, Murphy WJ. Utilization of mouse models to decipher natural killer cell biology and potential clinical applications. *Hematology Am Soc Hematol Educ Program*. 2013;2013:227-33. doi: 10.1182/asheducation-2013.1.227. PubMed PMID: 24319185.
10. Abel AM, Yang C, Thakar MS, Malarkannan S. Natural Killer Cells: Development, Maturation, and Clinical Utilization. *Front Immunol*. 2018;9:1869. Epub 20180813. doi: 10.3389/fimmu.2018.01869. PubMed PMID: 30150991; PMCID: PMC6099181.
11. Gingrich AA, Reiter TE, Judge SJ, York D, Yanagisawa M, Razmara A, Sturgill I, Basmaci UN, Brady RV, Stoffel K, Murphy WJ, Rebhun RB, Brown CT, Canter RJ. Comparative Immunogenomics of Canine Natural Killer Cells as Immunotherapy Target. *Front Immunol*. 2021;12:670309. Epub 20210914. doi: 10.3389/fimmu.2021.670309. PubMed PMID: 34594320; PMCID: PMC8476892.
12. Regan DP, Chow L, Das S, Haines L, Palmer E, Kurihara JN, Coy JW, Mathias A, Thamm DH, Gustafson DL, Dow SW. Losartan Blocks Osteosarcoma-Elicited Monocyte Recruitment, and Combined With the Kinase Inhibitor Toceranib, Exerts Significant Clinical Benefit in Canine Metastatic Osteosarcoma. *Clin Cancer Res*. 2022;28(4):662-76. doi: 10.1158/1078-0432.CCR-21-2105. PubMed PMID: 34580111; PMCID: PMC8866227.

13. Weiss MC, Eulo V, Van Tine BA. Truly Man's Best Friend: Canine Cancers Drive Drug Repurposing in Osteosarcoma. *Clin Cancer Res.* 2022;28(4):571-2. doi: 10.1158/1078-0432.CCR-21-3471. PubMed PMID: 34880110.
14. Jin WJ, Jagodinsky JC, Vera JM, Clark PA, Zuleger CL, Erbe AK, Ong IM, Le T, Tetreault K, Berg T, Rakhmilevich AL, Kim K, Newton MA, Albertini MR, Sondel PM, Morris ZS. NK cells propagate T cell immunity following in situ tumor vaccination. *Cell Rep.* 2023;42(12):113556. Epub 20231213. doi: 10.1016/j.celrep.2023.113556. PubMed PMID: 38096050; PMCID: PMC10843551.
15. Smith SL, Kennedy PR, Stacey KB, Worboys JD, Yarwood A, Seo S, Solloa EH, Mistretta B, Chatterjee SS, Gunaratne P, Allette K, Wang YC, Smith ML, Sebra R, Mace EM, Horowitz A, Thomson W, Martin P, Eyre S, Davis DM. Diversity of peripheral blood human NK cells identified by single-cell RNA sequencing. *Blood Adv.* 2020;4(7):1388-406. doi: 10.1182/bloodadvances.2019000699. PubMed PMID: 32271902; PMCID: PMC7160259.
16. Dogra P, Rancan C, Ma W, Toth M, Senda T, Carpenter DJ, Kubota M, Matsumoto R, Thapa P, Szabo PA, Li Poon MM, Li J, Arakawa-Hoyt J, Shen Y, Fong L, Lanier LL, Farber DL. Tissue Determinants of Human NK Cell Development, Function, and Residence. *Cell.* 2020;180(4):749-63.e13. Epub 20200213. doi: 10.1016/j.cell.2020.01.022. PubMed PMID: 32059780; PMCID: PMC7194029.
17. Lopes N, Galluso J, Escalière B, Carpentier S, Kerdiles YM, Vivier E. Tissue-specific transcriptional profiles and heterogeneity of natural killer cells and group 1 innate lymphoid cells. *Cell Rep Med.* 2022;3(11):100812. doi: 10.1016/j.xcrm.2022.100812. PubMed PMID: 36384102; PMCID: PMC9729827.
18. Chen C, Wang C, Pang R, Liu H, Yin W, Chen J, Tao L. Comprehensive single-cell transcriptomic and proteomic analysis reveals NK cell exhaustion and unique tumor cell evolutionary trajectory in non-keratinizing nasopharyngeal carcinoma. *J Transl Med.*

2023;21(1):278. Epub 20230425. doi: 10.1186/s12967-023-04112-8. PubMed PMID: 37098551; PMCID: PMC10127506.

19. Moreno-Fernandez ME, Damen MSMA, Divanovic S. A protocol for isolation of primary human immune cells from the liver and mesenteric white adipose tissue biopsies. *STAR Protoc.* 2021;2(4):100937. Epub 20211102. doi: 10.1016/j.xpro.2021.100937. PubMed PMID: 34778849; PMCID: PMC8577113.

20. Reichard A, Asosingh K. Best Practices for Preparing a Single Cell Suspension from Solid Tissues for Flow Cytometry. *Cytometry A.* 2019;95(2):219-26. Epub 20181206. doi: 10.1002/cyto.a.23690. PubMed PMID: 30523671; PMCID: PMC6375754.

21. Razmara AM, Farley LE, Harris RM, Judge SJ, Lammers M, Iranpur KR, Johnson EG, Dunai C, Murphy WJ, Brown CT, Rebhun RB, Kent MS, Canter RJ. Preclinical evaluation and first-in-dog clinical trials of PBMC-expanded natural killer cells for adoptive immunotherapy in dogs with cancer. *J Immunother Cancer.* 2024;12(4). Epub 20240416. doi: 10.1136/jitc-2023-007963. PubMed PMID: 38631708; PMCID: PMC11029326.

22. Judge SJ, Darrow MA, Thorpe SW, Gingrich AA, O'Donnell EF, Bellini AR, Sturgill IR, Vick LV, Dunai C, Stoffel KM, Lyu Y, Chen S, Cho M, Rebhun RB, Monjazebe AM, Murphy WJ, Canter RJ. Analysis of tumor-infiltrating NK and T cells highlights IL-15 stimulation and TIGIT blockade as a combination immunotherapy strategy for soft tissue sarcomas. *J Immunother Cancer.* 2020;8(2). doi: 10.1136/jitc-2020-001355. PubMed PMID: 33158916; PMCID: PMC7651745.

23. Korsunsky I, Millard N, Fan J, Slowikowski K, Zhang F, Wei K, Baglaenko Y, Brenner M, Loh PR, Raychaudhuri S. Fast, sensitive and accurate integration of single-cell data with Harmony. *Nat Methods.* 2019;16(12):1289-96. Epub 20191118. doi: 10.1038/s41592-019-0619-0. PubMed PMID: 31740819; PMCID: PMC6884693.

24. Jin S, Guerrero-Juarez CF, Zhang L, Chang I, Ramos R, Kuan CH, Myung P, Plikus MV, Nie Q. Inference and analysis of cell-cell communication using CellChat. *Nat Commun.*

2021;12(1):1088. Epub 20210217. doi: 10.1038/s41467-021-21246-9. PubMed PMID: 33597522; PMCID: PMC7889871.

25. Subramanian A, Nemat-Gorgani N, Ellis-Caleo TJ, van IJzendoorn DGP, Sears TJ, Somani A, Luca BA, Zhou MY, Bradic M, Torres IA, Oladipo E, New C, Kenney DE, Avedian RS, Steffner RJ, Binkley MS, Mohler DG, Tap WD, D'Angelo SP, van de Rijn M, Ganjoo KN, Bui NQ, Charville GW, Newman AM, Moding EJ. Sarcoma microenvironment cell states and ecosystems are associated with prognosis and predict response to immunotherapy. *Nat Cancer*. 2024;5(4):642-58. Epub 20240301. doi: 10.1038/s43018-024-00743-y. PubMed PMID: 38429415; PMCID: PMC11058033.

26. Ammons DT, Harris RA, Hopkins LS, Kurihara J, Weishaar K, Dow S. A single-cell RNA sequencing atlas of circulating leukocytes from healthy and osteosarcoma affected dogs. *Front Immunol*. 2023;14:1162700. Epub 20230519. doi: 10.3389/fimmu.2023.1162700. PubMed PMID: 37275879; PMCID: PMC10235626.

27. Ammons DT, Hopkins LS, Cronise KE, Kurihara J, Regan DP, Dow S. Single-cell RNA sequencing reveals the cellular and molecular heterogeneity of treatment-naïve primary osteosarcoma in dogs. *Commun Biol*. 2024;7(1):496. Epub 20240424. doi: 10.1038/s42003-024-06182-w. PubMed PMID: 38658617; PMCID: PMC11043452.

28. Wienke J, Visser LL, Kholosy WM, Keller KM, Barisa M, Poon E, Munnings-Tomes S, Himsworth C, Calton E, Rodriguez A, Bernardi R, van den Ham F, van Hooff SR, Matser YAH, Tas ML, Langenberg KPS, Lijnzaad P, Borst AL, Zappa E, Bergsma FJ, Strijker JGM, Verhoeven BM, Mei S, Kramdi A, Restuadi R, Sanchez-Bernabeu A, Cornel AM, Holstege FCP, Gray JC, Tytgat GAM, Scheijde-Vermeulen MA, Wijnen MHWA, Dierselhuis MP, Straathof K, Behjati S, Wu W, Heck AJR, Koster J, Nierkens S, Janoueix-Lerosey I, de Krijger RR, Baryawno N, Chesler L, Anderson J, Caron HN, Margaritis T, van Noesel MM, Molenaar JJ. Integrative analysis of neuroblastoma by single-cell RNA sequencing identifies the NECTIN2-TIGIT axis as

- a target for immunotherapy. *Cancer Cell*. 2024;42(2):283-300.e8. Epub 20240104. doi: 10.1016/j.ccell.2023.12.008. PubMed PMID: 38181797; PMCID: PMC10864003.
29. DeMartino J, Meister MT, Visser LL, Brok M, Groot Koerkamp MJA, Wezenaar AKL, Hiemcke-Jiwa LS, de Souza T, Merks JHM, Rios AC, Holstege FCP, Margaritis T, Drost J. Single-cell transcriptomics reveals immune suppression and cell states predictive of patient outcomes in rhabdomyosarcoma. *Nat Commun*. 2023;14(1):3074. Epub 20230527. doi: 10.1038/s41467-023-38886-8. PubMed PMID: 37244912; PMCID: PMC10224926.
30. Crinier A, Milpied P, Escalière B, Piperoglou C, Galluso J, Balsamo A, Spinelli L, Cervera-Marzal I, Ebbo M, Girard-Madoux M, Jaeger S, Bollon E, Hamed S, Hardwigsen J, Ugolini S, Vély F, Narni-Mancinelli E, Vivier E. High-Dimensional Single-Cell Analysis Identifies Organ-Specific Signatures and Conserved NK Cell Subsets in Humans and Mice. *Immunity*. 2018;49(5):971-86.e5. Epub 20181106. doi: 10.1016/j.immuni.2018.09.009. PubMed PMID: 30413361; PMCID: PMC6269138.
31. Wong JL, Berk E, Edwards RP, Kalinski P. IL-18-primed helper NK cells collaborate with dendritic cells to promote recruitment of effector CD8+ T cells to the tumor microenvironment. *Cancer Res*. 2013;73(15):4653-62. Epub 20130612. doi: 10.1158/0008-5472.CAN-12-4366. PubMed PMID: 23761327; PMCID: PMC3780558.
32. Rebuffet L, Melsen JE, Escalière B, Basurto-Lozada D, Bhandoola A, Björkström NK, Bryceson YT, Castriconi R, Cichocki F, Colonna M, Davis DM, Diefenbach A, Ding Y, Haniffa M, Horowitz A, Lanier LL, Malmberg KJ, Miller JS, Moretta L, Narni-Mancinelli E, O'Neill LAJ, Romagnani C, Ryan DG, Sivori S, Sun D, Vagne C, Vivier E. High-dimensional single-cell analysis of human natural killer cell heterogeneity. *Nat Immunol*. 2024;25(8):1474-88. Epub 20240702. doi: 10.1038/s41590-024-01883-0. PubMed PMID: 38956378; PMCID: PMC11291291.
33. Zhang J, Le Gras S, Pouxvielh K, Faure F, Fallone L, Kern N, Moreews M, Mathieu AL, Schneider R, Marliac Q, Jung M, Berton A, Hayek S, Vidalain PO, Marçais A, Dodard G, Dejean

- A, Brossay L, Ghavi-Helm Y, Walzer T. Sequential actions of EOMES and T-BET promote stepwise maturation of natural killer cells. *Nat Commun.* 2021;12(1):5446. Epub 20210914. doi: 10.1038/s41467-021-25758-2. PubMed PMID: 34521844; PMCID: PMC8440589.
34. Tietscher S, Wagner J, Anzeneder T, Langwieder C, Rees M, Sobottka B, de Souza N, Bodenmiller B. A comprehensive single-cell map of T cell exhaustion-associated immune environments in human breast cancer. *Nat Commun.* 2023;14(1):98. Epub 20230106. doi: 10.1038/s41467-022-35238-w. PubMed PMID: 36609566; PMCID: PMC9822999.
35. Panjwani MK, Grassmann S, Sottile R, Le Luduec JB, Kontopoulos T, van der Ploeg K, Sun JC, Hsu KC. Single-Cell Profiling Reveals a Naive-Memory Relationship between CD56. *bioRxiv.* 2023. Epub 20230924. doi: 10.1101/2023.09.23.559062. PubMed PMID: 37790504; PMCID: PMC10543008.
36. Tang F, Li J, Qi L, Liu D, Bo Y, Qin S, Miao Y, Yu K, Hou W, Peng J, Tian Z, Zhu L, Peng H, Wang D, Zhang Z. A pan-cancer single-cell panorama of human natural killer cells. *Cell.* 2023;186(19):4235-51.e20. Epub 20230821. doi: 10.1016/j.cell.2023.07.034. PubMed PMID: 37607536.
37. Shen X, Zuo X, Liang L, Wang L, Luo B. Integrating machine learning and single-cell trajectories to analyze T-cell exhaustion to predict prognosis and immunotherapy in colon cancer patients. *Front Immunol.* 2023;14:1162843. Epub 20230503. doi: 10.3389/fimmu.2023.1162843. PubMed PMID: 37207222; PMCID: PMC10191250.
38. Wells SB, Rainbow DB, Mark M, Szabo PA, Ergen C, Maceiras AR, Caron DP, Rahmani E, Benuck E, Amiri VVP, Chen D, Wagner A, Howlett SK, Jarvis LB, Ellis KL, Kubota M, Matsumoto R, Mahbubani K, Saeb-Parsy K, Dominguez-Conde C, Richardson L, Xu C, Li S, Mamanova L, Bolt L, Wilk A, Teichmann SA, Farber DL, Sims PA, Jones JL, Yosef N. Multimodal profiling reveals tissue-directed signatures of human immune cells altered with age. *bioRxiv.* 2024. Epub 20240104. doi: 10.1101/2024.01.03.573877. PubMed PMID: 38260588; PMCID: PMC10802388.

39. Ohs I, van den Broek M, Nussbaum K, Münz C, Arnold SJ, Quezada SA, Tugues S, Becher B. Interleukin-12 bypasses common gamma-chain signalling in emergency natural killer cell lymphopoiesis. *Nat Commun.* 2016;7:13708. Epub 20161216. doi: 10.1038/ncomms13708. PubMed PMID: 27982126; PMCID: PMC5172358.
40. Han Y, Ru GQ, Mou X, Wang HJ, Ma Y, He XL, Yan Z, Huang D. AUTS2 is a potential therapeutic target for pancreatic cancer patients with liver metastases. *Med Hypotheses.* 2015;85(2):203-6. Epub 20150501. doi: 10.1016/j.mehy.2015.04.029. PubMed PMID: 25962312.
41. Limsakul P, Choochuen P, Charupanit G, Charupanit K. Transcriptomic Analysis of Subtype-Specific Tyrosine Kinases as Triple Negative Breast Cancer Biomarkers. *Cancers (Basel).* 2023;15(2). Epub 20230107. doi: 10.3390/cancers15020403. PubMed PMID: 36672350; PMCID: PMC9856281.
42. Wang D, Malarkannan S. Transcriptional Regulation of Natural Killer Cell Development and Functions. *Cancers (Basel).* 2020;12(6). Epub 20200616. doi: 10.3390/cancers12061591. PubMed PMID: 32560225; PMCID: PMC7352776.
43. Crinier A, Dumas PY, Escalière B, Piperoglou C, Gil L, Villacreces A, Vély F, Ivanovic Z, Milpied P, Narni-Mancinelli É, Vivier É. Single-cell profiling reveals the trajectories of natural killer cell differentiation in bone marrow and a stress signature induced by acute myeloid leukemia. *Cell Mol Immunol.* 2021;18(5):1290-304. Epub 20201125. doi: 10.1038/s41423-020-00574-8. PubMed PMID: 33239726; PMCID: PMC8093261.
44. Manaster I, Gazit R, Goldman-Wohl D, Stern-Ginossar N, Mizrahi S, Yagel S, Mandelboim O. Notch activation enhances IFN γ secretion by human peripheral blood and decidual NK cells. *J Reprod Immunol.* 2010;84(1):1-7. Epub 20091211. doi: 10.1016/j.jri.2009.10.009. PubMed PMID: 20004979.
45. Horowitz A, Strauss-Albee DM, Leipold M, Kubo J, Nemat-Gorgani N, Dogan OC, Dekker CL, Mackey S, Maecker H, Swan GE, Davis MM, Norman PJ, Guethlein LA, Desai M,

- Parham P, Blish CA. Genetic and environmental determinants of human NK cell diversity revealed by mass cytometry. *Sci Transl Med.* 2013;5(208):208ra145. doi: 10.1126/scitranslmed.3006702. PubMed PMID: 24154599; PMCID: PMC3918221.
46. Netskar H, Pfefferle A, Goodridge JP, Sohlberg E, Dufva O, Teichmann SA, Brownlie D, Michaëlsson J, Marquardt N, Clancy T, Horowitz A, Malmberg KJ. Pan-cancer profiling of tumor-infiltrating natural killer cells through transcriptional reference mapping. *Nat Immunol.* 2024;25(8):1445-59. Epub 20240702. doi: 10.1038/s41590-024-01884-z. PubMed PMID: 38956379; PMCID: PMC11291284.
47. Yang C, Siebert JR, Burns R, Gerbec ZJ, Bonacci B, Rymaszewski A, Rau M, Riese MJ, Rao S, Carlson KS, Routes JM, Verbsky JW, Thakar MS, Malarkannan S. Heterogeneity of human bone marrow and blood natural killer cells defined by single-cell transcriptome. *Nat Commun.* 2019;10(1):3931. Epub 20190902. doi: 10.1038/s41467-019-11947-7. PubMed PMID: 31477722; PMCID: PMC6718415.
48. Xu L, Saunders K, Huang SP, Knutsdottir H, Martinez-Algarin K, Terrazas I, Chen K, McArthur HM, Maués J, Hodgdon C, Reddy SM, Roussos Torres ET, Chan IS. A comprehensive single-cell breast tumor atlas defines epithelial and immune heterogeneity and interactions predicting anti-PD-1 therapy response. *Cell Rep Med.* 2024;5(5):101511. Epub 20240412. doi: 10.1016/j.xcrm.2024.101511. PubMed PMID: 38614094; PMCID: PMC11148512.
49. Dong DH, Zhang XF, Lopez-Aguilar AG, Poultsides G, Makris E, Rocha F, Kanji Z, Weber S, Fisher A, Fields R, Krasnick BA, Idrees K, Smith PM, Cho C, Beems M, Schmidt CR, Dillhoff M, Maithel SK, Pawlik TM. Tumor burden score predicts tumor recurrence of non-functional pancreatic neuroendocrine tumors after curative resection. *HPB (Oxford).* 2020;22(8):1149-57. Epub 20191209. doi: 10.1016/j.hpb.2019.11.009. PubMed PMID: 31822386.
50. Huuhtanen J, Kasanen H, Peltola K, Lönnberg T, Glumoff V, Brück O, Dufva O, Peltonen K, Vikkula J, Jokinen E, Ilander M, Lee MH, Mäkelä S, Nyakas M, Li B, Hernberg M, Bono P, Lähdesmäki H, Kreutzman A, Mustjoki S. Single-cell characterization of anti-LAG-3 and anti-PD-

1 combination treatment in patients with melanoma. *J Clin Invest.* 2023;133(6). Epub 20230315. doi: 10.1172/JCI164809. PubMed PMID: 36719749; PMCID: PMC10014104.

51. Dean I, Lee CYC, Tuong ZK, Li Z, Tibbitt CA, Willis C, Gaspal F, Kennedy BC, Matei-Rascu V, Fiancette R, Nordenvall C, Lindforss U, Baker SM, Stockmann C, Sexl V, Hammond SA, Dovedi SJ, Mjösberg J, Hepworth MR, Carlesso G, Clatworthy MR, Withers DR. Rapid functional impairment of natural killer cells following tumor entry limits anti-tumor immunity. *Nat Commun.* 2024;15(1):683. Epub 20240124. doi: 10.1038/s41467-024-44789-z. PubMed PMID: 38267402; PMCID: PMC10808449.

52. Noone CM, Paget E, Lewis EA, Loetscher MR, Newman RW, Johnson PA. Natural killer cells regulate T-cell proliferation during human parainfluenza virus type 3 infection. *J Virol.* 2008;82(18):9299-302. Epub 20080709. doi: 10.1128/JVI.00717-08. PubMed PMID: 18614637; PMCID: PMC2546889.

53. Waggoner SN, Cornberg M, Selin LK, Welsh RM. Natural killer cells act as rheostats modulating antiviral T cells. *Nature.* 2011;481(7381):394-8. Epub 2011/11/20. doi: 10.1038/nature10624. PubMed PMID: 22101430; PMCID: PMC3539796.

54. Chen W, Huang W, Xue Y, Chen Y, Qian W, Ma J, August A, Wang J, Zheng SG, Lin J. Neuropilin-1 Identifies a New Subpopulation of TGF- β -Induced Foxp3. *Front Immunol.* 2022;13:900139. Epub 20220504. doi: 10.3389/fimmu.2022.900139. PubMed PMID: 35603221; PMCID: PMC9114772.

55. Chuckran CA, Liu C, Bruno TC, Workman CJ, Vignali DA. Neuropilin-1: a checkpoint target with unique implications for cancer immunology and immunotherapy. *J Immunother Cancer.* 2020;8(2). doi: 10.1136/jitc-2020-000967. PubMed PMID: 32675311; PMCID: PMC7368550.

56. Werba G, Weissinger D, Kawaler EA, Zhao E, Kalfakakou D, Dhara S, Wang L, Lim HB, Oh G, Jing X, Beri N, Khanna L, Gonda T, Oberstein P, Hajdu C, Loomis C, Heguy A, Sherman MH, Lund AW, Welling TH, Dolgalev I, Tsigos A, Simeone DM. Single-cell RNA sequencing

reveals the effects of chemotherapy on human pancreatic adenocarcinoma and its tumor microenvironment. *Nat Commun.* 2023;14(1):797. Epub 20230213. doi: 10.1038/s41467-023-36296-4. PubMed PMID: 36781852; PMCID: PMC9925748.

57. Dufva O, Gandolfi S, Huuhtanen J, Dashevsky O, Duàn H, Saeed K, Klievink J, Nygren P, Bouhlal J, Lahtela J, Näätänen A, Ghimire BR, Hannunen T, Ellonen P, Lähteenmäki H, Rumm P, Theodoropoulos J, Laajala E, Härkönen J, Pölönen P, Heinäniemi M, Hollmén M, Yamano S, Shirasaki R, Barbie DA, Roth JA, Romee R, Sheffer M, Lähdesmäki H, Lee DA, De Matos Simoes R, Kankainen M, Mitsiades CS, Mustjoki S. Single-cell functional genomics reveals determinants of sensitivity and resistance to natural killer cells in blood cancers. *Immunity.* 2023;56(12):2816-35.e13. doi: 10.1016/j.immuni.2023.11.008. PubMed PMID: 38091953.

58. Lau CM, Adams NM, Geary CD, Weizman OE, Rapp M, Pritykin Y, Leslie CS, Sun JC. Epigenetic control of innate and adaptive immune memory. *Nat Immunol.* 2018;19(9):963-72. Epub 20180806. doi: 10.1038/s41590-018-0176-1. PubMed PMID: 30082830; PMCID: PMC6225771.

59. Amin SB, Anderson KJ, Boudreau CE, Martinez-Ledesma E, Kocakavuk E, Johnson KC, Barthel FP, Varn FS, Kassab C, Ling X, Kim H, Barter M, Lau CC, Ngan CY, Chapman M, Koehler JW, Long JP, Miller AD, Miller CR, Porter BF, Rissi DR, Mazcko C, LeBlanc AK, Dickinson PJ, Packer RA, Taylor AR, Rossmeisl JH, Woolard KD, Heimberger AB, Levine JM, Verhaak RGW. Comparative Molecular Life History of Spontaneous Canine and Human Gliomas. *Cancer Cell.* 2020;37(2):243-57.e7. doi: 10.1016/j.ccell.2020.01.004. PubMed PMID: 32049048; PMCID: PMC7132629.

60. Simpson RM, Bastian BC, Michael HT, Webster JD, Prasad ML, Conway CM, Prieto VM, Gary JM, Goldschmidt MH, Esplin DG, Smedley RC, Piris A, Meuten DJ, Kiupel M, Lee CC, Ward JM, Dwyer JE, Davis BJ, Anver MR, Molinolo AA, Hoover SB, Rodriguez-Canales J, Hewitt SM. Sporadic naturally occurring melanoma in dogs as a preclinical model for human

- melanoma. *Pigment Cell Melanoma Res.* 2014;27(1):37-47. Epub 2013/11/21. doi: 10.1111/pcmr.12185. PubMed PMID: 24128326; PMCID: PMC4066658.
61. Tarone L, Barutello G, Iussich S, Giacobino D, Quagliano E, Buracco P, Cavallo F, Riccardo F. Naturally occurring cancers in pet dogs as pre-clinical models for cancer immunotherapy. *Cancer Immunol Immunother.* 2019;68(11):1839-53. Epub 20190620. doi: 10.1007/s00262-019-02360-6. PubMed PMID: 31222484.
62. Gardner HL, Fenger JM, London CA. Dogs as a Model for Cancer. *Annu Rev Anim Biosci.* 2016;4:199-222. Epub 20151109. doi: 10.1146/annurev-animal-022114-110911. PubMed PMID: 26566160; PMCID: PMC6314649.
63. Simpson S, Dunning MD, de Brot S, Grau-Roma L, Mongan NP, Rutland CS. Comparative review of human and canine osteosarcoma: morphology, epidemiology, prognosis, treatment and genetics. *Acta Vet Scand.* 2017;59(1):71. Epub 2017/10/24. doi: 10.1186/s13028-017-0341-9. PubMed PMID: 29065898; PMCID: PMC5655853.
64. Seelig DM, Avery AC, Ehrhart EJ, Linden MA. The Comparative Diagnostic Features of Canine and Human Lymphoma. *Vet Sci.* 2016;3(2). Epub 20160609. doi: 10.3390/vetsci3020011. PubMed PMID: 28435836; PMCID: PMC5397114.
65. Magee K, Marsh IR, Turek MM, Grudzinski J, Aluicio-Sarduy E, Engle JW, Kurzman ID, Zuleger CL, Oseid EA, Jaskowiak C, Albertini MR, Esbona K, Bednarz B, Sondel PM, Weichert JP, Morris ZS, Hernandez R, Vail DM. Safety and feasibility of an in situ vaccination and immunomodulatory targeted radionuclide combination immuno-radiotherapy approach in a comparative (companion dog) setting. *PLoS One.* 2021;16(8):e0255798. Epub 20210812. doi: 10.1371/journal.pone.0255798. PubMed PMID: 34383787; PMCID: PMC8360580.
66. Wang Y, Pattarayan D, Huang H, Zhao Y, Li S, Zhang M, Yang D. Systematic investigation of chemo-immunotherapy synergism to shift anti-PD-1 resistance in cancer. *Nat Commun.* 2024;15(1):3178. Epub 20240412. doi: 10.1038/s41467-024-47433-y. PubMed PMID: 38609378; PMCID: PMC11015024.

67. Dowell AC, Oldham KA, Bhatt RI, Lee SP, Searle PF. Long-term proliferation of functional human NK cells, with conversion of CD56(dim) NK cells to a CD56 (bright) phenotype, induced by carcinoma cells co-expressing 4-1BBL and IL-12. *Cancer Immunol Immunother.* 2012;61(5):615-28. Epub 20111022. doi: 10.1007/s00262-011-1122-3. PubMed PMID: 22021067; PMCID: PMC11029033.
68. Hollyoake M, Campbell RD, Aguado B. NKp30 (NCR3) is a pseudogene in 12 inbred and wild mouse strains, but an expressed gene in *Mus caroli*. *Mol Biol Evol.* 2005;22(8):1661-72. Epub 20050504. doi: 10.1093/molbev/msi162. PubMed PMID: 15872155.
69. Fend L, Rusakiewicz S, Adam J, Bastien B, Caignard A, Messaoudene M, Iribarren C, Cremer I, Marabelle A, Borg C, Semeraro M, Barraud L, Limacher JM, Eggermont A, Kroemer G, Zitvogel L. Prognostic impact of the expression of NCR1 and NCR3 NK cell receptors and PD-L1 on advanced non-small cell lung cancer. *Oncoimmunology.* 2017;6(1):e1163456. Epub 20160513. doi: 10.1080/2162402X.2016.1163456. PubMed PMID: 28197362; PMCID: PMC5283624.